The Role of CREB3L3 in Adipose Biology and Obesity

BY

MAXIMILIAN A. McCANN
B.S., University of Pittsburgh, 2014

THESIS

Submitted as partial fulfillment of the requirements for the degree of Doctor of Philosophy in Physiology and Biophysics in the Graduate College of the University of Illinois at Chicago, 2021

Chicago,IL

Defense Committee:
Chong Wee Liew, Advisor
Carlos Stocco, Chair
Mark Brodie
Giamila Fantuzzi, Kinesiology and Nutrition
Rhonda Kineman, Endocrinology, Diabetes, and Metabolism

ACKNOWLEDGEMENTS

There are so many people who have helped me get to this point and are deserving of praise. Firstly, I would not have made it to this point without the mentorship of my advisor, Dr. Chong Wee Liew. Thank you for teaching me how to design an experiment and for being patient with my mistakes. Thank you for making my ideas feel valued and giving me the freedom to pursue those ideas. Thank you for pushing me out of my comfort zone and helping me grow in unexpected ways. I will always be grateful for your patience and your belief in me.

To my thesis committee – Dr. Carlos Stocco, Dr. Rhonda Kineman, Dr. Mark Brodie, and Dr. Giamila Fantuzzi – thank you for your wisdom and getting me to think critically. I would still be wandering in the woods if you did not push me to focus my research. And to Dr. José Córdoba-Chacón, thank you for all the insightful advice, conversations about metabolism, and most importantly, laughs.

It is often said that it “takes a village to raise a child,” and my development as a scientist has felt akin to that. Both in the amount of growth I have undergone since I picked up a pipette for the first time, and all the wonderful people that have guided me along the different stages of my development. From my days as an “infant” at the University of Pittsburgh, I would like to thank Sandra Deslouches, Jake Richards, and Dr. Yvette Conley for their patience and humor as I toddled around the lab. To my early time at UIC when Guifen Qiang and Victoria Gil helped me to find my footing. To the last couple years when Yanliang, Phil, and Marcos became not just labmates, but friends and collaborators. Thank you for making every day in lab fun, or at least interesting. I also need to thank “Microscope” Mike Mkrtschjan and Kyle Ditloff for always being there, across the bench, whether I needed to bounce an idea off someone or discuss important NBA minutia.

I would also like to thank the rest of the Physiology Department for making this a great village to “grow up” in.

I also would like to thank the people who actually did raise me. To my mom, Judy, thank you for your fervent support and giving me your curious nature. To my dad, Tom, thank you for being my role model and always being willing to lend a helping hand. To my sister, Katie, thank you for being a calming presence and friend since the day I was born. To Granny and Rocco, thank you for being my biggest fans and shaping my mind with both Pavarotti and The Stones when I was a baby. To my niece, Gloria, thank you for always bringing out the best side of everyone you meet. You bring so much joy to our lives and I am proud to be a part of your village. And to Lisa, thank you for being my partner: for picking me up when I fall, for broadening my horizons, and for always keeping me on my toes. You and Clem have given me a home and carried me through this final stretch, and I am so thankful that I get to share life with you.

MAM

TABLE OF CONTENTS

CHAPTER PAGE

I. Introduction: Adipose Physiology & Obesity 1
1. Adipose Tissue Development 1
1A. Tissue Origins 1
1B. Adipogenesis 3
2. Adipose Tissue Function 6
2A. Anatomical introduction to fat depots 6
2B. White Adipose Tissue Functions 10
2B.1. Lipid Droplet Formation 10
2B.2. *De novo* Lipogenesis 11
2B.3. Lipolysis 12
2B.4. Fatty Acid Oxidation 15
2B.5. Adipokine Secretion 17
2C. Brown Adipose Tissue Functions 18
2C.1 Thermogenesis 20
2C.2. “BAT”okines 22
2C.3. Beige fat 23
3. Obesity & Metabolic Dysfunction 25
3A. Obesity: Modern Society’s Public Health Crisis 25
3B. Adipose Tissue Dysfunction during Obesity 28
3C. Global physiological changes during obesity 29
3C.1 Insulin Resistance 31
4. Subcutaneous vs. Visceral Fat 33
4A. Differential contributions to metabolic dysfunction 33
4B. Features Unique to Visceral Fat 34
4C. Features Unique to Subcutaneous Fat 35
4D. Cellular Mechanisms behind functional differences 36
5. CREB3L3 36
5A. An Introduction 36
5B. Expression 37
5C. Regulation 39
5D. Role in Inflammation 41

5E. Role in Metabolism 41
6. Statement of Hypothesis and Aims 43
II. Materials and Methods 45
1. Animal handling 45
2. Human subjects 45
3. RNA isolation and real-time qPCR 45
4. Human real-time qPCR 46
5. Western blotting 49
6. Isolation of mature adipocytes and stromal vascular fraction 50
7. Adipocyte differentiation 50
8. ER stress induction 51
9. Generation of CREB3L3 fat-specific knockout mouse model 51
10. Body and tissue weight studies 51
11. Tolerance tests 51
12. ELISA and multiplex 52
13. Food intake, energy expenditure, physical activity, and body composition 52
14. Insulin stimulation 52
15. Measurement of mouse lipid and ketone body contents 53
16. Histological analyses 53
17. Adipocyte area quantification 53
18. RNA sequencing 54
19. Environmental and pharmacological stimulation of adipose browning 54
20. Lipolysis assays 55
21. WAT CREB3L3 overexpression 55
22. iWAT overexpression of CREB3L3 55
23. Statistical Analyses 56
III. CREB3L3 is expressed in adipose tissue and selectively downregulated in obese subcutaneous fat 57
1. Introduction 57
2. Results 58
A. Differential expression of CREB3L3 in obese white adipose tissues 58
B. CREB3L3 is expressed in adipose tissues 58
C. CREB3L3 is downregulated in adipose tissue in response to fasting 60

D. ER stress modulates CREB3L3 expression during obesity 60
3. Discussion 65
IV. Adipose ablation of CREB3L3 enhances diet-induced obesity and insulin resistance 67
1. Introduction 67
2. Results 67
A. Adipose ablation of CREB3L3 enhances fat mass in mice fed a chow diet 67
B. CREB3L3 ablation promotes diet-induced obesity and insulin resistance 69
C. CREB3L3 ablation enhances visceral inflammation during obesity 70
3. Discussion 81
V. CREB3L3 fKO promotes weight gain by reducing energy expenditure and metabolic flexibility 83
1. Intro 83
2. Results 83
A. Fat-specific ablation of CREB3L3 reduces global energy expenditure during obesity 83
B. Ablation of CREB3L3 promotes whitening of brown fat 84
C. fKO subcutaneous adipocytes possess less browning potential 85
D. CREB3L3 differentially regulates lipid metabolism in white adipose tissue 86
3. Discussion 95
VI. Increasing expression of CREB3L3 in subcutaneous adipose tissue prevents diet-induced obesity 97
1. Introduction 97
2. Results 97
A. Increased expression of CREB3L3 in subcutaneous adipose tissue prevents diet-induced obesity 97
B. Subcutaneous adipose overexpression of CREB3L3 prevents obesity associated metabolic dysfunction 98
3. Discussion 104
VII. General Conclusions and Future Directions 107
VIII. Appendices 113
IX. Cited Literature 119
X. Vita 132

LIST OF TABLES

TABLE PAGE

QUANTITATIVE PCR PRIMERS 48

WESTERN BLOT ANTIBODIES 49

LIST OF FIGURES

FIGURE PAGE

1: Map of embryonic patterning 4

2: Map of adipose tissues 8

3: Lipid metabolism in adipocytes 13

4: Activation of brown fat 21

5: Obesity trends in the 21st century 27

6: Mechanisms of insulin resistance 32

7: CREB3L3 expression is limited to the liver and GI tract 38

8: CREB3L3 is selectively downregulated in obese subcutaneous fat 61

9: CREB3L3 is present in adipose tissues and adipocytes 62

10: Fasting reduced CREB3L3 expression in adipose tissues 63

11: ER stress induces differential express of CREB3L3 during obesity 64

12: CREB3L3 is knocked out of mature adipocytes in the fKO mice 73

13: Chow-fed fKO mice have enhanced fat mass, but no change in body weight 74

14: CREB3L3 ablation lowers RER in chow-fed mice 75

15: Fat-specific ablation of CREB3L3 enhances diet-induced obesity and insulin resistance 76

16: CREB3L3 fKO promotes selective hepatic insulin resistance 77

17: CREB3L3 fKO promotes eWAT insulin resistance without hypertrophy 78

18: CREB3L3 KO differentially regulates inflammation in obese eWAT and iWAT 79

19: Ablation of CREB3L3 promotes visceral fat inflammation 80

20: CREB3L3 ablation reduces energy expenditure and RER 88

21: Adipose ablation of CREB3L3 reduces food intake 89

22: CREB3L3 ablation promotes lipid accumulation in obese brown fat 90

LIST OF FIGURES (continued)

FIGURE PAGE

23: CREB3L3 ablation prevents β3-induced browning of iWAT adipocytes 91

24: Body weight effects of CREB3L3 ablation lost at thermoneutrality..... 92

25: CREB3L3 differentially regulates lipid metabolism in obese iWAT and eWAT 93

26: CREB3L3 ablation does not alter free fatty release from obese WAT..... 94

27: Adipose expression of CREB3L3 is induced using AAV 100

28: Increased expression of CREB3L3 in iWAT prevents diet-induced obesity 101

29: Increased iWAT CREB3L3 prevents glucose intolerance and insulin resistance .. 102

30: Increased iWAT CREB3L3 shifts global energy homeostasis..... 103

31: Summary of the effects that CREB3L3 modulation has on energy and metabolic homeostasis. 112

LIST OF ABBREVIATIONS

CREB3L3	Cyclic-AMP responsive element-binding protein 3-like-3
fKO	Fat-specific knockout
iWAT	Inguinal white adipose tissue
eWAT	Epididymal white adipose tissue
WAT	White adipose tissue
BAT	Brown adipose tissue
HFD	High-fat diet
Adipo-Cre	Adiponectin Cre recombinase
ER	Endoplasmic Reticulum
BMAL1	Brain and Muscle ARNT-Like 1
Tm	Tunicamycin
TUDCA	Tauroursodeoxycholic acid
FGF21	Fiboblast growth factor 21
SREBP1c	Sterol Regulatory Element-Binding Protein 1c
ChREBP	Carbohydrate response element binding protein
qPCR	Quantitative real-time PCR
RER	Respiratory exchange ratio
EE	Energy expenditure
VCO2	Volume of CO2 produced
VO2	Volume of oxygen consumed
CL	CL 316,243

NPY	Neural peptide Y
IPGTT	Intraperitoneal glucose tolerance test
IPITT	Intraperitoneal insulin tolerance test
CTT	Cold Tolerance Test
Iso	Isoproterenol
Akt	Protein Kinase B
IRS	Insulin receptor substrate
Igfbp1	Insulin-like growth binding protein 1
NEFA	Non-esterified fatty acid
TG	Triglyceride
3-HB	3-hydroxy butyrate
MA	Mature Adipocyte
SVF	Stromal Vascular Fraction
UCP1	Uncoupling protein 1
MIP-2	Macrophage inflammatory protein 2
DNL	*De novo* lipogenesis
Acc1/2	Acertyl-CoA Carboxylase 1/2
Fasn	Fatty Acid Synthase
Fabp4/aP2	Fatty Acid binding protein 4/adipocyte protein 2
GLUT4	Glucose transporter 4
C/EBP	CCAAT-enhancer-binding proteins

PPARγ	Peroxisome proliferator-activated receptor gamma
CLS	Crown-like structure
DEG	Differentially expressed gene
MCP1/Ccl2	Monocyte chemoattractant protein 1
F4/80	EGF-like module-containing mucin-like hormone receptor-like 1
TNFα	Tumor necrosis factor alpha
CD74	Cluster of Differentiation 74/Macrophage Migration Inhibitory Factor Receptor
PKA	Protein Kinase A
Elovl3	Elongation Of Very Long Chain Fatty Acids Protein 3
Adrb3	β-3 adrenergic receptor
Cox8b	Cytochrome c oxidase subunit 8B
PGC1α	Peroxisome proliferator-activated receptor gamma coactivator 1-alpha
Cidea	Cell Death-Inducing DFFA Like Effector A
Prdm16	PR domain containing 16
CPT1	Carnitine palmitoyl transferase
Plin1/2	Perilipin 1/2
HSL	Hormone sensitive lipase
ATGL	Adipocyte triglyceride lipase
AAV	Adeno-associated virus

FLEx-AAV	Flip-excision AAV
sOE	Subcutaneous fat-specific overexpression
BAC	Bacterial artificial chromosome

SUMMARY

The obesity epidemic affects the lives of the 39.6 percent of the American population that are obese and places a massive burden upon the healthcare system. The association of obesity with several dangerous comorbidities elicits an urgent need for effective therapies to induce weight loss and/or treat the complications associated with obesity. One issue that is central to this endeavor is the heterogeneity of adipose tissues. The metabolic contributions of adipose tissues vary based on their location in the body, and while we know some physiological factors behind these differences, cellular mechanisms for these differences have not been unmasked.

The most noteworthy example of adipose heterogeneity is the difference between visceral and subcutaneous white adipose tissue. Despite being comprised of seemingly the same type of adipocytes, visceral fat expansion associates with the development of metabolic dysfunction. This is due to its limited expansion potential, lack of metabolic flexibility, and propensity to become inflamed.

In this thesis, I studied the contributions of cyclic-AMP Responsive Element Binding Protein 3-like-3 (CREB3L3) to adipose biology. CREB3L3 is an ER-bound transcription factor that is an important regulator of lipid metabolism and has previously been described as liver specific. We became interested in CREB3L3 when data mining for other projects and discovering that its expression in adipose tissues is modulated by obesity. In the first chapter, we confirmed that CREB3L3 is expressed in adipose tissue and found that CREB3L3 is downregulated in the more “metabolically protective” subcutaneous fat of obese mice and patients in response to ER stress, while expression is unchanged in the visceral fat.

To investigate how this transcription factor contributes to adipose biology, we created a CREB3L3 fat-specific knockout (fKO) mouse in the second chapter. The fKO mice became significantly heavier than floxed controls when fed high-fat diet and had greater expansion of their epididymal and inguinal fat depots. The epididymal fat from the fKO mice become more inflammatory without more hypertrophic adipocytes. This tissue had more crown-like structures, higher expression of pro-inflammatory cytokines and leptin, and reduced expression of anti-inflammatory markers and adiponectin. These changes manifested in the reduced insulin sensitivity in the fKO mice during obesity.

In the third chapter we investigated the cause of the larger adipose tissues in the fKO mice. While CREB3L3 differentially regulated lipid metabolism in subcutaneous and visceral fat and shifted them towards more lipid synthesis and less lipolysis, respectively, there did not appear to be significant functional changes that explain the larger adipose tissues. Instead, indirect calorimetry experiments show that a reduction in whole-body energy expenditure is the causing the enhanced adiposity of the fKO mice following high-fat feeding. In addition to having a shift in brown fat metabolism from fatty acid oxidation to lipid synthesis, fKO subcutaneous adipocytes were more resistant to browning upon treatment with the β3-adrenergic receptor agonist CL316,243. Additionally, the fKO mice no longer exhibited their enhanced adiposity when housed at thermoneutrality during high-fat feeding. These findings show that the fKO mice have a reduced ability to undergo adaptive thermogenesis, leading to their larger adipose tissues and body weight.

In the last chapter, we created a subcutaneous fat-specific overexpression model to address whether increased CREB3L3 expression in this tissue would prevent the

development of obesity. I found that with only a modest increase in expression of CREB3L3 in subcutaneous fat, diet-induced obesity and insulin resistance is prevented.

Taken together, our data show that this transcription factor is important for regulating body weight and inflammation during high-fat feeding. Our comprehensive phenotyping of our mouse models leads us to propose that the amount of CREB3L3 present in adipose tissues negatively associates with adiposity. Together, our results suggest that CREB3L3 plays an important role in energy homeostasis in adipose tissues during obesity and its ability to modulate body weight suggests that this transcription factor possesses therapeutic potential for the treatment of obesity and obesity-associated disorders.

I. Introduction: Adipose Physiology & Obesity

1. Adipose Tissue Development

1A. Tissue Origins

During the development of an organism, a single fertilized egg cell is able to divide and differentiate into all of the many different cell types within the body that create and support the life of the organism. A crucial step of this process in vertebrates is gastrulation, where the embryo transitions from a single-layered blastula to a structure featuring three distinct layers known as the gastrula. This shift sets the stage for the development of different cell types and the formation of all the organs in the body. The three primary germ layers of the gastrula are the endoderm (inner), mesoderm (middle), and ectoderm (outer) [8]. Fat cells or adipocytes are derived from the mesoderm layer, which has been known since the 1870's when Walther Flemming discovered that adipocytes are derived from a connective tissue that was known to come from the mesoderm [9; 10]. While recent work has complicated our understanding of adipocyte lineage with the discovery that adipocytes from the salivary gland in mice arise from ectoderm-derived $Sox10^{+}$ neural crest cells [11], it is currently accepted that most adipocytes are derived from mesoderm progenitor cells [12].

After gastrulation, the mesoderm consists of three sections. Of these, the somites and lateral plates have been shown to give rise to adipocytes, whereas the intermediate mesoderm has not [12]. The somites are a pair of structures that form at the dorsal end of the mesoderm and consist of the sclerotome, myotome, and dermomyotome (Fig 1) [13]. The most lateral section, the dermomyotome, consists of cells that will make up muscle, the dorsal dermis, and adipocytes in multiple depots in the body.

The adipocytes derived from the dermomyotome will not just end up in anatomically different spaces, but consist of different types of adipocytes as well. It was previously believed that adipocyte progenitors expressing the myogenic transcription factor Myf5 solely differentiated into brown adipocytes. However, lineage-tracing studies have shown that while brown adipocytes in the interscapular, subscapular, and cervical regions come from a $Myf5^+$ lineage, other brown adipocytes were not from $Myf5^+$ progenitors. Additionally, some $Myf5^+$ progenitors even gave rise to white adipocytes in the anterior subcutaneous and the retroperitoneal fat pads [14; 15]. Pax3 and Meox1 fate mapping have confirmed that retroperitoneal brown adipocytes come from a non-$Myf5^+$ progenitor lineage and shown that progenitors on the ventrolateral lip of the dermomyotome develop into perigonadal white adipocytes in male, but not female mice [14; 16; 17]. These findings and further fate mapping using Pax7 have suggested that the location of progenitor cells within the dermomyotome, rather than Myf5 expression, dictates the type of adipocyte a progenitor population will give rise to [12].

In addition to the dermomyotome of the somites, the lateral plate also contains cells that will differentiate into adipocytes. The lateral plate consists of two separate pouches, the somatic and splanchnic (Fig 1), which both give rise to mature adipocytes in different parts of the body ([14; 18]). Progenitors in the splanchnic lateral plate have been shown to give rise to adipocytes located in all of the visceral adipose depots, but not in any subcutaneous or brown adipose tissues [19]. Prx1-Cre labeling was used to discover that progenitors from the somatic lateral plate give rise to limb-associated subcutaneous adipocytes [20; 21]. Additionally, progenitor cells from the splanchnic and the somatic lateral plate have recently been shown to give rise to adipocytes in the subcutaneous inguinal and the visceral mesenteric and female perigonadal fat [18]. Interestingly, the

perigonadal fat of males and females develops from two separate regions of the mesoderm, suggesting genetic sex differences in this visceral adipose depot.

1B. Adipogenesis

Now that we know the lineages that adipocytes come from during development, let's take a look at how adipocytes form from these progenitor cells. This process by which adipocyte precursor cells differentiate into mature adipocytes is called adipogenesis and there are two main processes that occur: determination and terminal differentiation.

The process of determination involves narrowing down the potential fates of progenitor cells until they become preadipocytes and are determined to become adipocytes. Determination has mostly been studied using mesehnchymal cells from bone marrow, so much of the work has focused on the fate decision between becoming a bone cell or an adipocyte [22]. Zfp423 is a transcription factor that has been identified as a promoter of adipocyte determination [23] and is inhibited by Zfp521, which instead promotes osteogenesis [24]. Of the signaling pathways that have been studied, the Wnt and hedgehog pathways promote differentiation into bone cells via osteogenesis, while inhibiting adipogenesis. These signaling pathways meet at the transcription factor COUP-TFII, which inhibits the induction of PPARγ and C/EBP-α, important drivers of adipogenesis [25; 26]. While Wnt signaling inhibits adipogenesis, non-canonical Wnt5b signaling promotes adipogenesis by preventing the inhibitory canonical Wnt signals from reaching the nucleus [27]. Additionally, IGF/insulin signaling has been shown to be a strong promoter of adipogenesis [28]. Our lab has shown that the loss of insulin signaling via the ablation of the insulin receptor in adipose tissue leads to a drastic reduction in the size of adipose tissue [29]. While these signaling pathways have been established as

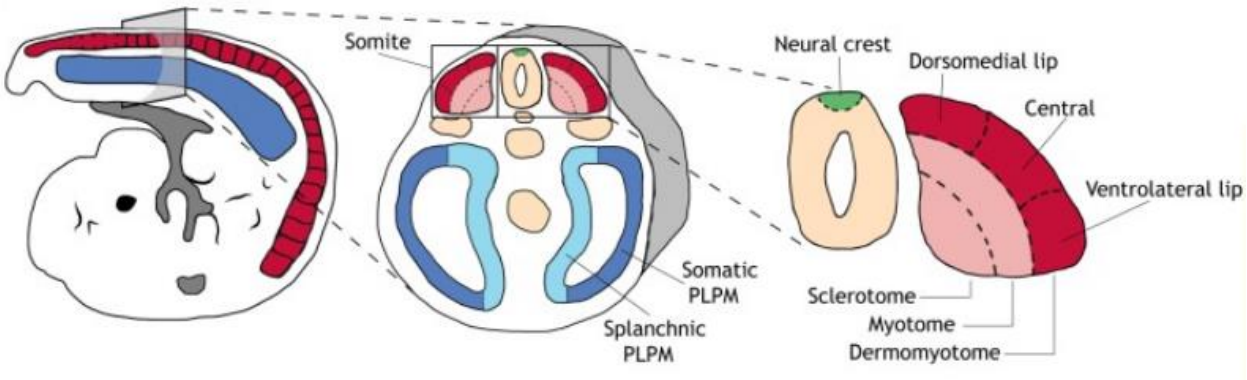

Figure 1: Map of embryonic patterning

Cross-sectional diagram depicting regions of the mesoderm and neuro-ectoderm [12].

contributors to the determination of preadipocytes, studies examining the effect of other signaling pathways like TGF-β/BMP, Notch, and FGF have had conflicting results [30].

Differentiation of adipocyte precursor cells is dependent upon a cascade of transcription factor activity that leads to the adipogenic program of genes being expressed. The key transcription factors involved in this cascade are the C/EBP family (α, β, and δ) and PPARγ, which is known as the master regulator of adipogenesis. PPARγ regulates most of the genes involved in adipocyte metabolism [22] and is such a powerful driver of adipogenesis that it can push precursors of other lineages like myoblasts and fibroblasts to differentiate into adipocytes [31; 32]. While only some of the PPARγ binding sites are conserved between mice and humans, the genes they regulate are very similar. Additionally, PPARγ loss of function mutations lead to lipodystrophy, a condition characterized by a lack of adipocytes and insulin resistance [33-35].

The C/EBP family of bZIP transcription factors work in concert with PPARγ to execute the terminal differentiation of adipocytes. Small amounts of C/EBP-β are present in committed preadipocytes and bind to transcription factor “hotspots” that will later be bound by PPARγ before differentiation is even induced [36]. C/EBP-δ is also active early during terminal differentiation. C/EBP-α is induced later during differentiation and forms a positive feedback loop with PPARγ that “locks in” differentiation into adipocytes [37; 38]. PPARγ also forms feedback loops with C/EBP-β and subsequently the insulin receptor that act to finalize the differentiation process [39]. These feedback loops drive the expression of the gene program necessary for adipocyte differentiation and expression of all three of these transcription factors is needed to maintain the expression of target genes like adiponectin and adipocyte protein 2 in mature adipocytes [40].

2. Adipose Tissue Function

2A. Anatomical introduction to fat depots

These adipocytes can form individually or in clusters around blood and lymph vessels, but the majority will exist within distinct adipose tissues called depots [4]. These depots belong to two main types of adipose tissue – white and brown – that serve vastly different functions. The white adipose tissue (WAT) functions as an energy reservoir, storing excess energy inside its large lipid droplets in the form of triglycerides. The brown adipose tissue (BAT) works as a heat generating organ that combusts metabolic fuels to maintain the animal's body temperature. While metabolically these are the classical roles that adipose tissues fulfill, there are many other functions that adipose tissues serve. In this section we are going to highlight the extensive heterogeneity of adipose tissues and touch on some of the unique profiles of individual fat depots.

There are three main regions of the body where fat depots reside: the anterior subcutaneous, posterior subcutaneous, and the intra-abdominal region. Within the anterior subcutaneous region of mice, there are the axillary, cervical, and interscapular subcutaneous white fat pads, the latter of which encapsulates the interscapular brown fat depot (Fig 2) [41]. The interscapular brown fat is the major brown fat depot in mice, but other brown fat exists within the cervical, axillary, and perirenal regions [5].

In the posterior subcutaneous region of mice, there are three continuous fat pads, the dorsolumbar, inguinal, and gluteal, which make up the subcutaneous inguinal fat depot (Fig 2). This is the main subcutaneous fat depot in mice, and it is rather similar to the gluteofemoral fat in humans [42]. In addition to this fat depot, humans have a substantial amount of subcutaneous fat in the abdomen. Within this region, Scarpa's fascia is used as a landmark to demarcate two distinct fat depots. The tissue located

under Scarpa's fascia has a metabolic profile more akin to visceral fat. This "deep" subcutaneous fat has higher inflammatory cytokine expression, more saturated fatty acids, and is different morphologically from the superficial subcutaneous fat that surrounds it [43-46]. Much like the distinct behaviors of human subcutaneous fat, the fat pads of murine inguinal fat have metabolic differences as well, with the inguinal fat pad at the center having a higher capacity to form brown-like adipocytes than the dorsolumbar and gluteal fat pads [47].

The intra-abdominal region houses the visceral adipose tissue that surrounds the internal organs. The depots contained in this region include: (1) the mesenteric fat that surrounds the intestine; (2) the omentum, a fat apron that covers the spleen, stomach, pancreas, and colon [48]; (3) the retroperitoneal fat that is located at the rear of the peritoneal cavity; (4) the perirenal fat which forms a layer around the kidney and connects to the retroperitoneal fat; (5) a perigonadal depot in mice that is associated with the ovaries in females and is connected to the epididymis in males, and thusly referred to as the epididymal white adipose tissue (eWAT) (Fig 2). Among the visceral fat depots, the mesenteric, perirenal, and retroperitoneal are all present in both humans and mice. The omental (humans) and perigonadal fat (mouse) are the most commonly used models of visceral fat. However, humans do not possess a perigonadal fat depot, while mice have so little/rarely seen omentum that its presence is not always acknowledged [4; 49]. This represents a limitation of visceral fat research, but one that is a function of practicality. The omental fat is the least invasive biopsy to acquire and while murine mesenteric fat most closely resembles human visceral fat, the perigonadal fat is larger, more accessible, and easier to manipulate surgically and dissect, and is therefore more commonly used [41].

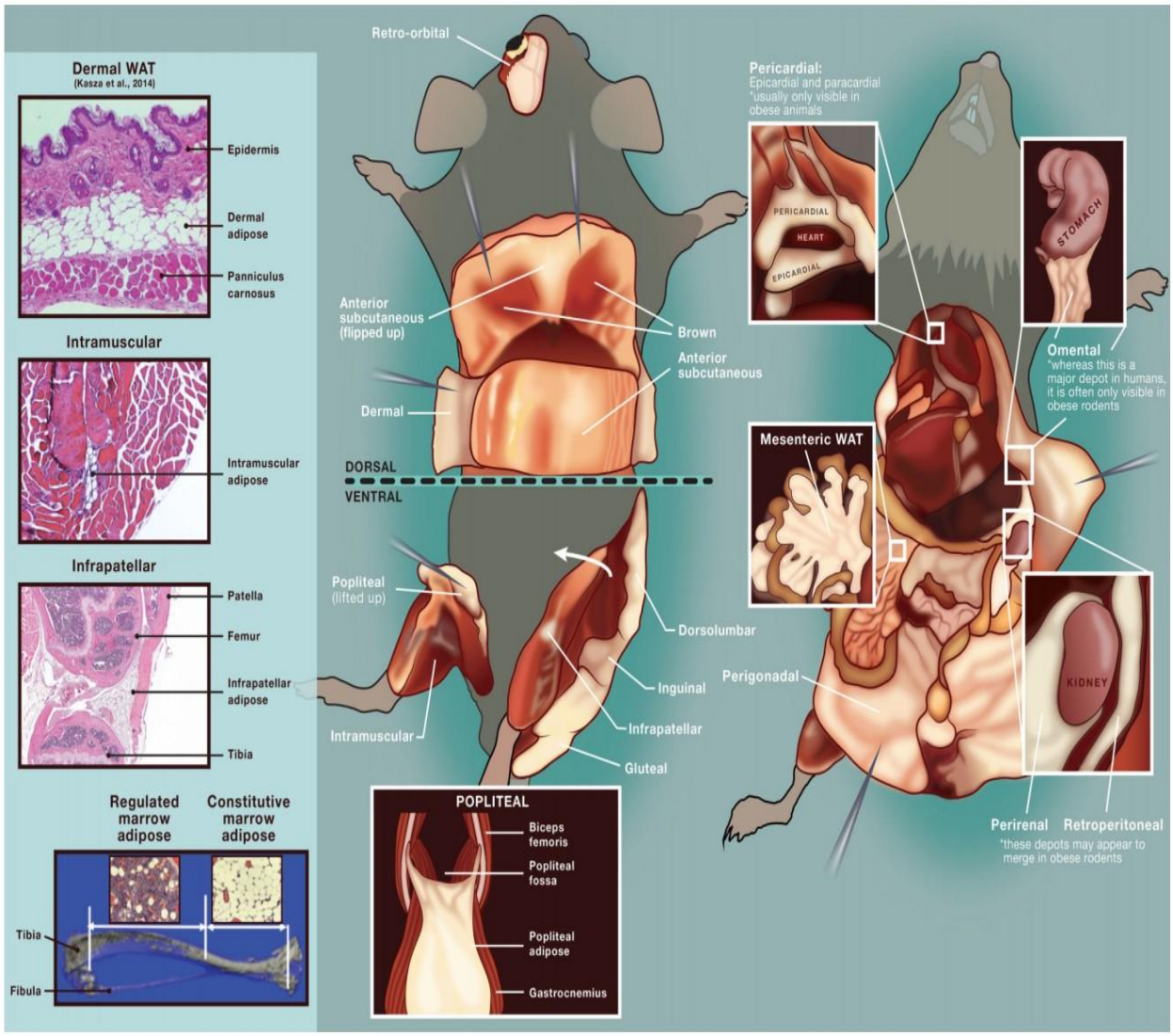

Figure 2: Map of adipose tissues

Diagram depicting the location of different adipose tissues in the body [4].

In addition to these main fat depots, adipocytes exist throughout the body in various forms and take on a number of functions (Fig 2). Adipose tissue exists within the bone marrow and makes up about 10% of the total fat mass in humans. Marrow adipose tissue is an important metabolic tissue due to its role in lipid storage, bone homeostasis, and its high proportional secretion of the hormone adiponectin [47]. Dermal adipose tissue – located just under the dermis layer of the skin has been a new avenue of metabolic research, and it was recently discovered that these adipocytes have the ability to dedifferentiate, proliferate, then redifferentiate to modulate the mass of the tissue [50]. It normally functions to provide insulation, fight infection, promotes wound healing, and the growth of hair follicles [51]. The adipose tissue within the mammary gland is noted for its ability to undergo cyclic remodeling of expansion and a shift towards lipid production during pregnancy [52], followed by retraction and reversible transdifferentiation into secretory mammary epithelial cells during lactation [53]. The omentum, the visceral fat organ that covers the abdominal organs, was termed “the policeman of the abdomen” in the early 1900’s due to its ability to move around the peritoneal cavity and plug up surgical wounds and inflammation [54]. The omentum is also known for its “milky spots,” clusters of leukocytes that Ranvier identified to be embedded between adipocytes [55]. Similar lymphoid clusters exist in mesenteric and pericardial fat [56]. The pericardial WAT forms the layer of fat surrounding the heart, although the epicardial WAT takes up an estimated 80% of the surface area of the heart [57]. The epicardial WAT also has a unique profile of smaller white adipocytes that express high levels of the brown fat marker UCP1 [58] and releases large amounts of free fatty acids to assumedly fuel the heart [59]. Lastly, muscle tissue features both intermuscular adipocytes between muscle groups, and intramuscular adipocytes that form between muscle and fibers. Increased number of

intramuscular adipocytes correlates with the development of type 2 diabetes [60]. To conclude, adipocytes perform a bevy of metabolic, immune, structural, and secretory functions throughout the body. Next, let's take a look at the cellular processes that allow adipocytes to perform these functions.

2B. White Adipose Tissue Functions

While the white adipose tissues may serve different roles based on their anatomical locations, they have one feature that unites them: energy storage. In this section we will discuss the processes that adipose tissues use to store, utilize, and distribute energy to other tissues in the form of fatty acids.

2B.1. Lipid Droplet Formation

The defining feature of adipocytes is their lipid droplet. This organelle is filled with triglycerides and can take up as much as 95% percent of the volume of adipocytes [61], shunting the other organelles to the periphery of the cell. Fat makes up 80% of the weight of adipose tissue, with triglycerides making up over 90% of the lipids stored in the adipose tissues [62]. The presence of this much intracellular lipid would be toxic to any other cell type, yet the formation and maintenance of this central lipid droplet allows adipocytes to safely store lipids and serve as an energy reservoir for the rest of the body.

The formation of lipid droplets is still a relatively new field of research and the exact mechanism has not been fully pinpointed yet. However, here is the proposed mechanism by which it is believed that lipid droplets form: (1) Triacylglycerols are synthesized within the ER. (2) An oil lens forms in the membrane of the ER at the tubules. It is proposed that the curvature of the tubules disturbs the local bilayer of the ER membrane and may promote formation of the oil lens [63; 64]. (3) This oil lens buds off the ER membrane and creates a nascent lipid droplet. The prevailing model is that nascent lipid droplets bud off

into the cytosol and then break off, although it has not been ruled out that they remain connected to the ER [65]. (4) Expansion of the lipid droplet occurs when the lipid droplet itself begins synthesizing TG, after lipid droplet proteins like DGAT2 appear in and around the lipid droplet [66; 67]. This shift from an initial (iLD) to expanding lipid droplet (eLD) synthesizing its own TG occurs over the course of minutes to hours and occurs as lipid synthesis enzymes relocate from the ER to the lipid droplet [68]. ARF1/COP1 trafficking proteins are necessary for this process [69], and a lack of either of these proteins leads to smaller and fewer lipid droplets in drosophila [70; 71]. (5) Growth of lipid droplets is believed to occur via one of two processes, either fusion of two existing lipid droplets [65], or facilitated diffusion of lipids from a small lipid droplet to a larger neighboring droplet via proteins located at inter-droplet contact zones like FSP27/CIDE-C [72]. Together, these mechanisms of lipid droplet formation, growth, and lipid droplet protein targeting form our expanding knowledge base of how the cellular architecture that helps drive adipocyte function is created.

2B.2. *De novo* Lipogenesis

The lipids that are stored in the lipid droplets can either come from the diet and are absorbed in the intestine, or they are synthesized from carbohydrates in a process called *de novo* lipogenesis (Fig 3). *De novo* lipogenesis (DNL) consists of a series of reactions that takes citrate from the TCA cycle and converts it into a fatty acid chain, which can undergo further modifications to make the wide range of lipid species needed to support life. To start, citrate is exported from the mitochondria and converted to acetyl-coA by ATP citrate lyase. Then, acetyl-coA carboxylase (ACC) adds a carboxyl group to this molecule, turning it into malonyl-coA. The enzyme complex fatty acid synthase (FASN) takes the malonyl-coA molecule and begins elongation, adding carbons to the nascent

fatty acid chain [73]. After the fatty acid is synthesized, it can be condensed to glycerol to form phospholipids to go into membranes or form a triglyceride and be stored in the lipid droplet (Fig 3). Additionally, elongase and desaturase enzymes add variety to the potential lipids that cells can produce by altering the length, structure, and physical properties that adipocytes and other cells produce [74]. The two main enzymes of DNL are ACC and FASN. They are both transcriptionally regulated by SREBP1c and ChREBP, but SREBP1c is the most important regulator of DNL in the liver, while ChREBP is in the adipose tissue [75; 76]. DNL in these tissues also has opposite effects on global metabolic homeostasis, with increased hepatic DNL leading to negative outcomes, and adipose DNL promoting insulin sensitivity [76].

2B.3. Lipolysis

Adipocytes are able to access the fatty acids that have been stored in the lipid droplet during periods of negative energy balance via a process known as lipolysis. Lipolysis is the breakdown of triglyceride molecules stored within the lipid droplet that results in the release of free fatty acids (FFA) and glycerol. Lipolysis is a series of reactions that starts with the hydrolysis of triglycerides via adipose triglyceride lipase (ATGL) that produces diacylglycerol (DAG) and releases one FFA molecule. That DAG molecule then gets hydrolyzed by hormone-sensitive lipase (HSL), which results in monoacylglycerol and another FFA molecule. The process is then completed by the enzyme monoacylglycerol lipase (MGL), which hydrolyzes the bond between glycerol and the remaining fatty acid molecule and separates them. Overall, the products of catabolizing one triglyceride molecule are one glycerol and three FFA molecules (Fig 3) [77].

The process of lipolysis is mainly controlled by the activity of protein kinase A (PKA), a kinase that is activated by elevated cyclic-AMP (cAMP) concentrations.

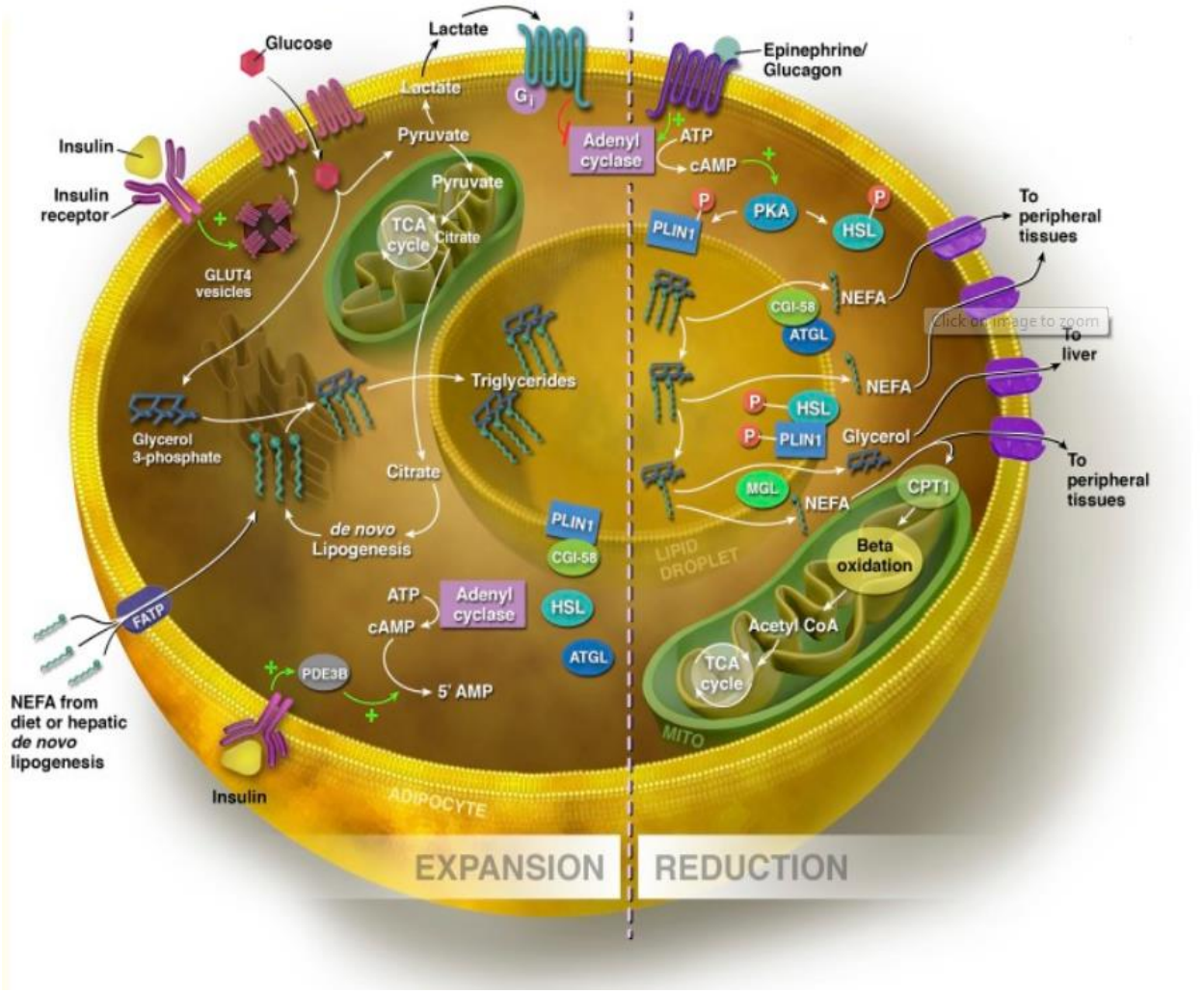

Figure 3: Lipid metabolism in adipocytes

Diagram depicting lipolysis, fatty acid uptake, *de novo* lipogenesis, and Beta oxidation in adipocytes [7].

The concentration of cAMP is modulated by many signaling pathways via many G-protein coupled receptors (GPCR). When intracellular cAMP levels rise, PKA becomes activated and phosphorylates HSL, causing it to translocate to the lipid droplet and hydrolyze diacylglycerol molecules [77]. PKA also phosphorylates the lipid droplet protein perilipin, which restricts lipase access to the lipid droplet under basal conditions (Fig 3) [78]. This phosphorylation causes perilipin to release comparative gene identification 58 (CGI-58), an ATGL co-activator, which allows ATGL to dock on the lipid droplet membrane. PKA can also phosphorylate CGI-58, enhancing its dispersal in the cytoplasm and promoting its interaction with ATGL [79].

There are several regulatory mechanisms that control the rate of lipolysis that occurs within adipocytes. The autonomic nervous system is one of the main regulators of lipolysis. The adipose tissue is highly innervated by both the sympathetic (SNS) and parasympathetic (PNS) nervous system, allowing for tight regulatory control [80]. The SNS controls the body's response to stress and mobilizes metabolic substrates like fatty acids so they are available for quick consumption. Catecholamines, the signaling molecules of the SNS, stimulate lipolysis via binding to adrenoceptors, which are GPCRs that activate adenylyl cyclase and thus PKA. In humans, the B1 and B2 adrenoceptors are the most active in lipolysis, while the contributions of the more adipose-specific B3 adrenoceptor is not well established [81], and has even failed to induce lipolysis and weight loss when stimulated in obese patients [82; 83]. The a2-adrenoceptor is coupled to G-inhibitory proteins that inhibit cAMP production, so the balance of the inputs of the different adrenoceptors is important for lipid mobilization in humans [84; 85].

The name of the enzyme hormone-sensitive lipase derives from its regulatory inputs from multiple hormones. The main hormonal regulator of lipolysis is insulin, which

rapidly inhibits lipolysis within minutes of binding to its receptor [77]. This binding leads to activation of phosphodiesterase-3B, which catalyzes cAMP breakdown. This drops the cAMP concentration and prevents PKA activation. Insulin signaling may also phosphorylate the regulatory subunit of protein phosphatase-1, which removes phosphate from HSL [86]. The drop in circulating insulin during periods of fasting removes its inhibitory effect and allows for lipolysis and the release of free fatty acids to occur.

In addition to insulin, other hormones regulate lipolysis, albeit with a less potent effect. Growth hormone promotes lipolysis by disinhibiting adenylyl cyclase, especially during longer fasting, allowing it to produce more cAMP [87]. Cortisol creates a stress-induced increase in lipolysis that has a more delayed effect than the minutes it takes the epinephrine from the SNS to stimulate lipolysis [88; 89]. The stimulatory effect of cortisol is also undermined by its promotion of insulin release. Lastly, parathyroid hormones seem to stimulate lipolysis in human adipose tissue [90; 91], but may also promote weight gain by preventing catecholamine-induced lipolysis [92].

2B.4. Fatty Acid Oxidation

Following uptake via membrane transporters like CD36 or lipolysis, free fatty acids are able to be metabolized for energy production. β-oxidation consists of four steps that lead to the cleavage of two carbons from the fatty acid and the creation of NADH, $FADH_2$, and an acetyl-CoA molecule. The shortened fatty acyl co-A molecule is then able to undergo subsequent rounds of β-oxidation. The acetyl co-A molecule is able to enter the TCA cycle and produces more NADH and $FADH_2$ molecules, and in the liver can be used to generate ketone bodies [93]. The NADH and $FADH_2$ produced become participants in the electron transport chain to produce ATP. All in all, the oxidation of one 16 carbon palmitate molecule generates upwards of 100 ATP molecules [94].

In order for oxidation to occur, fatty acids must be activated via conjugation to acetyl-coA, creating a fatty acyl-coA molecule in the cytoplasm. Short-chain fatty acyl-coA molecules are able to freely diffuse across the mitochondrial membrane for oxidation; however, medium and long chain fatty acids are not. These larger fatty acyl-coA molecules require the carnitine shuttle system to transport them across the mitochondrial membrane and into the matrix for oxidation. Carnitine palmitoyl transferase 1 (CPT1) in the outer mitochondrial membrane adds a carnitine molecule to fatty acyl-coA, creating a fatty acyl-carnitine. This molecule is then able to diffuse across the mitochondrial membrane using the carnitine-acylcarnitine translocase. Once in the mitochondrial matrix carnitine palmitoyl transferase 2 (CPT2) removes the carnitine, and the fatty acyl-CoA is able to undergo β-oxidation (Fig 3) [95].

The carnitine shuttle system is regulated in conjunction with *de novo* ligogenesis. When acetyl-coA molecules produced by glycolysis are carboxylated, they form malonyl-coA, which serves as a substrate for *de novo* lipogenesis and palmitate production. Malonyl-coA has also been shown to inhibit beta oxidation through inhibition of CPT1 [95]. This makes CPT1 the rate-limiting step of fatty acid oxidation and means that fatty acids get pushed towards storage as triglycerides instead of oxidation during periods of positive energy balance [96]. The rate-limiting status of CPT1 makes its downregulation in the visceral adipose biopsies from obese patients [97] a hindrance to potential body weight interventions, and adipocytes become less oxidative during obesity [98; 99]. To summarize, fatty acid oxidation is an important metabolic process that allows adipocytes and other cell types to make use of the vast energy stores contained within adipocytes.

2B.5. Adipokine Secretion

In recent years, the ability of adipose tissue to function as an endocrine organ, and not solely as an inert energy storage organ, was recognized. There are several hormones that the adipose tissue secretes that contribute to the global metabolic regulation of the organism. The first adipokine to be discovered was the appetite-suppressing hormone, leptin. Discovery of the effects of leptin are attributed to Douglas Coleman, Rudolph Leibel, and Jeffrey M. Friedman at the Jackson Laboratory. They identified its effects in a non-obese mouse line that developed a mutation which caused the mice to eat nonstop and become obese [100]. When the circulation of an “ob/ob” mouse was joined with that of a mouse lacking the mutation, the ob/ob mouse ate less and lost weight, demonstrating that a mutated circulating factor was responsible for its excessive food intake [101]. The mutated circulating factor was later identified as leptin, which we now know is secreted from adipocytes and helps to suppress appetite and increase energy expenditure by stimulating several regions in the hypothalamus including the arcuate, dorsomedial, lateral, and ventromedial nuclei [102; 103]. Leptin also has pro-inflammatory effects. It has been shown to stimulate production of pro-inflammatory cytokines like IL-1, IL-6, and TNFα, to stimulate ROS production, to promote T helper 1 differentiation, and to promote macrophage activation [104; 105].

Adiponectin is the other main adipokine. It is adipose specific and use of its promoter has become the gold standard for creation of adipose-specific genetic manipulations [29; 106]. While adiponectin is expressed only in adipocytes, its receptors are expressed throughout the body, causing adiponectin to have widespread metabolic effects. Adiponectin has been shown to suppress glucose production in the liver [107], to improve pancreatic beta cell function, to promote cardiovascular health [108], and to

enhance fatty acid oxidation in liver and muscle via activation of AMPK and other signaling pathways [109]. Adiponectin is also known as an insulin-sensitizing hormone because it stimulates translocation of the glucose transporter GLUT-4 to the plasma membrane in skeletal muscle [110]. Adiponectin also stimulates the hypothalamus to promote food intake, and the overexpression of this adipokine in ob/ob mice created a mouse model that weighed around 100 grams, but had improved glucose homeostasis relative to ob/+ littermates [111]. Like leptin, adiponectin also affects inflammation, although the effects of adiponectin are more anti-inflammatory. Adiponectin has been shown to prevent production of TNFα and IFN-γ, while promoting the secretion anti-inflammatory cytokines like IL-10 and IL-1RA [112].

In addition to leptin and adiponectin, adipocytes also secrete several other cytokines. Resistin is an adipokine that is secreted more during obesity, and as the name suggests, promotes insulin resistance in obese animals [113]; however, human studies involving resistin have not concluded this [114]. RBP4 is expressed mostly in visceral adipose tissue and has been shown to be elevated in obesity and contribute to insulin resistance [115]. While aP2 usually functions in the cytosol to coordinate lipolysis, secretion of this protein through exosomes has been observed, leading to promotion of hepatic glucose production [116]. Lastly, signaling properties of fatty acid derivatives have begun to be characterized in recent years, creating a new class of non-protein adipokines called “lipokines” [22].

2C. Brown Adipose Tissue Functions

Brown adipose tissue exists as a hybrid between white adipose tissue and muscle. It still features lipid droplets and is capable of lipid storage; however, brown adipocytes are mostly derived from the same lineage as muscle cells and feature a similar expression

profile [117]. While white adipose tissue focuses on storing energy as triglycerides, brown adipose tissue exists to metabolize fatty acids and glucose in order to maintain the body's temperature. In order to achieve this, brown adipose tissue needs a large amount of blood vessels to supply it with metabolic substrates and mitochondria to break them down. The iron within these key features of brown adipose tissue gives it its trademark color and name. In addition to being rich in blood vessels and mitochondria, brown adipocytes contain different lipid droplets than those found in white adipocytes. Instead of the unilocular appearance of white adipocytes where the cytoplasm is dominated by one large lipid droplet, brown adipocytes have a multilocular appearance that features numerous smaller lipid droplets.

In addition to the differences in form and function of brown adipose tissue, the interspecies variability in the amount of brown adipose tissue is much larger than white adipose tissue. Brown adipose tissue is housed as distinct interscapular, axillary, and cervical pads in mice [5]. In humans, infants have a layer of interscapular brown adipose tissue akin to the brown adipose tissue seen in mice [118; 119]. As humans grow during development, they lose relative surface area and the need for brown adipose tissue to maintain body temperature. Brown adipocytes are replaced by white adipocytes [120] as the body develops and until recently it was believed that infants were the only humans that possess brown fat [121]. However, functional imaging that traces cellular glucose uptake using ^{18}flurodeoxyglucose positron emission tomography (18F-FDG PET) was used in the late 2000's to identify supraclavicular and cervical regions in adult humans that contained brown adipose tissue that expressed brown fat markers [122-124] and was more prevalent during cooler months [125]. This was a landmark finding and opened up

the possibility of utilizing this high energy consuming tissue for the treatment of obesity and metabolic dysfunction.

2C.1 Thermogenesis

The unique feature of brown adipocytes that makes them an appealing therapeutic target is their ability to consume large amounts of energy due to the heat-producing process called thermogenesis. Thermogenesis occurs in response to cold-induced release of norepinephrine from sympathetic nerves or beta adrenergic stimulation. This stimulation leads to $G_{s\alpha}$ stimulation of adenylyl cyclase and the production of cAMP. This rise in cAMP activates protein kinase A, which phosphorylates CREB and p38 MAPK (Fig 4) [126]. These kinases phosphorylate and activate the transcriptional co-activator PGC1α, a key transcriptional regulator of mitochondrial biogenesis and fatty acid oxidation [127]. In adipocytes, PGC1α promotes expression of thermogenic proteins like uncoupling protein 1 (UCP1) [127; 128]. UCP1 is a proton channel that allows protons to leak back across the inner mitochondrial membrane and removes the membrane potential that drives the highly efficient oxidative phosphorylation pathway, uncoupling it from respiration (Fig 4) [129].

This short circuiting of the most efficient pathway for ATP production forces brown adipocytes to consume more metabolic fuels in order to meet cellular energy needs. The high volume of catabolic reactions occurring within brown adipocytes allows them to generate heat and makes them an important contributor to basal metabolic rate. Despite the small amount of brown fat that adults have, it has been estimated that after stimulation, brown adipose tissue can account for 16% of the resting metabolic rate in humans [130]. While stimulated brown fat can have large contributions to the energy

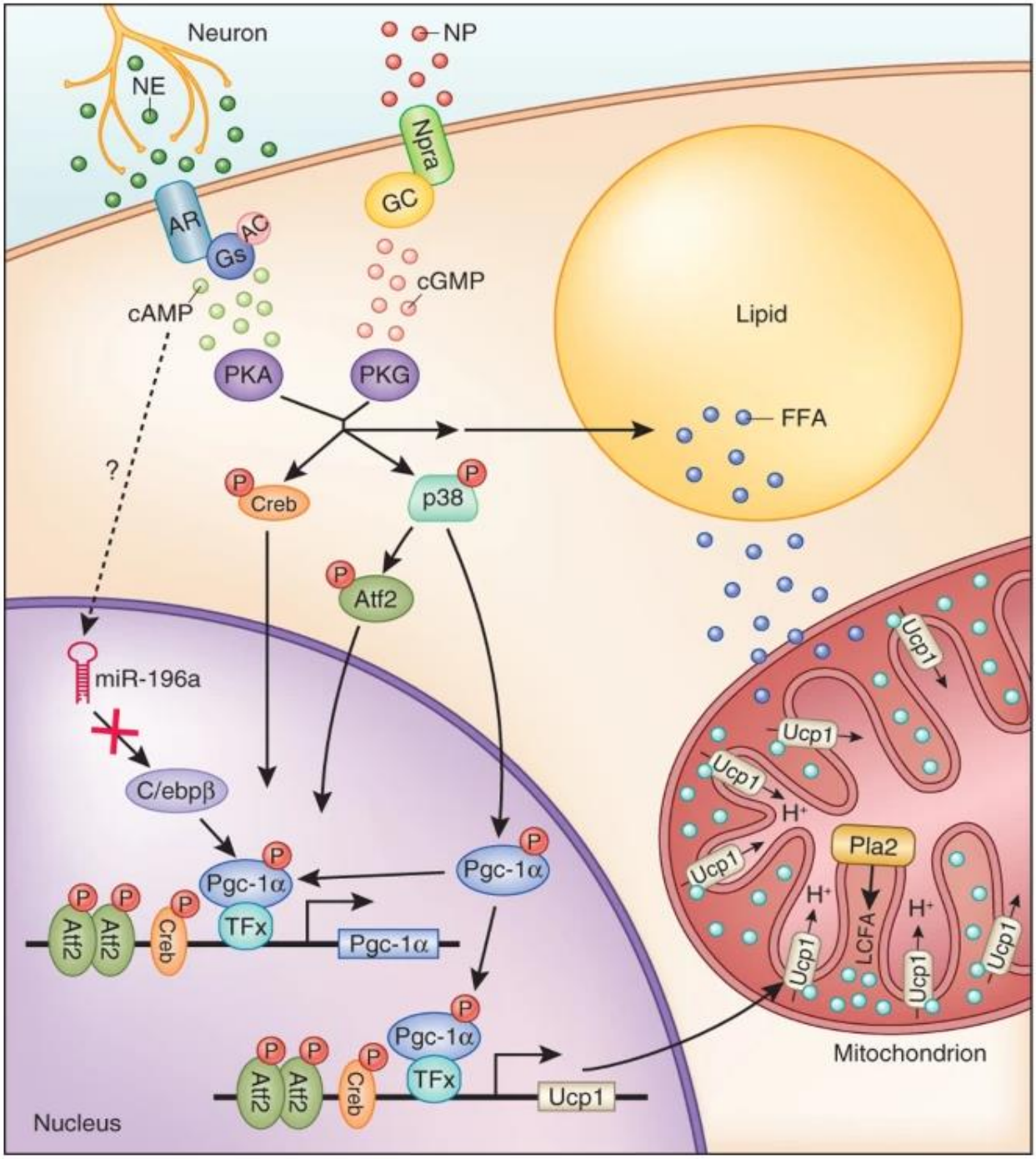

Figure 4: Activation of brown fat

Diagram depicting brown fat activation via PKA signaling in response to cold or β-adrenergic stimulation [5].

expenditure of humans, many humans do not face sustained exposure to cold temperatures that stimulate the brown adipose tissue.

2C.2. “BAT”okines

Although humans are usually not exposed to cold long enough to stimulate brown fat activity under normal conditions; under experimental conditions, brown fat stimulation leads to improved insulin sensitivity and glucose homeostasis in adult humans [131; 132]. These effects appear to be due to more than just changes in body weight or fat mass. When PRDM16, a transcriptional coregulator important in brown fat development, was overexpressed in the fat of obese transgenic mice, the mice showed small improvements in insulin sensitivity and fat mass, but large improvements in their glucose tolerance [133]. Conversely, fat-specific ablation of PRDM16 or its coregulator EHMT1, lead to insulin resistance in lean mice and led to hepatic steatosis [134; 135]. These findings suggest that brown fat and brown adipocytes located within WAT depots have a greater contribution to global glucose homeostasis than solely its boost in energy expenditure. One potential reason for the improvements in glucose tolerance associated with brown fat activity is the ability of brown fat to act as a “metabolic sink,” where glucose, fatty acids, and other metabolic substrates are dumped, and prevented from getting into other metabolic organs [136].

Another potential reason is that brown fat might secrete its own adipokines that improve glucose homeostasis. Some evidence exists for the secretion of metabolically-beneficial hormones being secreted from brown or brown-like adipocytes in WAT, called beige cells, following exercise. Endurance exercise has been shown to promote the formation of beige adipocytes, and the transplantation of inguinal WAT following exercise training improved insulin sensitivity and glucose tolerance in recipient mice [137].

Additionally, neuregulin 4 has been shown to be secreted from brown fat and negatively regulates lipid synthesis in the liver [138]. In addition to neuregulin 4, stimulated beige fat has been shown to secrete irisin and METRNL, two proteins that are secreted by the muscle following exercise, and cold-exposed adipose tissues secrete brown-inducing hormones FGF21 and BMP8b. While “BATokines” likely work in tandem with the metabolic sink capacity of brown adipocytes to improve glucose homeostasis, they offer a relatively new class of metabolic hormones and add a layer of complexity to our rapidly evolving knowledge of brown adipose tissue.

2C.3. Beige fat

In addition to brown fat, adipocytes within white adipose tissues are also capable of expressing UCP1 and performing non-shivering thermogenesis. These “beige” adipocytes appear in response to cold exposure or stimulation of the β_3-adrenoceptor (Adrb3) by the sympathetic nervous system. There are two leading hypotheses for how beige adipocytes form. The first is that existing white adipocytes transdifferentiate into beige adipocytes and begin expressing UCP1. The other is that beige adipocytes are formed from perivascular precursor cells that undergo *de novo* adipogenesis to form beige cells. There is substantial evidence for both sides of this argument. The presence of intermediate cells that fall between white and beige phenotypes provide evidence of transdifferentiation [139; 140], but tracing studies have shown that new adipogenesis is required for beige adipocyte formation in response to cold [141].

Recent fate-mapping studies have suggested that cold and beta-adrenergic stimulation may make use of different sources for their induction of beige adipocytes. Acta2+ or Myh11+ smooth muscle cells have been shown to differentiate into beige cells [142; 143]. Fate mapping of these cells during Adrb3 stimulation demonstrated that they

were not the source of beige cell generation. This suggests that transdifferentiation of existing white adipocytes is responsible for beige cell formation following Adrb3 stimulation, which was confirmed using an adipocyte-specific ablation of Prdm16, resulting in inguinal fat that was unable to form beige adipocytes [144]. Expression studies of beta adrenoceptors provides further support for Adrb3-induced beige cells coming from existing adipocytes. Mature adipocytes express the Adrb3 receptor, but smooth muscle cells do not [142; 145]. They do, however, express Adrb1, which is not expressed in adipocytes [146]. This study also used pharmacological inhibitors to suggest that Adrb1, and not Adrb3 stimulation, is responsible for the formation of beige cells in response to cold, which backs up previous reports of Adrb3 being dispensable for cold-induced browning [147]. Additionally, Adrb1 null mice are cold intolerant [148], and overexpression of this receptor amplifies browning potential [149]. Together, these data suggest that cold and Adrb3 stimulation utilize different cell sources and signaling pathways to induce beige cell formation. In addition to confirming the source of beige adipocytes in response to different stimuli, the metabolism of beige cells formed from each induction method should be characterized to ascertain the ideal therapeutic strategy.

While brown and beige fat have intriguing therapeutic potential for the treatment of obesity and metabolic dysfunction, there are some caveats that should be considered regarding the comparison of mouse and human thermogenic tissues. Firstly, the thermogenic tissue identified in humans more closely resembles beige rather than brown fat found in mice [150; 151]. Humans and mice also have different tissues with higher expression of browning markers. In mice, expression is higher in subcutaneous fat. In humans, expression is actually higher in the omental fat compared to the abdominal subcutaneous fat [152]. Additionally, exercise increases markers of browning within

subcutaneous fat in mice; however, exercise reduces brown fat markers in human subcutaneous fat [137; 153]. Together, these differences highlight the limitations that undermine data interpretation and the care that must be taken to extrapolate findings from murine brown adipose tissue and apply it to human beings.

3. Obesity & Metabolic Dysfunction

Body weight regulation is a delicate balance between energy expenditure and energy consumption. If energy consumption does not meet the energy expenditure needs of an animal, the animal will starve. However, if energy consumption is greater than its energy expenditure, the animal will store the extra energy, usually in the lipid droplets of adipocytes. This is the body's natural response to acute overnutrition. When overnutrition occurs chronically, fat begins to accumulate and eventually the animal becomes obese.

3A. Obesity: Modern Society's Public Health Crisis

Starting in middle of the 1970's, the prevalence of obesity began to climb. A comparative study of obesity rates of Americans between 1976-1980 estimated the prevalence of obesity in American adults was around 14.5 percent [154]. In 2015-2016, the prevalence of obesity was 39.6 percent in American adults and 18.5 percent in children (age 2-19) (Fig 5) [3]. That number is even higher in the non-Hispanic Black (46.8%) and Hispanic (47%) populations. This is a dangerous situation due to the association of obesity with many comorbidities including diabetes and insulin resistance, heart disease, liver diseases, Alzheimer's, depression, reproductive issues, and certain types of cancers [155], and obesity creates an estimated 147-210 billion dollars of healthcare costs in the United States each year [156]. But what has caused this dramatic shift in the size of the

American population? And how does increased body weight predispose individuals to some of the most deadly diseases?

For most of human existence, food resources were scarce and uncertainty over when (or if) a next meal would happen were common. Therefore, the human body evolved to meet the energy conservation needs of a food insecure society. Survival was more likely if humans were able to consume as many calories as possible when food was present, then conserve leftover calories until the next time food was available. In the meantime, the body would store any unused calories from the meal as fat, which the body could draw from while searching for the next meal.

In other words, the human body was not prepared for Taco Bell. The emergence of fast food alone did not doom modern society to a future of obesity and chronic health problems, but it certainly did not help. The appearance of cheap, delicious, high-calorie foods that are ready at a moment's notice was not the death knell for America's waistlines, but a byproduct of a society that now had something the human body did not evolve for: plenty. While food insecurity exists as a still too common problem that affected 10.5 percent of American households in 2019 [157], society has progressed so that acquiring food is no longer the mass critical venture it had been throughout history. Instead of needing to go out and hunt for dinner, or ration the yields of a harvest, grocery stores are stocked with any food a person could want, year round. And the human body has responded to surplus the way it has responded to food for centuries, by conserving excess calories as fat. Along with the excess of food available in today's society, increasingly sedentary lifestyles, less cigarette smoke (appetite suppressant), the rise of food deserts, and the steep price of vegetables, modern society has created an environment that sets up Americans, and the rest of the world, to be obese.

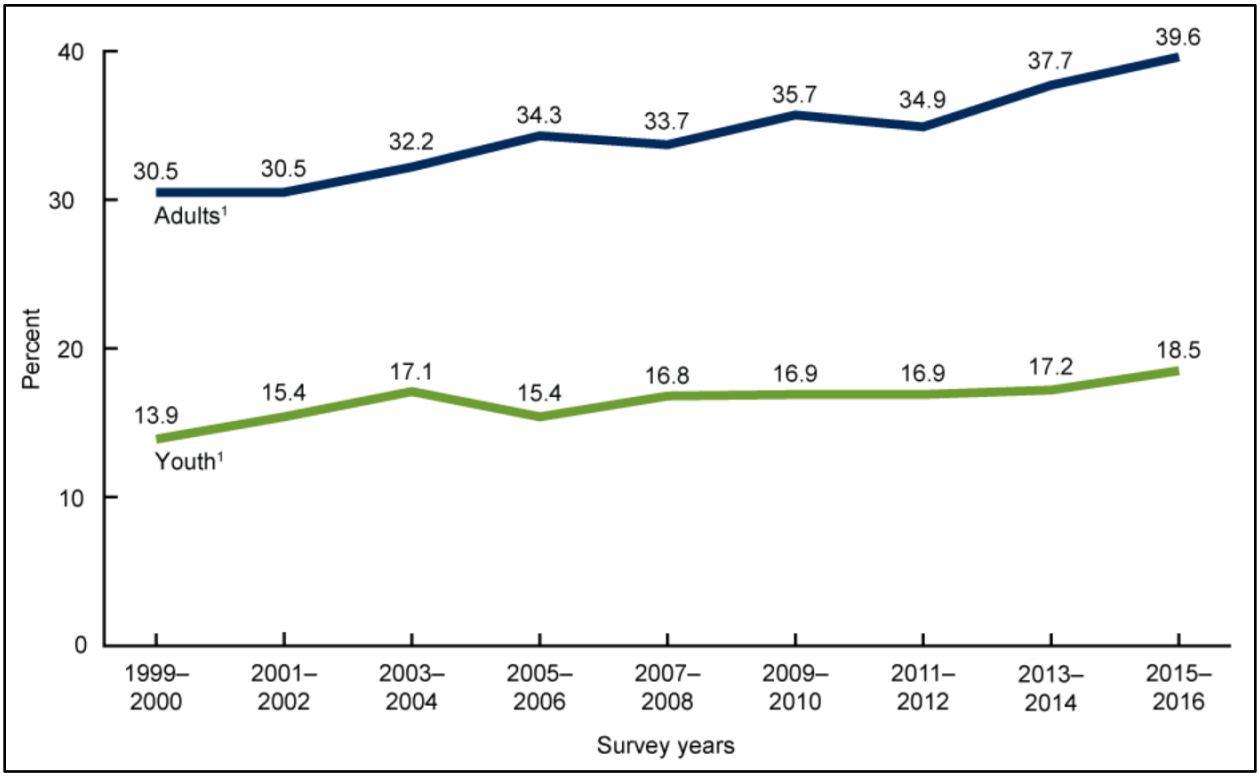

Figure 5: Obesity trends in the 21st century

Percent of American adults and youths with obesity between 1999-2016 [3].

3B. Adipose Tissue Dysfunction during Obesity

When the body has a positive energy balance, adipocytes expand to compensate for this until a threshold, usually around 0.7-0.8 μg/cell, is reached. At this point, cells start to secrete signals to induce proliferation and differentiation of surrounding progenitor cells [158]. This preference for hypertrophy manifests as an increase in adipocyte size, but not number, following several months of overnutrition in humans [159]. Additionally, stable isotope tracing of people exposed to nuclear weapons testing in the middle of the 20th century revealed that the number of adipocytes remains relatively constant after early adulthood, although obese individuals had an upward shift in their number of adipocytes [160]. This study also confirmed that weight loss results in decreased adipocyte volume [161; 162], but not a reduction in their number, meaning that once you acquire fat cells, you are not likely to lose them.

The expansion of adipose tissue by hypertrophy of the adipocytes can lead to problems as space is limited within the adipose tissue. Adipocyte hypertrophy creates physical constraints within the tissue as the adipocytes press up against the rigid extracellular matrix, which can lead to stress and inflammation [163]. This is exacerbated by the tendency of obese adipose tissue to become fibrotic [163]. The expansion of the adipocytes stresses themselves and the greater demand for protein synthesis and lipid processing and storage elicits ER stress [164]. Adipose expansion also strains the vasculature, which typically fails to expand enough to sufficiently supply oxygen and nutrients to the hypertrophic adipocytes [165]. These adipocytes can become hypoxic and hypoxia inducible factor 1a (HIF-1a) usually becomes activated in adipocytes during obesity [97]. It has been suggested that HIF-1a induces multiple changes in obese

adipocytes including inhibition of fatty acid oxidation by inactivating PGC1α [97], reducing adiponectin expression [166], and inducing inflammation and fibrosis [167].

3C. Global physiological changes during obesity

These changes in adipose biology during obesity create a set of organs that behave very differently than under normal physiological conditions. Three main changes in lipid metabolism, adipokine secretion, and inflammation in obese adipose tissues lead to disturbances in whole body metabolism and physiology. The changes in adipose lipid metabolism center around increased lipolysis and less oxidation within obese adipocytes, leading to more free fatty acids being released into the circulation [22]. These excess fatty acids are taken up into other organs that are not equipped to handle high lipid loads and are susceptible to lipotoxicty. This leads to ectopic lipid accumulation, which promotes the development of insulin resistance in the liver and muscles [168]. The loss of insulin signaling causes regulatory control over hepatic glucose production to be lost, which when coupled with the reduced glucose uptake into resistant skeletal muscles, leads to elevated blood glucose, known as hyperglycemia. Hyperglycemia stimulates the pancreas to secrete more insulin, as does the elevated circulating free fatty acids. This creates a short-lived “compensatory” phase of insulin resistance where the beta cells are maximally producing insulin to meet the body’s elevated demands. Eventually, the insulin-producing beta cells in the pancreas succumb to lipotoxicity and exhaustion from hyperproduction of insulin and the individual is no longer able to supply their body with the necessary insulin for proper blood glucose management [169]. This is how Type 2 Diabetes Mellitus develops.

In addition to the changes in lipid metabolism and free fatty acid release into the circulation, changes in the secretion of hormones called “adipokines” from adipose tissue

also contributes to the global metabolic dysfunction that occurs as a result of obesity. Under normal physiological conditions, leptin secreted from adipose tissue acts in the hypothalamus to restrict hunger and promote energy expenditure. However, the logical idea of treating obese patients with a hormone that limits food intake and boosts energy expenditure has only been mildly effective [170; 171]. This may be due to the elevated leptin secretion observed in the larger adipose tissues of obese patients [172]. It is believed that the increase leptin leads to leptin resistance, and results in the loss of the appetite-suppressing and metabolism-promoting effects. In fact, recent work by Phil Scherer's group has shown that reducing circulating leptin using genetic or neutralization approaches actually improves hypothalamic response and reduces weight gain by increasing energy expenditure and reducing food intake [173]. In addition to leptin, the secretion of the insulin-sensitizing hormone, adiponectin, is also modulated by obesity. Adiponectin secretion is paradoxically reduced during obesity, despite the increase in fat mass [174]. Since this adipokine has far-ranging effects that promote insulin sensitivity, this drop in circulating concentration contributes to the insulin resistance in the adipose tissue (autocrine/paracrine effects) and in other metabolic organs throughout the body [175]. Increases in secretion of RBP4 and resistin also contribute to global insulin resistance during obesity [113; 115].

In addition to the cytokines that adipocytes secrete to regulate metabolism, they also secrete inflammatory cytokines during obesity that alter adipose tissue physiology, as well as global metabolic homeostasis. Macrophages are recruited to the adipose tissue in an attempt to phagocytose and clear away dead and dying adipocytes. As the macrophages clear away adipocytes from obese adipose tissue, they shift from the anti-inflammatory M2 polarization to the pro-inflammatory M1 polarization [176; 177].

Similarly, the anti-inflammatory regulatory CD4+ Foxp3+ T cells present in lean adipose tissues shift to cytotoxic CD4+ and CD8+ T cells [178; 179]. This shift further pushes macrophage differentiation away from the M2 polarization [180], which correlates with the development of insulin resistance [181]. The macrophages which take on the M1 phenotype secrete pro-inflammatory cytokines like TNFα, which has long been shown to interrupt insulin signaling [182]. They also secrete MCP1, which reduces insulin sensitivity, alters adipocyte gene expression, and recruits more macrophages to the tissue [183]. These proinflammatory cytokines amplify the inflammation within the tissue, creating an environment of chronic inflammation that potentiates insulin resistance and metabolic dysfunction.

3C.1 Insulin Resistance

One of the main ways that these pathophysiological changes that occur during obesity manifest in metabolic dysfunction is through the development of insulin resistance. Insulin is a peptide hormone that pancreatic beta cells secrete in response to elevated blood glucose during the postprandial phase. This anabolic hormone has a multitude of effects including the promotion of glucose uptake and the synthesis of glycogen, lipids, and proteins, while inhibiting gluconeogenesis, lipolysis, and protein degradation [184]. Insulin induces these effects through a network of signaling pathways stemming from its receptor, which induces its insulin receptor tyrosine kinase activity upon binding to insulin. Following autophosphorylation, the tyrosine residues bind the insulin receptor substrate (IRS), which is phosphorylated by the insulin receptor. This phosphorylated IRS activates PI3K [185]. PI3K phosphorylates PIP2 to create PIP3, which recruits and activates Akt through PDK1. Activated Akt then phosphorylates several effectors like mTorc1, Foxo1, GSK3B, and PDE3B to bring about its effects on cell growth and survival [184].

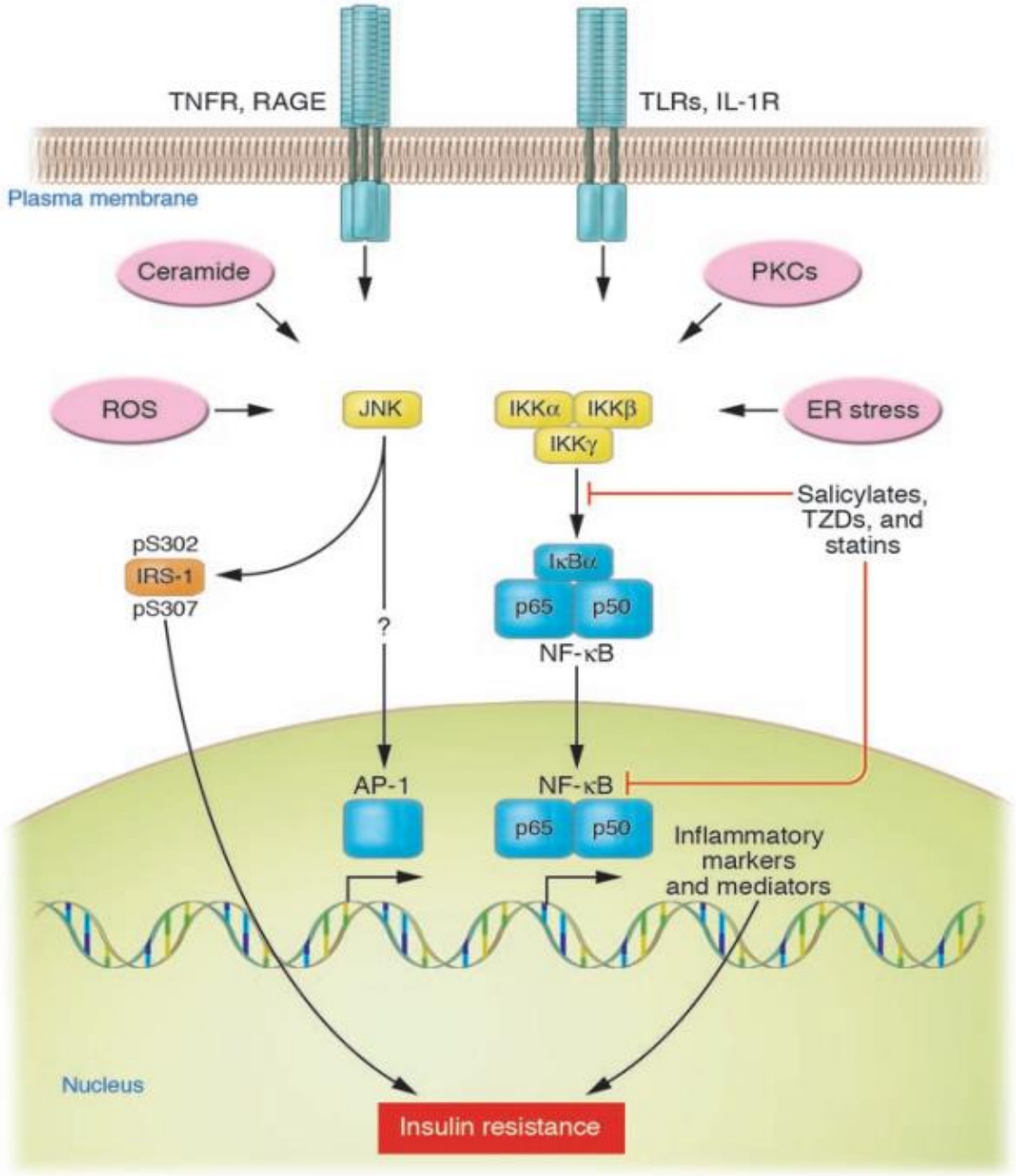

Figure 6: Mechanisms of insulin resistance

Diagram depicting changes in cell signaling that cause insulin resistance [6].

During obesity, this signaling can be disrupted by the presence of ER stress, ceramides, ROS, and inflammation (Fig 6) [6]. These pathological changes impact insulin signaling by activating JNK and the IKK/NF-κB pathway. JNK reduces insulin sensitivity by phosphorylating serine residues on the IRS, inhibiting its function. IKK activation leads to NF-κB translocation and the induction of inflammatory mediators that further amplify insulin resistance [6]. PKC also phosphorylates IRS serine residues, and has been shown to be activated by diacylglycerols, a metabolite produced by lipolysis [186]. Together, these changes manifest in a resistance to insulin signaling in metabolic tissues and a paradoxical selective insulin resistance in the livers of patients. Insulin inhibition of glucose production is lost but lipid synthesis is pushed higher by elevated insulin levels [187], although recent evidence suggests that lipid synthesis promotion by insulin is also impaired in humans [188].

4. Subcutaneous vs. Visceral Fat

4A. Differential contributions to metabolic dysfunction

Overall, the expansion of adipose tissue during obesity creates a pathophysiological state and contributes to the development of metabolic dysfunction; however, expansion of visceral and subcutaneous adipose tissues have different impacts on global metabolic homeostasis. The enlargement of visceral fat strongly correlates with the development of metabolic syndrome [189], whereas subcutaneous fat is seen as being more “metabolically protective” during obesity and individuals with more subcutaneous fat deposition are less likely to develop metabolic syndrome [190; 191]. Transplantation of subcutaneous fat into the visceral area of recipient mice improves insulin sensitivity and

glucose tolerance, while visceral fat transplantation did not produce beneficial effects [192; 193].

4B. Features Unique to Visceral Fat

There are several factors that are believed to cause the differential metabolic contributions of these white adipose tissues. Visceral fat is believed to contribute to metabolic dysfunction due to its more inflammatory nature [194], as well as its enhanced ability to mobilize fatty acids via lipolysis [42]. It is also associated with ectopic fat accumulation in other metabolic organs [195] as well as reduced secretion of the insulin-sensitizing hormone adiponectin, despite expansion of the tissue during obesity [196]. These changes in visceral adipose biology may have outsized effects on whole-body metabolism due to the visceral fat draining into the portal vein. It has been proposed that this system exposes the liver to elevated concentrations of fatty acids and cytokines, but the metabolic impact of this connection is still being evaluated[197].

Inflammation within the visceral fat plays an important role in the development of metabolic dysfunction. Not only does the visceral omental fat have more substantial macrophage infiltration compared to the subcutaneous fat in obese patients, but macrophage infiltration into the omentum associated with liver dysfunction, while subcutaneous fat infiltration did not [198]. The visceral adipose tissue also contains higher abundances of pro-inflammatory cytokines like TNFα, MCP1, IFNγ, and interleukins [199] and the obese murine visceral fat has larger populations of IFNγ-producing CD4+ T cells. The proportion of Foxp3+ anti-inflammatory T cells lowered by 70% compared to lean VAT. While the subcutaneous fat from these mice still had a (smaller) increase in the number of IFNγ-producing CD4+ T cells during obesity, Foxp3+ regulatory T cells accounted for the same proportion as in lean subcutaneous fat [179].

4C. Features Unique to Subcutaneous Fat

Subcutaneous fat is believed to be more protective because it has higher secretion of protective adipokines, like leptin and perhaps adiponectin, and it has more metabolic flexibility than visceral fat [196; 200]. Subcutaneous fat much more readily undergoes browning in response to cold or beta adrenergic stimulation [5]. Murine visceral fat is highly resistant to browning, even when Prdm16, a key driver of brown and beige adipocyte formation, is overexpressed [133]. Visceral fat browning capacity has been recently demonstrated, but has only been shown in a few select models [201-204].

In addition to these metabolic and secretory changes, the methods adipose tissues use to expand seem to contribute to their divergent behaviors during obesity. In response to chronic nutrient excess, preadipocytes proliferate and differentiate into new adipocytes to aid subcutaneous fat expansion, whereas intra-abdominal fat expands via adipocyte hypertrophy in humans [205]. Similar patterns are observed in upper and lower body subcutaneous fat, with upper body fat tending to expand via hypertrophy, and lower body fat expanding via hyperplasia [206]. These differences in preferred expansion mechanism may account for the finding that adipocyte death rates are drastically different between visceral and subcutaneous fat, with a report of up to 80% of epididymal adipocytes dying after mice spent four months on high-fat diet, but only 3% of inguinal adipocytes died during the same time period [207].

Differences in the preadipocytes within these two types of adipose tissue may explain this phenomenon. Preadipocytes within subcutaneous fat have higher expression of PPARγ and the C/EBP family of transcription factors that drive adipocyte formation [208]. Subcutaneous preadipocytes can proliferate, differentiate, and accumulate more lipid than differentiated preadipocytes from visceral fat [208]. Thus, the elevated PPARγ

and C/EBP transcription factors could contribute to the more plastic nature of subcutaneous fat and its ability to avoid hypertrophy during obesity.

4D. Cellular Mechanisms behind functional differences

Although the physiological reasons underpinning the divergent behaviors of visceral and subcutaneous fat have been described, the cellular mechanisms behind them have not been fully described. However, some cell autonomous features of visceral and subcutaneous adipocytes have been unearthed. For example, different expression of developmental patterning genes in isolated adipocytes and the stromal vascular fraction from subcutaneous and visceral fat suggests that these tissues have different developmental origins [209]. One of these developmental genes that have been studied is Short stature homeobox 2 (Shox2). It has much higher expression in subcutaneous adipocytes, especially in patients with central obesity. While it appears that developmental lineage may be responsible for the heterogeneity among white adipose tissues and fat distribution, further study is required to determine how these developmental differences manifest in the metabolic profiles of visceral and subcutaneous fat.

5. CREB3L3

5A. An Introduction

Cyclic-AMP responsive element-binding protein 3-like-3 (CREB3L3) is an endoplasmic reticulum (ER)-bound transcription factor from the cyclic-AMP response element-binding protein (CREB) family of transcription factors that binds to DNA via a basic leucine zipper domain. CREB3L3 has been previously described in the literature as being a liver-specific gene, and has even been termed CREB hepatocyte specific (CREBH). In addition to

CREB3L3 mRNA being highly expressed in the liver [1; 210], it has also been shown to be present in the ileum, and to a lesser extent, in the stomach and duodenum (Fig 7B) [2].

What separates this transcription factor from canonical CREB is the presence of a transmembrane domain located that tethers the protein to the endoplasmic reticulum (ER) membrane. When this transcription factor was first cloned, four key structural features that were identified (Fig 7A) [210]. (1) Protein database homology searches showed that the b-Zip domain of CREB3L3 features strong homology to the known b-Zip transcription factors BBF-2 in drosophila, CREB3/LZIP in humans, and OASIS in mice, with CREB3L3 having 71, 84, and 69% homology to these factors, respectively. (2) A second leucine zipper motif containing three 'LXNXTXX' repeats was found in the C-terminal in addition to the b-Zip domain. (3) A string of 17 amino acids that could potentially make up a hydrophobic transmembrane domain. (4) A short sequence of 'GDEL' at sites 458-461 that could make up a KDEL-like sequence and function to traffic CREB3L3 to the ER membrane following synthesis [211].

5B. Expression

There are numerous stimuli that alter the expression of CREB3L3 in studies performed in the liver. One of the earliest identified regulators of CREB3L3 expression in the liver was HNF4a, but ablation of this transcription factor in the small intestine did not alter CREB3L3 expression [2]. The inflammatory cytokines IL6, IL1β, and TNFα were also shown to induce hepatocyte expression of CREB3L3 [1]. ER stress is known to induce activation of this factor, but there is no clear consensus as to whether ER stress induces expression of CREB3L3 [1; 212], and there is *ex vivo* evidence that ER stress induction does not alter CREB3L3 expression in primary hepatocytes [213].

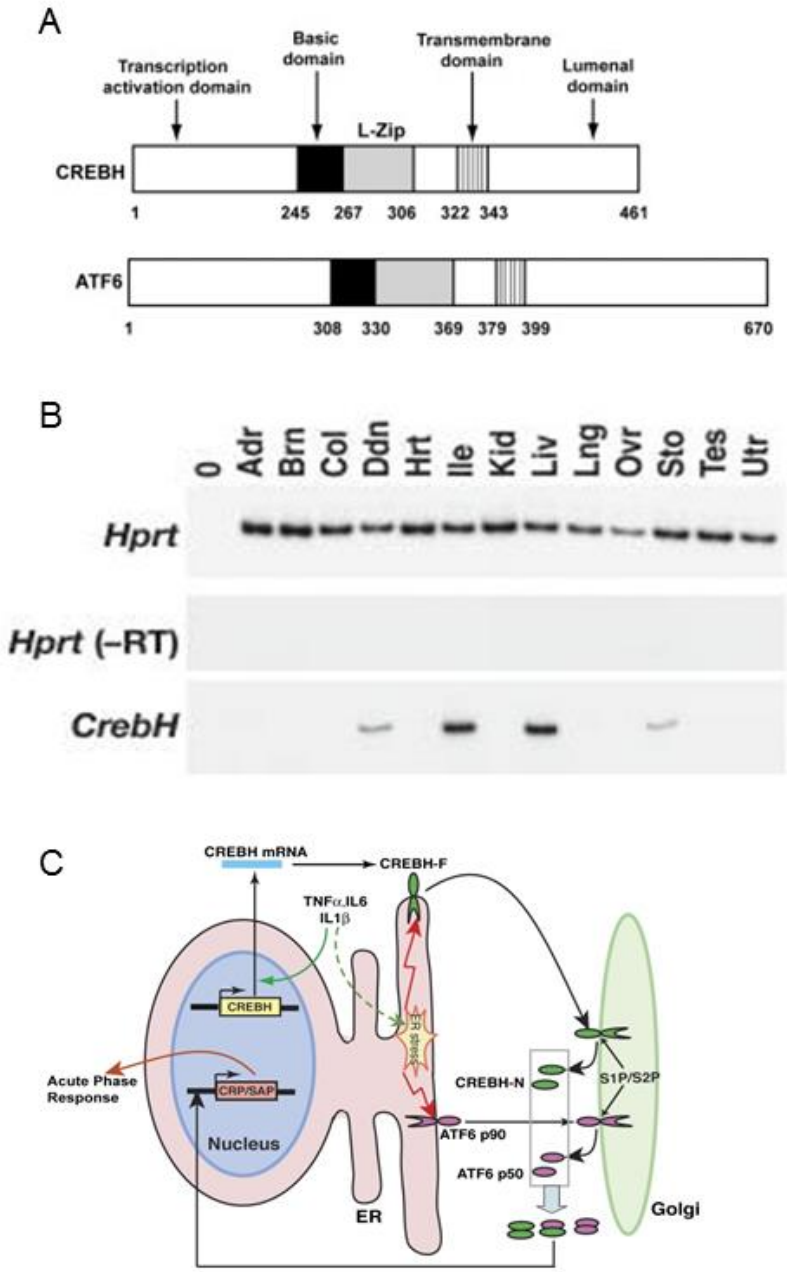

Figure 7: CREB3L3 expression is limited to the liver and GI tract

(A) Structure of CREB3L3 [1].

(B) Northern blot showing expression of CREB3L3 in various tissues [2].

(C) Diagram depicting activation of CREB3L3. CREB3L3 is tethered to ER membrane and is trafficked to Golgi where it is cleaved by site-1 and 2 proteases. The transcription activation domain is then able to transclocate to the nucleus [1].

Metabolic stimuli also play a key role in the regulation of CREB3L3 expression. Glucagon stimulation of PKA signaling during fasting induces CREB3L3 expression, while glucocorticoid receptors bind directly to the glucocorticoid response element within the CREB3L3 promoter to induce expression of this transcription factor [214]. Fasting itself has been shown to induce CREB3L3 expression, and while treatment of HepG2 cells with palmitate, oleic, and eicosapentanoic acid increased CREB3L3 expression [215], primary hepatocytes did not have a significant increase in CREB3L3 message following palmitate stimulation [213]. PPARα could also play a role in the expression of CREB3L3 in response to fasting, as treatment of HepG2 cells with PPARα agonists fenofibrate, Wy14643, and pemafibrate has increased hepatic CREB3L3 expression [215-217]. To this end, the CREB3L3 promoter has a PPRE site, and it has been proposed that PPARα and CREB3L3 create a mutual autoregulatory loop [215]. In addition to being induced by fasting, insulin has been shown to suppress hepatic CREB3L3 expression in the fed state [218]. To summarize, there is a complex network of factors that regulate the expression of CREB3L3 in the liver, with inflammation and fasting/refeeding standing as central factors in the transcriptional regulation of this protein.

5C. Regulation

The presence of the transmembrane domain that localizes the full length protein to the ER membrane means that the regulation of CREB3L3's activity is not driven by phosphorylation like other CREB transcription factors. Instead, its activity is regulated by the cleavage of the peptide, which releases the transcription activation domain to translocate to the nucleus (Fig 7C) [1]. ER stress occurs when unfolded or misfolded proteins accumulate within the ER lumen. This triggers the signaling pathways known as

the unfolded protein response (UPR), which attempt to clear the peptides from the ER lumen. In response to ER stress, fasting/elevated free fatty acids, insulin, and atherogenic high-fat diet, CREB3L3 is trafficked to the Golgi via COPII vesicles (Fig 7C) [219]. While TNFα and IL6 increased the mRNA expression of CREB3L3, they did not increase the *in vitro* abundance of the cleaved form of CREB3L3 in H2.35 cells [1]. However, *in vivo* co-injection of IL6 or IL-1B resulted in increased cleaved CREB3L3 in the liver [1].

Once in the Golgi, CREB3L3 is cleaved by site 1 and 2 proteases. This cleavage releases the N-terminus, allowing it to translocate to the nucleus and induce transcription (Fig 7C) [1]. In addition to ER stress, there are other mechanisms that regulate the activity of this transcription factor. CREB3L3 activation is also controlled by the circadian regulator BMAL in the liver. BMAL activates Akt, which phosphorylates GSK3β, which in turn phosphorylates CREB3L3, preventing it from complexing with COPII vesicles proteins and being transported to the Golgi for activation [219]. While there is not much change in the expression of hepatic CREB3L3 message during a 24-hour cycle, this circadian regulation leads to more CREB3L3 present in the nucleus during the light cycle than when the mouse is in the dark [219]. This allows the CREB3L3 to induce expression of genes that promote lipolysis, which contributes to the release of fatty acids from the liver during the light cycle when mice are typically inactive and fasting.

In addition to phosphorylation by GSK3β, there are additional post-translational modifications that regulate the activity of CREB3L3. It has been shown that CREB3L3 is ubiquitinated by the Sel1L-Hrd1 ER-associated degradation complex which targets it for degradation, especially during the fed state, when the abundance of Se1L and Hrd1 is higher. Ablation of Sel1L led to a drastic increase in the amount of active CREB3L3 in the nucleus, which led to increased FGF21 in the circulation [220]. In response to fasting or

glucagon stimulation, CREB3L3 is acetylated on its lysine 294 residue, which was required for the interaction of this transcription factor with PPARα [221].

5D. Role in Inflammation

One of the first functions of CREB3L3 to be identified was its contributions to inflammation within the liver via induction of acute phase response proteins. Luciferase studies using overexpression of the N-terminal of CREB3L3 show that this transcription factor induced expression of the promoters of acute phase proteins CRP and SAP, and the full-length CREB3L3 only did in response to ER stress [1]. The ablation of CREB3L3 abrogated the ability of hepatocytes to induce expression of these genes in response to ER-stress [2]. CREB3L3 has also been shown to induce expression of the iron-regulating hormone hepcidin, which is thought to limit iron availability for foreign microorganisms [222]. Feeding CREB3L3 global KO mice an atherogenic high-fat diet increased the expression of the proinflammatory cytokines TNFa and IL6 in the liver, although this could be a response to the steatosis occurring in this model [213]. Lastly, CREB3L3 has also been shown to contribute to osteoclast differentiation via induction of the master regulator of osteoclastogenesis, NFATc1, after being activated by RANKL [223].

5E. Role in Metabolism

CREB3L3 plays a variety of roles in metabolism, and has been established as an important regulator of energy homeostasis. Clinically, patients with hypertriglyceridemia have a high propensity for mutations that render CREB3L3 nonfunctional [224-226]. This has been recapitulated in mouse models as CREB3L3 deficiency led to hypertriglyceridemia in mice due to reduced expression of the Lpl coactivators Apoc2, Apoa4, and Apoa5 and increased expression of the inhibitor Apoc3. This led to reduced Lpl activity and triglyceride clearance [224]. This was also found in CREB3L3 knockout

mice fed atherogenic high-fat (AHF) diet that had plasma rich with triglycerides and a milky appearance [213]. The mice from this study also developed hepatic steatosis. This may be due to the reduction in fatty acid oxidation markers and FGF21 in these mice [213]. CREB3L3 has been shown to complex with PPARα to induce transcription of the "starvation" hormone FGF21, usually during periods of fasting [216; 221]. Steatosis was also observed in CREB3L3 knockout mice in another group, and Fgf21 was also able to partially rescue the steatosis observed following AHF dietary treatment [221]. In addition to its role as a regulator of lipolysis and fatty acid oxidation, CREB3L3 has also been shown to inhibit lipogenesis in the liver via suppression of SREBP1c expression. It appeared to achieve this through induction of Insig2 in hepatocytes and was sufficient to prevent insulin-stimulated initiation of lipogenesis [218]. CREB3L3 also plays an important role in the lipid metabolism outside of the liver. CREB3L3 has been shown to reduce expression of Npc1l1 expression in the small intestine, which reduces the absorption of cholesterol and prevented hypercholesterolemia in CREB3L3 transgenic mice [227].

In addition to its role in lipid metabolism, CREB3L3 also contributes to glucose homeostasis in the liver. CREB3L3 induces expression of the gluconeogenic genes PEPCK and G6Pase in hepatocytes, and ablation of this transcription factor in the liver reduced blood glucose levels [214]. Additionally, CREB3L3 has also been shown to induce expression of the liver form of glycogen phosphorylase to increase glycogenolysis [228]. To summarize, CREB3L3 serves a vast array of regulatory roles in hepatic glucose and lipid metabolism.

6. Statement of Hypothesis and Aims

The ability to modulate body weight is a sorely needed therapy given the omnipresence of obesity. The heterogeneity of adipose tissues represent a substantial barrier for harnessing the potential of this tissue as a weight loss tool. We have identified that the transcription factor CREB3L3 is differentially regulated in visceral and subcutaneous adipose tissues, which could contribute to the poorly understood differences between these tissues. Given the important role of this transcription factor in hepatic lipid metabolism, we aimed to elucidate the role of this factor in adipose tissue metabolism, using our fat-specific knockout mouse in addition to creating a novel technique for subcutaneous fat-specific overexpression. *The central hypothesis of this thesis is that CREB3L3 is present in adipocytes and its activity in these cells contributes to body weight regulation and global metabolic homeostasis.* To test this hypothesis the following aims were explored:

Specific Aim 1: Confirm adipose CREB3L3 expression and characterize effects of its ablation. Previous works neglected to measure the adipose expression of CREB3L3, as this key lipid metabolism regulator has been assumed to be liver-specific. In this aim, we measured the expression of CREB3L3 in adipose tissue, created an adipocyte-specific knockout (fKO) of this factor, and performed metabolic phenotyping to investigate its role in adipose biology.

Specific Aim 2: Identify the molecular mechanisms by which CREB3L3 regulates body weight. We hypothesized that CREB3L3 ablation shifts lipid metabolism towards synthesis and storage, leading to the enhanced adiposity in the fKO mice during obesity.

In this aim we performed functional analysis to determine why CREB3L3 ablation produced larger adipose tissues. Lastly, we overexpressed CREB3L3 in subcutaneous fat to further examine the role CREB3L3 plays in adipose metabolism and global energy balance.

II. Materials and Methods

1. Animal handling

Animal protocols were approved by the University of Illinois at Chicago Animal Care and Use Committee (IACUC). Institutional guidelines for care were followed. Mice were housed at environmentally controlled conditions including a 12 hour light/dark cycle with *ad libitum* feeding of a standard rodent chow diet and water. Changes in diet or environmental temperature are specified. Adiponectin-Cre, C57BL/6J, and *ob/ob* mice were acquired from Jackson Laboratories (Bar Harbor, ME, USA). Adiponectin-Cre mice used in this study were on a C57BL/6J background, and the CREB3L3 floxed mice were on a mixed (129Sv/CD-1) background.

2. Human subjects

In a cross-sectional study of 636 individuals (433 women, 203 men; BMI range: 14.7 – 88.8 kg/m², age range: 18-90 years), we investigated CREB3L3 mRNA expression in paired abdominal omental (Vis) and subcutaneous (SC) adipose tissue samples. The samples were harvested while elective laparoscopic abdominal surgery was performed, as described previously [27]. The samples were flash frozen in liquid nitrogen and stored at -80 degrees Celsius. This project received approval by the Ethics Committee of the University of Leipzig (approval no: 159-12-21052012) and followed the guidelines set in the declaration of Helsinki. All subjects gave written informed consent before taking part in this study.

3. RNA isolation and real-time qPCR

Total RNA was isolated from tissues and mature adipocytes using Trizol reagent (Invitrogen, Carlsbad, CA, USA) and the Direct-zol Kit (Zymo, Irvine, CA, USA). Tissue samples were homogenized using the Bead Blaster 24 homogenizer (Benchmark) at the

following settings: Power: 5 m/s, Time: 30 sec, 2 cycles. The homogenized tissue was then centrifuged at 4°C for 10 min. 350μL of the pink Trizol layer was removed, taking care not to disturb any white lipid layer that may have formed in more lipid-rich samples. An equal volume of ethanol was added to this Trizol homogenate, and the mixture was loaded onto a Direct-zol column. Isolation was then performed following the manufacturer's instructions. The concentration and integrity of the resultant RNA samples was measured with the Nanodrop ND-1000 spectrophotometer (Thermo Fisher Scientific, Waltham, MA, USA). 2μg of total RNA was used to generate cDNA using the High Capacity cDNA Reverse Transcription Kit (Invitrogen, Carlsbad, CA, USA) with random hexamer primers, following the manufacturer's instructions. The resultant cDNA was diluted to a concentration of 10ng/uL and 1.67uL was aliquoted for each 6.67uL real-time quantitative polymerase chain reaction (qPCR) (SYBR Green, Bio-Rad, Hercules, CA, USA). Reactions contained primers (Integrated DNA Technologies, Coralville, IA, USA) at a concentration of 300nM each, and 600nM for UCP1 in white adipose tissue. PCR reactions were run in duplicate and quantitated using the ViiATM7 Real-Time PCR system (Applied Biosystems, Foster City, CA, USA). Results were normalized to Beta-actin (B-actin), Ribosomal protein L19 (L-19), or TATA box binding protein (TBP) and expressed as arbitrary units (a.u.) or fold change over controls. Sequences for each primer set are listed in Table 1.

4. Human real-time qPCR

RNA was extracted from human adipose tissue samples using the RNeasy Lipid tissue Mini Kit (Qiagen, Hilden, Germany). RNA integrity and quantity was measured using the NanoVue Plus Spectrophotometer (GE Healthcare, Freiburg, Germany). From the resultant RNA samples, 1μg of RNA from SC and Vis adipose tissues was reverse

transcribed. The resultant cDNA was used for TaqMan-based qPCR reactions using the QuantStudio 6 Flex Real-Time PCR System (Life technologies, Darmstadt, Germany). CREB3L3 expression was determined using the standard curve method and was normalized to the housekeeping gene hypoxanthine guanine phosphoribosyltransferase 1 (HPRT1). The cDNA probes (Life technologies, Darmstadt, Germany) for CREB3L3 (Hs00261701_m1) and HPRT1 (Hs01003267_m1) were designed to span exon-exon boundaries to improve qPCR specificity.

TABLE 1 – QUANTITATIVE PCR PRIMERS

Gene name	Forward Sequence	Reverse Sequence
CREB3L3	GTGACGCTAGACAGAAACAGTAG	ACCTCCCAAAGATGCTGAAATA
CREB3L3 ORF	GAGAAGAAGCTGCTGGCTAAA	CCGGATCTTTCTGCGGATTT
Igfbp1	GCAGAGTGATGCTGCTTAGA	CTGTGTGAGACGATGAGGAAAT
Pparg1	CTGGCCTCCCTGATGAATAAAG	AGGCTCCATAAAGTCACCAAAG
Pparg2	TCGCTGATGCACTGCCTATG	GAGAGGTCCACAGAGCTGATT
Srebp1c	CCTCTGATCTCATGGCTCATAAC	CTAGGGAACTGTGTGTGTTTCT
Fasn	GCTGCGGAAACTTCAGGAAAT	AGAGACGTGTCACTCCTGGACTT
Fabp4	GATGCCTTTGTGGGAACCTG	CTGTCGTCTGCGGTGATTTC
PGC1a	GACAATCCCGAAGACACTACAG	AGAGAGGAGAGAGAGAGAGAGA
PGC1B	GGTGTTCGGTGAGATTGTAGAG	CTGAACACCGGAAGGTGATAAA
Cox8b	GAACCATGAAGCCAACGACT	GCGAAGTTCACAGTGGTTCC
Cpt1b	TGAGACCAGTCTTAGCCTCTAC	GGCCATTCTTGCAGGAGATAA
Acc1	TGTACAAGCAGTGTGGGCTGGCT	CCACATGGCCTGGCTTGGAGGG
Acc2	GAGGCCGAGAACACAAGAAA	CACCTTCTCTATGACCCTGTTG
Ppara	AAGACTACCTGCTACCGAAATG	AACATTGGGCCGGTTAAGA
Ucp1	CTGCCAGGACAGTACCCAAG	TCAGCTGTTCAAAGCACACA
Elovl3	TCCGCGTTCTCATGTAGGTCT	GGACCTGATGCAACCCTATGA
Cidea	ATCACAACTGGCCTGGTTACG	TACTACCCGGTGTCCATTTCT
Cyc1	GCTACCCATGGTCTCATCGT	CATCATCATTAGGGCCATCC
Tfam	GTCCATAGGCACCGTATTGCG	CCCATGCTGGAAAAACACTTCG
Adrb3	GCTCTGTGTCTCTGGTTAGTTT	GTCCAAGATGGTGCTTAGAGAG
Prdm16	CAGCACGGTGAAGCCATTC	GCGTGCATCCGCTTGTG
F4/80	TTTCCTCGCCTGCTTCTTC	CCCCGTCTCTGTATTCAAC
Ccl2/MCP1	CCACTCACCTGCTGCTACTCAT	TGGTGATCCTCTTGTAGCTCTCC
IL-1b	TGGAGAGTGTGGATCCCAAGCAAT	TGTCCTGACCACTGTTGTTTCCCA
TNF-a	GCCTCTTCTCATTCCTGCTTGT	GGCCATTTGGGAACTTCTCAT
CD74	CCCAGAGAATCTGAAGCATCTTA	CAGGGAGTTCTTGCTCATCTC
Mif	CCAGAACCGCAACTACAGTAAG	GGCAGCGTTCATGTCGTAATA
Resistin	TCAACAAGAAGGAGCTGTGGGACA	ATGGCTTCATCGATGGGACACAGT
Rbp4	ACCTTCTCTAGGTGGACATTAAAC	CATCTTTCAGGGACCTTCAGTAA
Leptin	CCTCATCAAGACCATTGTCACC	TCTCCAGGTCATTGGCTATCTG
Adiponectin	TGTTGCAAGCTCTCCTGTTCCTCT	CATCCAACCTGCACAAGTTCCCTT
Cxcl2/MIP-2	AGTTTGCCTTGACCCTGAAG	TCAGTTAGCCTTGCCTTTGT
Dio2	AAGGCTGCCGAATGTCAACGAATG	TGCTGGTTCAGACTCACCTTGGAA
Fgf21	GCTCTCTATGGATCGCCTCAC	GGTACACATTGTAACCGTCCTC
Chrebp	CACTCAGGGAATACACGCCTAC	ATCTTGGTCTTAGGGTCTTCAGG
Glut4	ACATACCTGACAGGGCAAGG	CGCCCTTAGTTGGTCAGAAG
Scd1	CCCTGCGGATCTTCCTTATC	TGTGTTTCTGAGAACTTGTGGTG
Scd2	CAGTCCCACTCTGACGATAATG	ACAGCTGGGTCCAGTAAGA
Elovl1	GAAAGGGCTGGACACTTACTT	CCTCTTCAGTGTGAGGAGAAAG
Elovl6	TCAGCAAAGCACCCGAAC	AGCGACCATGTCTTTGTAGGAG
Dhcr24	CGCCTGTCACTTGGAACATTAG	CCTAGCTACCACCTGGATCATT
Hsl	ACGGATACCGTAGTTTGGTGC	TCCAGAAGTGCACATCCAGGT
Atgl	TAGCTAACAGTTGGGCTTCAC	CAGAGAGAACAGAGCAGCTTAC
Lpl	CCCACAAGTGTAGTCGTCATT	AGGGCTAACATTCCAGCATATC
Plin1	ACTGAAGGGCACCATCTCTA	GGAGGAACTCTACCACCTTCT
Plin2	GGAGGAAAGACTGCCTATTCTG	GTGAGAGGGAAGTACTGGTCTA

5. Western blotting

Tissues were homogenized in radioimmunoprecipitate (RIPA) buffer with protease inhibitor (Sigma Aldrich, St. Louis, MO, USA) and phosphatase inhibitor cocktails 2 and 3 (Sigma Aldrich, St. Louis, MO, USA) using the bead blaster homogenizer . Protein concentration was measured using at the following settings: Power: 5 m/s, Time: 30 sec, 2 cycles. Next, the homogenized tissue was centrifuged at max speed at 4 degrees Celsius for 10 min. The supernatant was transferred to another tube. Due to the presence of a significant lipid layer in adipose tissues, particular care was taken to avoid transfer of this layer. To ensure protein samples purity, adipose tissue samples were spun down again and the lysate was transferred to a clean tube. Protein concentration was measured next to a BSA standard curve using Pierce BCA assay (Thermo Fisher Scientific, Waltham, MA, USA) and lysates were denatured by boiling for 10 minutes in Laemli buffer with 2-mercaptoethanol (Sigma Aldrich, St. Louis, MO, USA). 20-80 µg of protein was loaded onto 8-10% SDS-PAGE gels. Proteins were transferred onto nitrocellulose membranes (Amersham Biosciences, Little Chalfont, UK) and developed using multiple exposures to determine signal linearity. Antibodies used for immunoblotting are presented In Table 2.

TABLE 2 – WESTERN BLOT ANTIBODIES

Antibody	Provider	Dilution Used
CREB3L3	Kezhong Zhang, Wayne State University	1:1000
S473-pAkt	Cell Signaling	1:1000
pan Akt	Cell Signaling	1:1000
S660-pHSL	Cell Signaling	1:1000
HSL	Cell Signaling	1:1000
ATGL	Proteintech	1:1000
Perilipin	Cell Signaling	1:1000
Fasn	Cell Signaling	1:1000
SCD1	Proteintech	1:1000
β-actin	Proteintech	1:1000

6. Isolation of mature adipocytes and stromal vascular fraction

Mature adipocytes were isolated from inguinal and epididymal adipose tissue following digestion with collagenase Type 1 (2mg/mL Worthington Biochemical, Lakewood, NJ, USA). Following resection, adipose tissues were minced and incubated in a solution of collagenase diluted with KRBA (Krebs-Ringer Buffer w/ 3.5% BSA) in a shaking water bath at 37 degrees. Epididymal fat was incubated for 30 minutes and the inguinal fat was incubated for 45 minutes. The digested tissues were then centrifuged at 4 degrees for 5 minutes to pellet the stromal vascular fraction (SVF). Due to the low density of the lipids that predominate the contents of adipocytes, these cells float to the top of aqueous solutions. Using this phenomenon, a pipette bulb was used to remove the liquid and SVF below the mature adipocytes. The cells were washed with cold PBS and then frozen in Trizol for RNA isolation. For cell culturing, SVF was pipetted into a separate tube, washed with PBS and plated in DMEM complete media onto collagen (Rat Tail Collagen Type 1: Corning) coated dishes.

7. Adipocyte differentiation

The SVF was allowed to grow and was split onto 12-well plates before reaching confluence. The cells continued to proliferate on the new plate until confluence. Once confluent, the media was changed to fresh DMEM F12 media to induce mitotic clonal expansion [229]. Two days later, the cells were given an induction cocktail consisting of insulin (50nM), dexamethasone (2 μg/mL), indomethacin (0.125mM), IBMX (0.5mM), and T3 (100nM). This marks D0 of the differentiation process. On D2, D4, and D6 the cells were given a maintenance media consisting of insulin (50nM) and T3 (1nM). On D6 the differentiated adipocytes were treated with tunicamycin or vehicle solution for 24 hours.

8. ER stress induction

To induce ER stress, 10 week old C57BL/6j mice were injected with 2.5mg/kg tunicamycin or vehicle for 6, 12, or 18 hours. Additionally, 6 week old C57BL/6j mice were fed a high-fat diet for 12 weeks to induce ER stress. The mice were then injected twice daily with vehicle or 250mg/kg of the ER chaperone tauroursodeoxycholic acid (TUDCA) for 15 days to ameliorate ER stress. The iWAT and eWAT were harvested to measure CREB3L3 expression using qPCR.

9. Generation of CREB3L3 fat-specific knockout mouse model

CREB3L3 floxed mice were rederived from frozen embryonic stem cells received from Stephen Duncan [2]. These mice were crossed with Adiponectin-Cre mice on a C57BL/6j background to generate a fat-specific knockout (fKO) of CREB3L3.

10. Body and tissue weight studies

During diet-induced obesity studies, mice were fed chow diet (17% fat, 25% protein and 58% carbohydrate by kcal; #7012, Envigo, Indianapolis, Indiana, USA) until 6 weeks of age. At this time, the mice were placed on high-fat diet (60% fat, 20% protein, and 20% carbohydrate by kcal; D12492, Research Diets, New Brunswick, NJ, USA) for the remainder of the experiment. Body weight was measured weekly until 16 weeks of age. For the measurement of body weight at thermoneutrality, the mice were housed in an environmental chamber (Powers Scientific, Pipersville, PA, USA) at 30 degrees Celsius for the duration of high-fat feeding.

11. Tolerance tests

Blood glucose was measured using an automated glucose monitor (Glucometer Elite, Bayer, Bayer AG, Leverkusen, Germany). Tolerance tests were performed as described previously [43]. Briefly, mice underwent a 16h overnight or 2h morning fast, before the

glucose (IPGTT) and insulin (IPITT) tolerance tests, respectively. During experiments with fKO mice, mice were injected intraperitoneally (IP) with a bolus of 2g/kg dextrose (Hospira, Lake Forest, IL, USA) for IPGTT or 1.5U/kg insulin (Eli Lilly, Indianapolis, IN, USA) for IPITT. During our overexpression studies, 1U/kg insulin was used for IPITT.

12. ELISA and multiplex

Enzyme-linked immunosorbent assays (ELISA) were performed to measure the fed and fasting plasma concentrations of insulin (Crystal Chem USA, Elk Grove, IL, USA), and adiponectin (RayBiotech Life, Peachtree Corners, GA, USA) following high-fat feeding. High-fat fed plasma concentrations of leptin and MIP-2 were measured via magnetic luminex assay (R&D Systems Inc., Minneapolis, MN, USA).

13. Food intake, energy expenditure, physical activity, and body composition

Food intake, oxygen consumption, carbon dioxide production, energy expenditure, and physical activity were measured using the Promethion System (Sable Systems International, Las Vegas, NV, USA). The energy expenditure was normalized to lean body mass. The respiratory exchange ratio (RER) was calculated using the VCO2/VO2 ratio from the gas exchange data. Body composition (lean and fat mass) was estimated using NMR (Bruker minispec LF50, Billerica, MA, USA).

14. Insulin stimulation

For the insulin stimulation assay, high-fat diet fed mice were fasted overnight for 16h before IP injection of PBS (baseline) or 1U insulin. Tissues were quickly harvested five minutes after injection and flash frozen in liquid nitrogen. Western blotting was performed to quantify the level of Akt phosphorylation in the liver and eWAT.

15. Measurement of mouse lipid and ketone body contents

Lipids were extracted from liver samples using Folch solution composed of a 2:1 (vol/vol) mixture of chloroform/methanol as described previously [42]. Lipids were solubilized in 10% Triton X-100 before evaporation. Non-esterified fatty acid (Fujifilm/Wako, Lexington, MA, USA), cholesterol (Stanbio, Boerne, TX, USA), and triglyceride content (Stanbio, Boerne, TX, USA) were measured in hepatic extracts and 3-hydroxybutyrate concentration (Fujifilm/Wako, Lexington, MA, USA) was measured in fasting plasma samples using colorimetric assays.

16. Histological analyses

For histological analyses, mice were sacrificed and tissues were excised, weighed, and processed for immunohistochemistry as described previously [44]. White adipose tissues were fixed for 48h in formalin and immediately processed, while liver and brown adipose tissues were fixed for 24h in formalin. Tissues were sectioned by the Human Tissue Resource Center (University of Chicago, Chicago, IL, USA). Representative images were taken from H&E-stained liver, eWAT, and brown fat tissue sections using the Zeiss Observer Z1 (Zeiss, Oberkochen, Germany) microscope. For quantification of crown-like structures within obese eWAT sections, the observer was blinded and counted the number of crown-like structures within each field of view. Images were grouped by genotype and analyzed using student's T-test [53].

17. Adipocyte area quantification

Tissue sections from eWAT were stained with anti-caveolin-1 antibody (1:200 dilution in normal goat serum; Abcam, Cambridge, United Kingdom) after antigen retrieval. Alexa Fluor 488-conjugated goat anti-rabbit secondary antibody (1:1000 dilution) was used to detect the bound caveolin. Images of the adipocyte outlines were taken. Adipocyte areas

were measured using a pipeline developed in CellProfiler [52]. Cell area frequencies were determined and graphed using GraphPad Prism 6 (Graphpad Software, San Diego, CA, USA).

18. RNA sequencing

Total RNA was isolated from epididymal white adipose tissues following high-fat feeding using Trizol reagent (Invitrogen, Carlsbad, CA, USA) and the Direct-zol Kit (Zymo, Irvine, CA, USA). Integrity of isolated RNA was determined using Tapestation 4200 (Agilent Technologies Santa Clara, CA, USA). Sequencing and library construction were performed by Novogene (Sacramento, CA, USA). Quality control consisted of determining the error distribution rate in illumina Casava 1.8 [45; 46] and the GC-content distribution. Library was mapped to mm10 as reference genome with STAR [47]. Reads were counted using FPKM (expected number of Fragments Per Kilobase of transcript sequence per Millions base pairs sequenced) [48]. Differentially expressed genes (DEGs) were obtained by performing one-way ANOVA (q value <0.05) and genes were filtered out for log2 fold change. Functional analysis was performed using the DAVID database [49; 50] and WebGestalt [51]. Heat maps were generated using the z-scores of the FPKM for each mouse for each gene in the most differentially expressed pathways (Mouse Genome Informatics).

19. Environmental and pharmacological stimulation of adipose browning

Mice were IP injected daily with 1mg/kg of the β3-adrenergic receptor agonist CL 316,243 (Tocris Bioscience, Minneapolis, MN, USA) or PBS (Corning, Corning, NY, USA) daily for 10 days, starting at 11 weeks of age. COLD To induce adipose browning using cold exposure, mice were housed in an environmental chamber (Powers Scientific, Pipersville, PA, USA) at 6 degrees for one week. To measure cold tolerance, a cold tolerance test

was performed using mice at 11-12 weeks of age. The mice were placed in the 4 degree cold room at hour 0, and their temperature was measured rectally every 2 hours using a Type T thermocouple probe (Digisense).

20. Lipolysis assays

To perform the *in vivo* lipolysis assay, mice fed a high-fat diet were fasted starting at 6am. The mice were injected with CL 316,243 to induce adipocyte lipolysis. Plasma sampled were collected one hour later. For the *ex vivo* lipolysis assay, 50-70mg eWAT and iWAT explants were harvested from mice in the fed state at 8:30am. The samples were incubated in KRBH (Krebs-Ringer Buffer with HEPES w/ 5% fatty acid free BSA) on ice for 1.5 hours, then minced with scissors for 20 seconds. The explants were then given 1mL warm KRBH with or without isoproterenol and placed on a slow shaker at 37 degrees. Samples were collected at 0, 1, 2, and 3 hour time points and non-esterified fatty acid concentrations from both assays were measured using colorimetric assay.

21. WAT CREB3L3 overexpression

To overexpress CREB3L3 in the white adipose tissues, adeno-associated virus (serotype 8, 4x10^11vg/mL, UIC Viral Core) encoding the processed form of CREB3L3 was injected directly into both the epididymal and inguinal fat pads of C57BL/6J mice at 9 weeks of age. Control mice were injected with an empty AAV vector. Each tissue received 5 injections of 5μL across the length of the tissue. The mice recovered from surgery for 10 days before being placed on high-fat diet for the remainder of the experiment.

22. iWAT overexpression of CREB3L3

To overexpress CREB3L3 in the subcutaneous adipose tissue, adeno-associated virus (serotype 8, 4x10^11vg/mL, Viral Core, Boston Children’s Hospital, Boston, MA, USA) encoding the inverted reading frame of the processed form of CREB3L3 flanked by both

loxP and lox 2272 sites was injected directly into both inguinal fat pads of Adiponectin-Cre mice and wild type littermates at 5wks of age. Each tissue received 8 injections of 3μL across the length of the tissue. The mice recovered from surgery for 10 days before being placed on high-fat diet for the remainder of the experiment. Body weight was measured weekly until 20 weeks of age and physiological experiments were performed.

23. Statistical Analyses

Results are shown as mean ± standard error of mean (SEM). Difference of means was calculated using unpaired two-tailed Student's t-test, with an α of 0.05. Gas exchange data from the metabolic cages were analyzed by two-way ANOVA. Sample sizes were determined using prior characterization experiments for the mouse models used for this study. Mice were randomized to treatment in a blinded manner when possible.

III. CREB3L3 is expressed in adipose tissue and selectively downregulated in obese subcutaneous fat

1. Introduction

Cyclic-AMP Responsive Element Binding Protein 3-like-3 (CREB3L3) is an endoplasmic reticulum (ER)-bound transcription factor, which features a transmembrane domain that tethers it to the ER membrane [210]. CREB3L3 is activated by various stimuli in the liver including ER stress, pro-inflammatory cytokines [1], fasting and fatty acids [213], and the circadian oscillator BMAL1 [219]. In response to these stimuli, CREB3L3 is trafficked to the Golgi. In the Golgi, CREB3L3 is cleaved by site-1 and 2 proteases. This releases the transcription activation domain, allowing it to translocate to the nucleus and induce transcription [1]. Previous works have shown that CREB3L3 promotes the transcription of genes involved in gluconeogenesis [214] and the acute phase response [1] in the liver, in addition to being an important regulator of lipid metabolism [230]. CREB3L3 has been shown to regulate several aspects of lipid metabolism in the liver by inducing expression of apolipoproteins [212; 224], FGF21 [221], genes involved in fatty acid oxidation [213], and suppresses de novo lipogenesis through inhibition of SREBP1c [218].

Previous works have all described the function of CREB3L3 within the liver. CREB3L3 has been described as having liver-specific expression [1; 2; 210], and has thus been termed hepatic CREB (CREBH) in the literature. However, these works neglected to measure the expression of CREB3L3 in the adipose tissues. Given the variety of roles that CREB3L3 plays in lipid metabolism in the liver, we sought to determine whether this transcription factor is present and plays a role in lipid metabolism in adipose tissue.

2. Results

A. Differential expression of CREB3L3 in obese white adipose tissues

In previous reports, our lab has identified multiple proteins that serve different functions in subcutaneous inguinal (iWAT) and visceral epididymal white adipose tissue (eWAT) [203; 231; 232]. As part of the data mining process for these studies, we identified the ER-bound transcription factor cyclic-AMP Responsive Element Binding Protein 3-like-3 (CREB3L3) as a protein differentially regulated in obese SAT and VAT. This phenomenon was observed in different cohorts of C57BL/6J mice that were fed a high-fat diet (HFD) for 12 weeks (Fig 8A). The mice at UIC and the Joslin Diabetes Center had been bred for several generations, meaning their microbiomes differed from the mice housed at Jackson Labs. We therefore conclude that microbiome, environment, and genetic drift have no influence on the changes in CREB3L3 expression in obese adipose tissue that we observed. Similarly, this differential downregulation of CREB3L3 was observed in the iWAT of *ob/ob* mice at three months of age (Fig 8B). A cohort of obese patients (BMI>30) were found to have a significant reduction in the CREB3L3 message present in their abdominal subcutaneous, but not omental fat, compared to lean patients (BMI<25) (Fig 8C).

B. CREB3L3 is expressed in adipose tissues

Since this transcription factor had been previously described as being specifically expressed in the liver and ileum [2], quantitative real-time PCR (qPCR) was performed using cDNA from various tissues from lean C57BL/6J mice to confirm the presence of CREB3L3 message within the adipose tissues under normal physiologic conditions (Fig 9A). CREB3L3 message was in high abundance in the liver and ileum but was also detected in several adipose tissues. CREB3L3 message was present in the brown

adipose tissue (BAT), iWAT, as well as the visceral eWAT, mesenteric, and retroperitoneal depots. The expression in adipose tissues was at levels similar to those observed in the stomach, which has been previously shown to express CREB3L3 [2]. In order to determine whether adipocytes express CREB3L3, mature adipocytes were isolated from the stromal vascular fraction (SVF), which contains fibroblasts, immune cells, pericytes, endothelial cells, and preadipocytes. The expression of CREB3L3 in these two cell populations was measured, and mature adipocytes and SVF were found to have similar contributions to the overall expression within white adipose tissues (Fig 9B).

To confirm our expression findings at the protein level, Western blotting was performed. CREB3L3 protein was detected in the iWAT, eWAT, BAT, and mesenteric fat, while lower abundance of the protein was found in the liver and stomach from the same mouse (Fig 9C). This represents the first reported CREB3L3 protein abundance data in various tissues and the relatively high expression of CREB3L3 in the liver did not translate to higher protein abundance. Since the abundance of protein in the liver does not match the higher mRNA expression, we included a fasting liver sample to demonstrate that the antibody could detect CREB3L3 in the liver. The abundance of CREB3L3 in the liver drops during the fed state [220]. Due to the higher abundance of CREB3L3, fasting liver samples were used as a positive control, along with iWAT from mice with adipose overexpression of CREB3L3. Additionally, the protein in the liver, as well as the brown and mesenteric fat samples, may be larger due to post-translational modifications, as the protein size in the iWAT and eWAT is closer to the expected protein size of 52 kD.

C. CREB3L3 is downregulated in adipose tissue in response to fasting

Interestingly, the expression of CREB3L3 in the adipose tissues during fasting is in opposition to that observed in the liver. In the liver, CREB3L3 message is upregulated in response to fasting. Here, we report that fasting induced a marked downregulation in the adipose tissue (Fig 10A). Additionally, we found that exposing mice to cold temperatures for one week to induce brown and beige fat activity had a limited effect on the expression of CREB3L3 in the BAT and iWAT, but did lead to a significant downregulation in the eWAT (Fig 10B).

D. ER stress modulates CREB3L3 expression during obesity

Obesity is known to induce ER stress [233], and in our investigation of the mechanism behind the differential expression of CREB3L3 during obesity, we observed that induction of ER stress mimicked the expression effects of obesity in adipocytes differentiated from iWAT and eWAT SVF (Fig 11A). Adipocytes differentiated from SVF isolated from these adipose tissues were treated with the ER stressor tunicamycin for 24 hours. These cells exhibited CREB3L3 upregulation in eWAT and downregulation in iWAT in response to ER stress. To determine whether ER stress modulates CREB3L3 expression *in vivo*, we stimulated mice with tunicamycin for up to 18 h. Interestingly, we observed that CREB3L3 was downregulated by ER stress in iWAT (Fig 11B). We have also observed that HFD induces a similar downregulation of CREB3L3 in iWAT (Fig. 8), and treatment of HFD-fed mice with the ER stress-inhibitor TUDCA returns CREB3L3 expression in iWAT and eWAT to levels observed in lean, CD-fed mice (Fig 11C). These results suggest that modulation of CREB3L3 in iWAT and eWAT is mediated by upregulation of ER stress in respective fat depots during obesity.

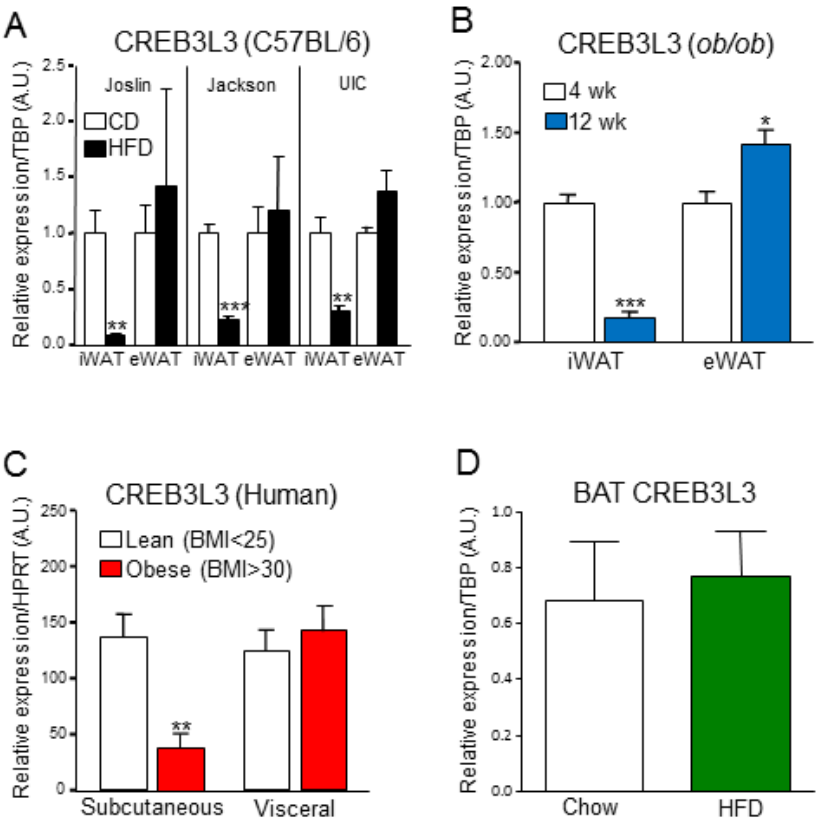

Figure 8: CREB3L3 is selectively downregulated in obese subcutaneous fat

(A-B) Quantitative PCR for CREB3L3 message in inguinal (iWAT) and epididymal (eWAT) white adipose tissue from (A) C57BL/6 mice fed a high-fat diet for 12 weeks at the indicated animal facility (n=6 mice per group) or (B) ob/ob mice before (4wk) and after (12wk) developing obesity (n=6 mice per group).

(C) Quantitative PCR for CREB3L3 message in subcutaneous abdominal and omental fat from patients with a BMI≤25kg/m² (lean, n=69) and BMI>30kg/m² (obese, n=504).

(D) Quantitative PCR for CREB3L3 message in brown adipose tissue from C57BL/6 mice fed a high-fat diet for 12 weeks (n=6 mice per group). Data presented as mean +/- SEM. The difference in means was analyzed using Student's t-test where *P<0.05, **P<0.01, and ***P<0.001.

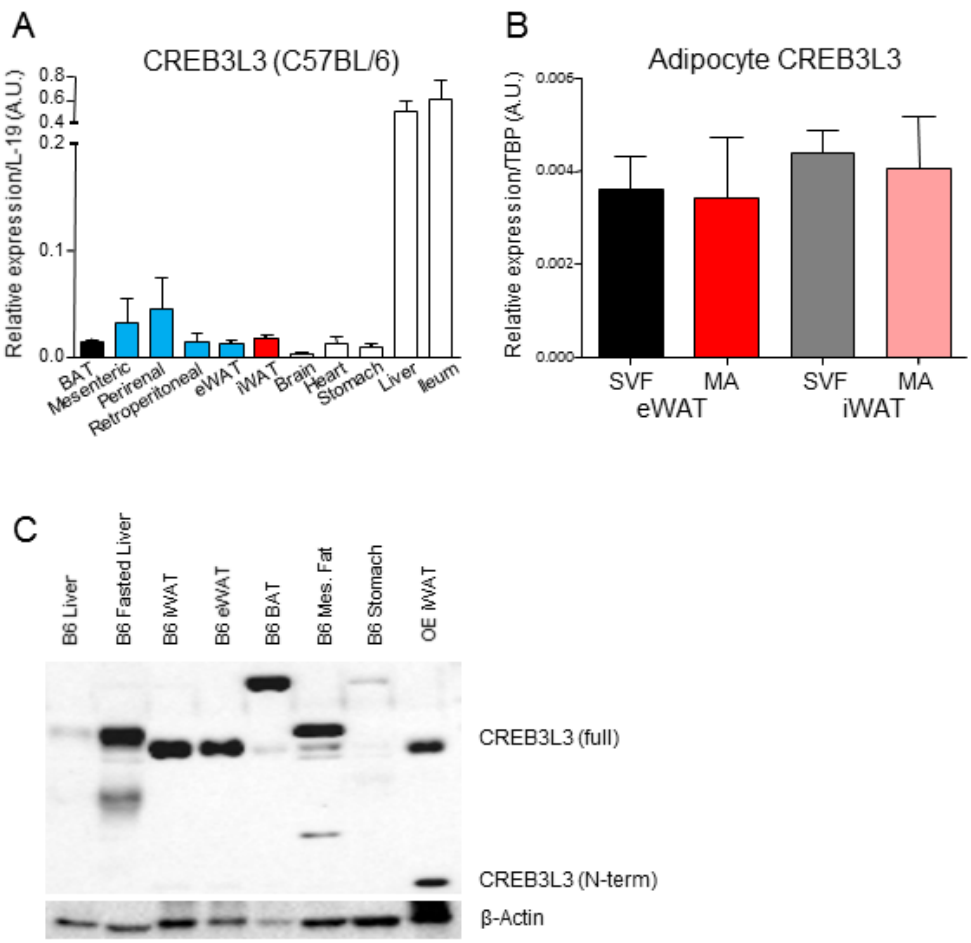

Figure 9: CREB3L3 is present in adipose tissues and adipocytes

(A) Quantitative PCR for CREB3L3 message in various tissues from lean C57BL/6 mice (n=3 mice).

(B) Quantitative PCR for CREB3L3 message in mature adipocytes (MA) and stromal vascular fraction (SVF) isolated from the eWAT and iWAT of lean C57BL/6 mice (n=4-6 mice per group).

(C) Western blot measuring abundance of CREB3L3 in various tissues from same lean C57BL/6 mouse, fasted C57BL/6 liver, or iWAT with forced overexpression of CREB3L3. Data presented as mean +/- SEM.

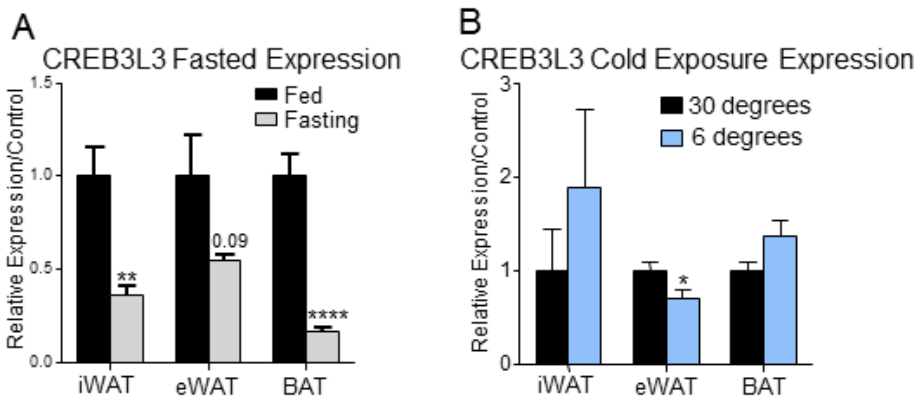

Figure 10: Fasting reduced CREB3L3 expression in adipose tissues

(A) Quantitative PCR for CREB3L3 message in iWAT, eWAT, and brown adipose tissue from C57BL/6 mice after 16h overnight fast (n=4-5 mice per group).

(B) Quantitative PCR for CREB3L3 message in iWAT, eWAT, and brown adipose tissue from C57BL/6 mice after 1wk at thermoneutrality or cold-exposure (n=5-7 mice per group). Data presented as mean +/- SEM. The difference in means was analyzed using Student's t-test where *P<0.05, **P<0.01, and ***P<0.001.

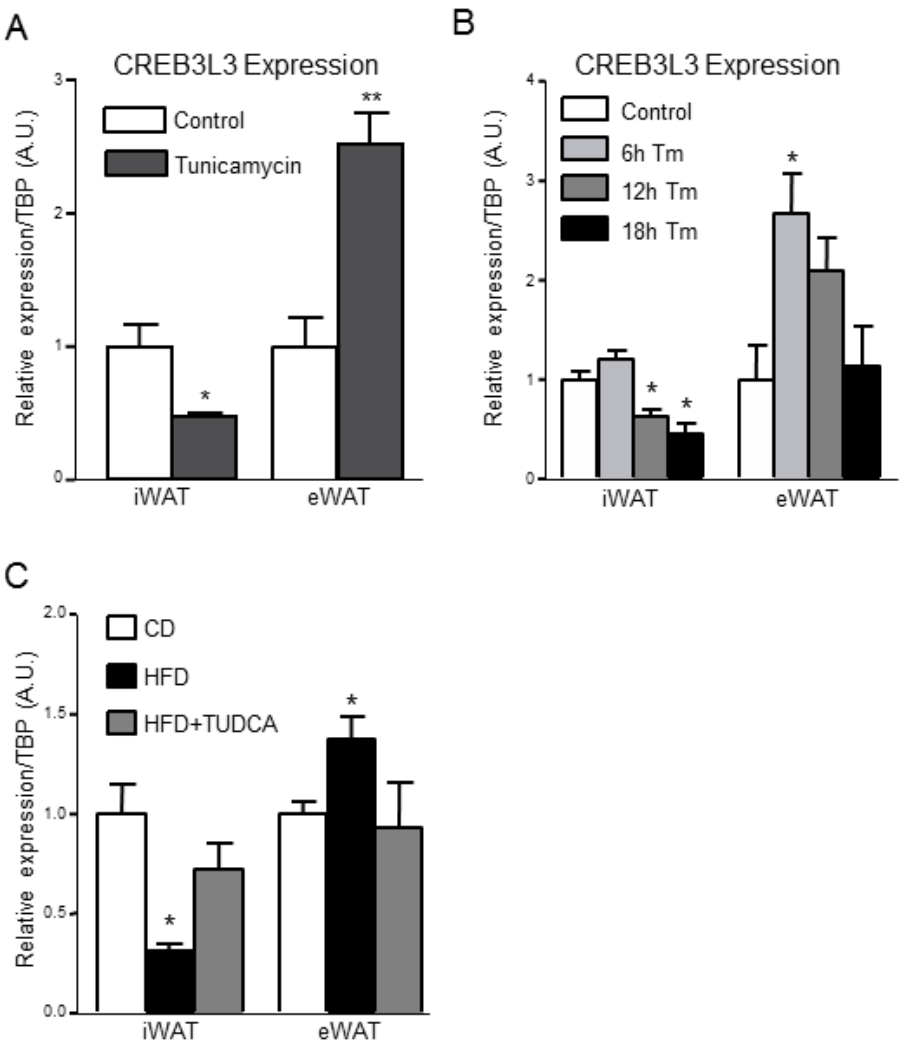

Figure 11: ER stress induces differential express of CREB3L3 during obesity
(A) Quantitative PCR for CREBL3 message in iWAT and eWAT adipocytes treated with tunicamycin (n=3).

(B) Quantitative PCR for CREBL3 message in iWAT and eWAT from mice treated with tunicamycin for various time points (n=5).

(C) Quantitative PCR for CREBL3 message in iWAT and eWAT from mice treated with CD, HFD, or HFD+TUDCA (n=5). Data presented as mean +/- SEM. *P<0.05, **P<0.01.

3. Discussion

Previous studies reported the expression of CREB3L3 in a variety of tissues, but did not examine the expression of this ER-bound transcription factor in adipose tissues. Here we report that CREB3L3 is not a liver-specific protein, and both CREB3L3 message and protein can be detected in the subcutaneous, brown, and multiple visceral adipose tissues. The abundance of CREB3L3 in these adipose tissues is much higher than in the liver, in addition to having different protein sizes (Fig 9C). The discrepancy between the liver RNA expression and protein abundance relative to other tissues could be due to the Sel1L-Hrd1-mediated degradation of CREB3L3 that occurs in the liver during the fed state. This complex is downregulated during fasting, and could be responsible for the smaller protein abundance in our fed liver samples.

The size of CREB3L3 appears different compared to the liver as well. While the mesenteric fat appears to have the same protein size as the liver, the iWAT and eWAT proteins were smaller and closer to the 52kD expected protein size. This may be due to the presence of post-translational modifications in the liver and mesenteric fat, or different splicing mechanisms occurring between the tissues. Similar differences could also account for the much larger protein size observed in the brown adipose tissue. Further study is needed to identify the structures of CREB3L3 within the adipose tissues.

In addition to being present in the adipose tissue, we also found that CREB3L3 is selectively downregulated in the subcutaneous fat during obesity, while the expression in the visceral fat is largely unchanged. By treating mice with the ER stressor tunicamycin, we determined that ER stress induces the same CREB3L3 expression pattern in iWAT and eWAT as obesity. We then demonstrated that ER stress is sufficient for the differential expression of CREB3L3 in the iWAT and eWAT during obesity by injecting the chaperone

protein TUDCA to ameliorate ER stress in mice fed a high-fat diet. We observed that the amelioration of ER stress returned expression of CREB3L3 to levels observed in lean mice. While we demonstrated that ER stress contributes to the differential expression of CREB3L3 during obesity, further studies are needed to identify the mechanism responsible for this phenomenon.

IV. Adipose ablation of CREB3L3 enhances diet-induced obesity and insulin resistance

1. Introduction

Previous studies have described the important role that CREB3L3 plays in lipid metabolism in the liver. This factor helps to transcriptionally regulate several processes in hepatocytes including lipolysis and triglyceride clearance [213; 224], fatty acid oxidation [213; 221], and *de novo* lipogenesis [218], in addition to contributing to the diurnal metabolic rhythms of mice [219; 228]. Despite the importance of adipose tissue in whole-body lipid metabolism, previous works did not measure the expression of this transcription factor in adipose tissues [1; 2; 234]. We report that CREB3L3 is not only present in adipose tissues (Fig 9A-C) and adipocytes (Fig 9B), but its expression is differentially regulated in adipose tissues during obesity (Fig 8A-C). We found that CREB3L3 is selectively downregulated in the subcutaneous fat during obesity, while the expression in the visceral fat is largely unchanged (Fig 8A-C). We therefore hypothesized that this downregulation of CREB3L3 in obese subcutaneous fat could contribute to the divergent metabolic profiles of subcutaneous and visceral fat during obesity.

2. Results

A. Adipose ablation of CREB3L3 enhances fat mass in mice fed a chow diet

To study the role of CREB3L3 in adipose biology, fat-specific knockout (fKO) mice were generated using adiponectin Cre mice [29; 106]. The specific knockout of CREB3L3 was confirmed by separating mature adipocytes from iWAT and eWAT in lean fKO and CREB3L3-floxed wildtype (WT) control mice (Fig 12A). Initial attempts to confirm the knockout using whole-adipose tissue RNA expression were unsuccessful (Fig 12B), perhaps due to the contributions of the SVF to adipose CREB3L3 expression (Fig 9B).

Our initial characterization of these mice revealed that adipose ablation of CREB3L3 did not alter body weight when the mice were fed a chow diet (Fig 13A), but did increase NMR-based fat mass (Fig 13B). Dissection of these mice revealed that there are slight, but not significant, increases in the size of the inguinal, epididymal, retroperitoneal, and mesenteric adipose tissues (Fig 13C). In contrast, the livers of the fKO mice were slightly smaller, suggesting that CREB3L3 ablation might enhance lipid storage in the adipose tissue, sequestering it from the liver. Despite the small changes in liver and adipose weights, and the increased fat mass, of the fKO mice, there were no changes to glucose homeostasis or insulin sensitivity, as measured by intraperitoneal (IP) glucose (Fig 13D) and insulin tolerance tests (Fig 13E). Despite no changes in insulin sensitivity, the fKO mice had a trend towards increasing circulating insulin during the fed state (Fig 13F).

To determine the physiological cause of the larger fat mass of the fKO mice, indirect calorimetry was measured. After acclimation to the cage system, the fKO mice had a slight increase in energy expenditure (Fig 14A), particularly during the dark cycles when mice are more active. The mice also had a significant decrease in their respiratory exchange ratio (RER) (Fig 14B), which is the ratio of CO2 produced to oxygen consumed and is a readout of the amount of carbohydrates (higher) and lipids (lower) that an animal is metabolizing. This downward shift during the daytime when mice mobilize and metabolize fats, suggests that ablation of CREB3L3 enhances the ability of adipocytes to mobilize fatty acids for oxidation via lipolysis. Additionally, the fKO mice were found to have no changes in activity (Fig 14C) or food intake (Fig 14D). Together, the phenotype of the fKO mice fed a chow diet was relatively mild, and is highlighted by higher energy expenditure, increased daytime lipid consumption, and enhanced fat mass.

B. CREB3L3 ablation promotes diet-induced obesity and insulin resistance

Based on the mild metabolic changes observed in the fKO mice fed chow diet, WT and fKO mice were placed on high-fat diet (HFD) to determine whether obesity would exacerbate the differences observed in fKO mice. Accordingly, when fKO mice were placed on HFD, they became significantly heavier than the WT controls after two weeks of high-fat feeding (Fig 15A). The changes in body weight are driven by significant enlargement of the iWAT and eWAT in the fKO mice (Fig 15B). The retroperitoneal and mesenteric fat also trends towards being larger in the fKO mice. Together, the fKO mice had a 60 percent increase in fat mass, while there were no changes in the lean mass (Fig 15C). Coinciding with their larger fat mass, the fKO mice fed a HFD have reduced insulin sensitivity, as evidenced by the upward shift in the 60 and 90 minute time points on the intraperitoneal (IP) insulin tolerance test (Fig 15D), which was associated with increased levels of plasma insulin in both the fed and fasted states (Fig 15F). Despite being more insulin resistant, fKO mice with diet-induced obesity show normal glucose clearance that suggests that beta cell function is not altered by fKO (Fig 15E).

In order to determine tissue-specific insulin sensitivity, we assessed insulin-mediated phosphorylation of AKT. Interestingly, insulin-mediated phosphorylation of AKT at the S473 residue was significantly reduced following insulin stimulation (Fig 16A-B), and the expression of insulin-like growth factor binding partner 1 was 4-fold higher in fKO livers (Fig 16C), indicative of hepatic insulin resistance [235]. Accordingly, the ability of insulin to promote de novo lipogenesis was increased as shown by the upregulation of Srebp1c, Acc1, Fasn, and Fabp4 (Fig 16D). [187]. Despite the dramatic upregulation of hepatic PPARγ (24-fold increase of Pparg2) (Fig 16D), and the well-known steatogenic

effect of PPARγ [236; 237]; 10 weeks of HFD did not significantly alter liver morphology (Fig 16E), or triglyceride, cholesterol, or non-esterified fatty acid contents (Fig 16F).

While the liver is a key contributor to insulin sensitivity [238], we also assessed the contributions of adipose tissue to the insulin resistance observed in the fKO mice (Fig 15D). Insulin-mediated phosphorylation of AKT was also reduced in the eWAT following insulin stimulation (Fig 17A-B). Adipocyte hypertrophy is known to induce metabolic changes in adipocytes, including promotion of insulin resistance [239]. To determine whether eWAT adipocytes lacking CREB3L3 become more hyperthrophic than WT cells during obesity, adipocyte areas were measured. The membrane of eWAT adipocytes was highlighted using a Caveolin-1 antibody and a pipeline in CellProfiler was used to measure the adipocyte areas (Fig 17C). Graphing the frequency distribution of these areas showed that there was no increase in the frequency of hypertrophic adipocytes in the fKO eWAT (Fig 17D), and is therefore unlikely to contribute to the insulin resistance observed.

C. CREB3L3 ablation enhances visceral inflammation during obesity

To decipher a potential cause of the insulin resistance in the fKO mice, RNA sequencing analysis was performed using whole-tissue RNA from the eWAT from WT and fKO mice following high-fat feeding. There were 728 genes that were differentially regulated. The vast majority (76%) of these differentially expressed genes were upregulated in the fKO eWAT (Fig 18A). Changes in gene expression were confirmed using qPCR (Fig 18B). The overwhelming majority (84%) of differentially expressed genes were downregulated in the fKO iWAT (Fig 18A). When gene ontology (GO) pathway analysis was performed with the iWAT dataset, it was determined that adaptive immune processes had the largest

decrease in gene expression. The most differentially expressed pathways were the adaptive immune response, leukocyte migration, and regulation of leukocyte activation (Fig 18C). However, these results could not be confirmed via qPCR (Fig 18D) and were not utilized for further investigation. When GO pathway analysis was performed with the validated eWAT dataset, it was determined that innate immune processes had the largest increase in gene expression. The processes with the largest fold increase in gene expression included myeloid leukocyte activation, phagocytosis, cell chemotaxis, leukocyte migration, positive regulation of response to external stimulus, cytokine-mediated signaling pathways, and positive regulation of cytokine production (Fig 18E).

To determine the extent of inflammation occurring in the fKO eWAT during obesity, the morphology of the tissue was analyzed. The eWAT from fKO mice had a significant increase in the number of crown-like structures (Fig 19A), which are formations of macrophages around apoptotic adipocytes. This result was confirmed by 4-fold higher expression of the macrophage marker F4/80 and upregulation of monocyte chemoattractant protein 1 (MCP1/Ccl2) in this tissue (Fig 19B). Along with the increase in macrophage infiltration, there was significant increase in the expression of the pro-inflammatory cytokine tumor necrosis factor alpha (TNFα), macrophage inflammatory protein 2 (MIP-2), and the macrophage migration inhibitory factor receptor CD74 (Fig 19B). In addition to increased expression of pro-inflammatory cytokines and macrophage markers, there was a reduction in the expression of the anti-inflammatory cytokines IL-4, IL-10, IL-12, IL-13, and IL-33, and reduced expression of Arginase 1, a marker of M2 macrophage polarization (Fig 19C).

Adipokine expression was also altered, as there was increased expression of leptin, which has pro-inflammatory effects [240] and reduced expression of the insulin-

sensitizing hormone adiponectin, which has anti-inflammatory effects [241] (Fig 19B). Measuring the plasma concentration of these adipokines revealed that these expression changes in the eWAT translate to systemic differences in leptin and adiponectin abundance, in addition to higher concentrations of macrophage inflammatory protein 2 (Fig 19D). Together, these results show that the eWAT from the fKO mice becomes more inflamed in the obese state, which contributes to the insulin resistance observed in the fKO mice.

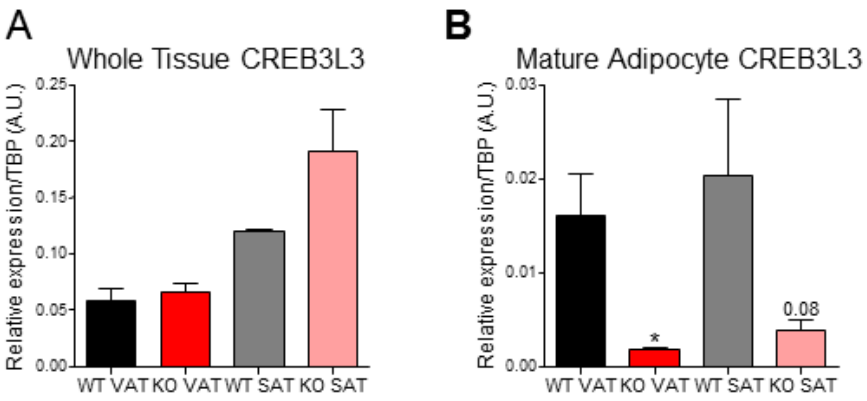

Figure 12: CREB3L3 is knocked out of mature adipocytes in the fKO mice
(A) Quantitative PCR for CREBL3 message in iWAT and eWAT from WT and KO mice (n=2-3 mice per group).

(B) Quantitative PCR for CREB3L3 message in mature adipocytes isolated from digested listed adipose tissues (n= 4-5 mice per group). Data presented as mean +/- SEM. The difference in means was analyzed using Student's t-test where *P<0.05.

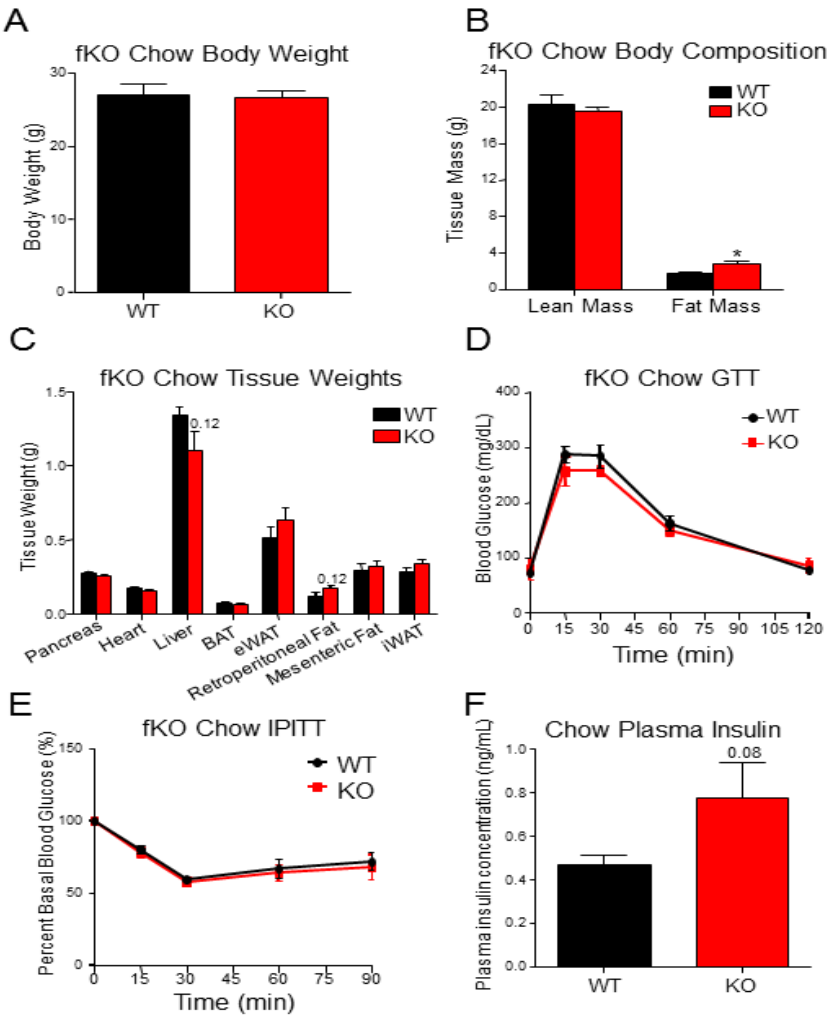

Figure 13: Chow-fed fKO mice have enhanced fat mass, but no change in body weight (A-B) (A) Body weight and (B) body composition NMR measurements of chow-fed CREB3L3 floxed (WT) and fat specific knockout (fKO) mice at 22 wks of age (n=7-9 mice per group).

(C) Tissue weight measurements for chow-fed (n=9 mice per group).

(D-E) Intraperitoneal (D) glucose and (E) insulin tolerance tests performed with chow-fed WT and fKO mice (n=9-10 mice per group).

(F) Fed and plasma insulin concentrations measured with ELISA (n=8 mice per group). Data presented as mean +/- SEM. The difference in means was analyzed using Student's t-test where *P<0.05.

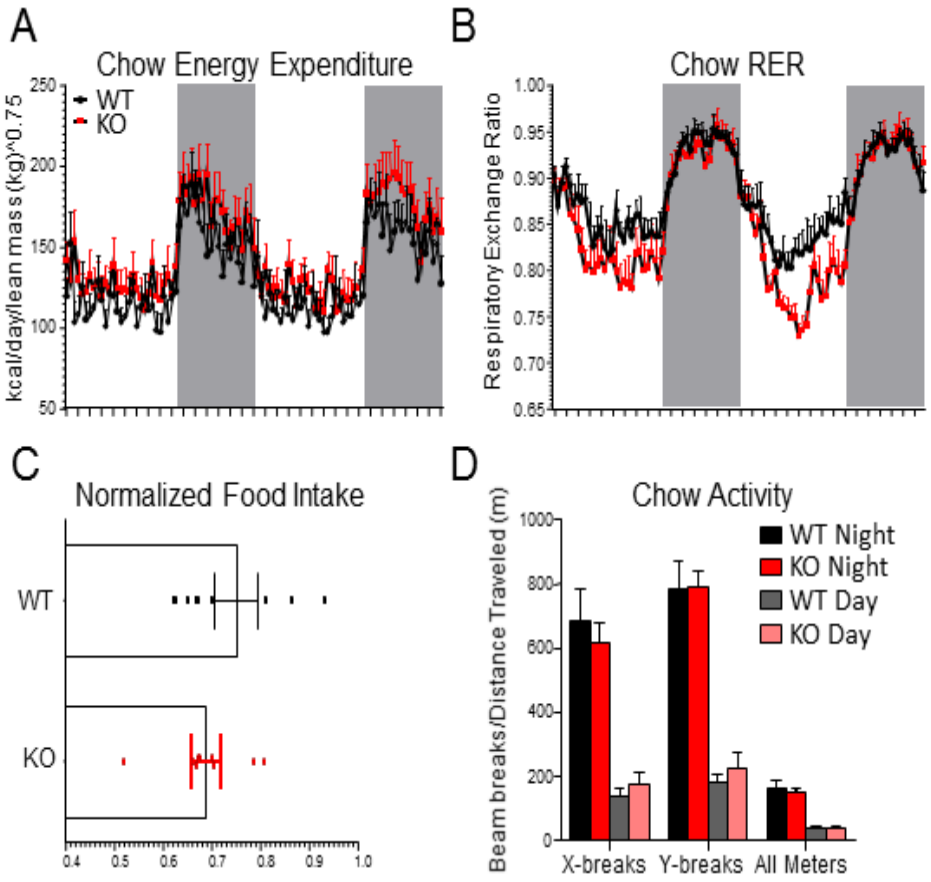

Figure 14: CREB3L3 ablation lowers RER in chow-fed mice

(A-B) Energy expenditure and (B) respiratory exchange ratios (RER) of WT and fKO mice fed chow diet (n=7-8 mice per group). Energy expenditure was normalized to the animal's lean mass. The curves for both measurements were analyzed using two-way ANOVA. P values for the column factor (genotype) for the energy expenditure and the RER were both <0.0001.

(C) Total consumption of chow diet while mice were in metabolic cages. Food intake was normalized to animal's body weight (n=5-8 mice per group).

(D) Activity measurements of WT and fKO mice fed chow diet. Data presented as x- and y-axis beam breaks and total movement per day following acclimation period (n=6-8 mice per group). Data presented as mean +/- SEM.

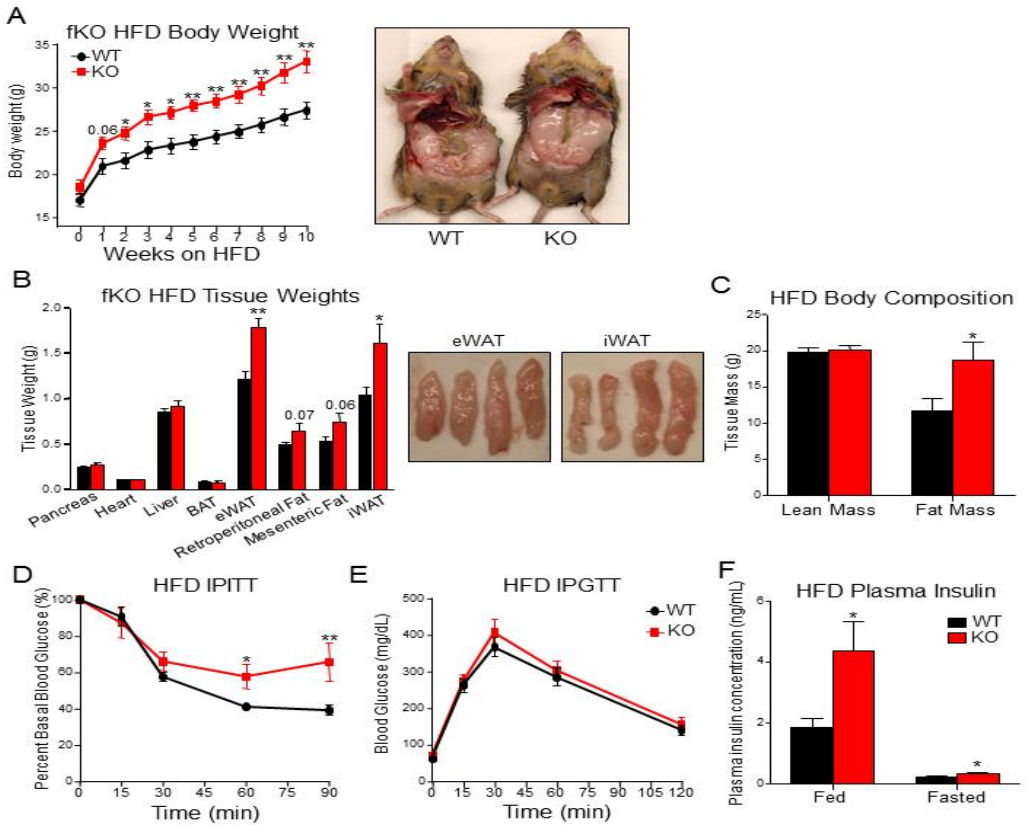

Figure 15: Fat-specific ablation of CREB3L3 enhances diet-induced obesity and insulin resistance

(A-B) (A) Weekly body weight measurements and (B) tissue weight measurements of WT and fKO mice during 10 wks of high-fat diet feeding (n=4-6 mice per group).

(C) Body composition following high-fat feeding measured by NMR (n=6-10 mice per group).

(D-E) Intraperitoneal (D) insulin and (E) glucose tolerance tests performed with high fat-fed WT and fKO mice (n=6-8 mice per group).

(F) Fed and fasted plasma insulin concentrations measured with ELISA (n=12-17 mice per fed group; 8 mice per fasted group). Data presented as mean +/- SEM with sample sizes listed above. The difference in means was analyzed using Student's t-test where *P<0.05 and **P<0.01.

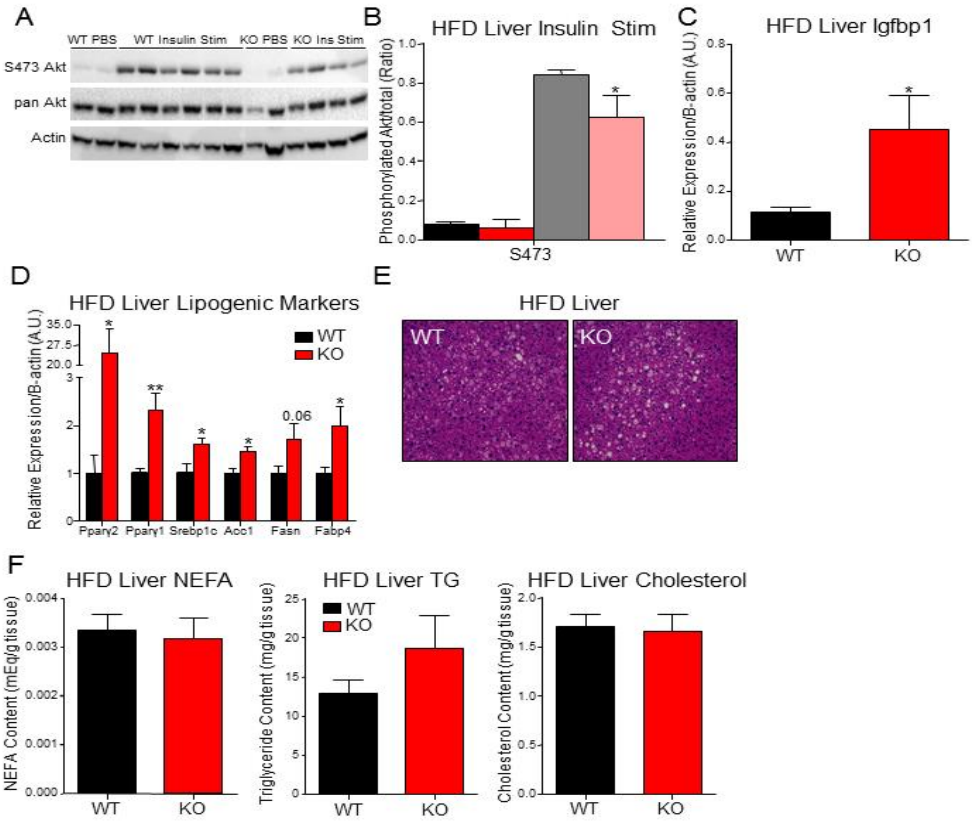

Figure 16: CREB3L3 fKO promotes selective hepatic insulin resistance

(A) Western blot measuring abundance of Akt and Akt phosphorylated at the S473 site in high fat-fed WT and fKO livers following injection with PBS or insulin.

(B) Quantification of Western blot results, with abundance of S473 phosphorylation normalized to abundance of total Akt in liver (n=2 mice per PBS group; n=4-6 insulin-stimulated mice per group).

(C-D) qPCR for (C) insulin-like growth factor binding protein 1 or (D) lipogenic markers in WT and fKO livers following high-fat feeding (n=5 mice per group).

(E) Representative images of H&E-stained liver sections following high-fat feeding.

(F) Quantification of lipid contents from liver extracts following high-fat feeding using colorimetric assays (n=7-8 mice per group). Data presented as mean +/- SEM with sample sizes listed above. The difference in means was analyzed using Student's t-test where *P<0.05 and **P<0.01.

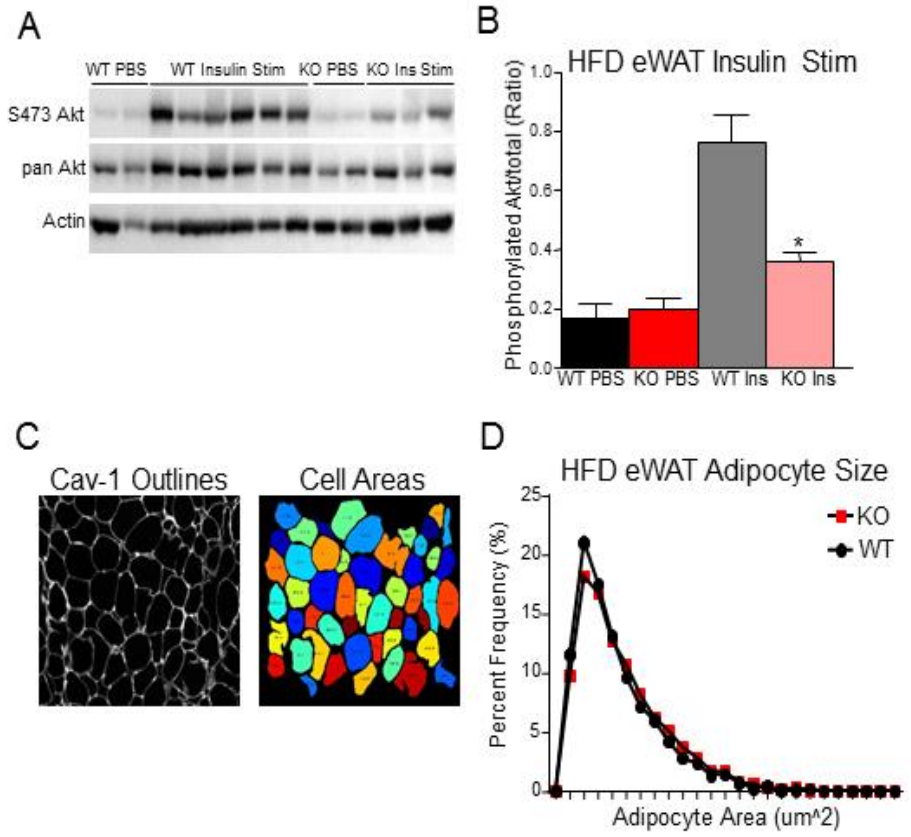

Figure 17: CREB3L3 fKO promotes eWAT insulin resistance without hypertrophy
(A) Western blot measuring abundance of Akt and Akt phosphorylated at the S473 site in high fat-fed WT and fKO eWAT following injection with PBS or insulin.

(B) Quantification of Western blot results, with abundance of S473 phosphorylation normalized to abundance of total Akt in eWAT (n=2 mice per PBS group; n=3-6 insulin-stimulated mice per group).

(C) Example images of the input and output of the CellProfiler pipeline designed to measure adipocyte area

(D) Frequency distribution of the adipocyte areas of WT and fKO eWAT following high-fat diet (10 images per mouse were used. n= 5 mice per group). Data presented as mean +/- SEM with sample sizes listed above. The difference in means was analyzed using Student's t-test where *P<0.05.

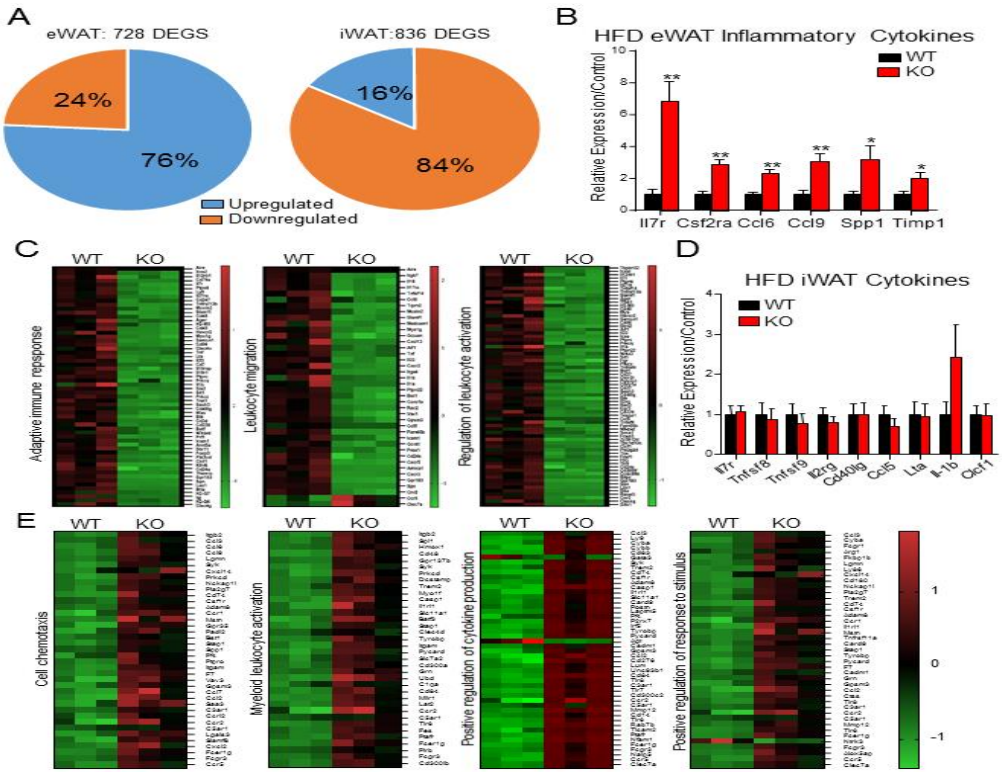

Figure 18: CREB3L3 KO differentially regulates inflammation in obese eWAT and iWAT (A) Pie charts showing the percentage of differentially expressed genes upregulated or downregulated in the eWAT and iWAT following high-fat feeding (n=4 mice per group).

(B) Quantitative PCR for high-fat fed eWAT expression of cytokines that were differentially expressed genes in the fKO eWAT RNASeq dataset. (n=8-9 mice per group).

(C) Heat map of z-scores of genes from the most differentially regulated pathways between WT and fKO iWAT following high-fat feeding (n=3 mice per group).

(D) Quantitative PCR for high-fat fed iWAT expression of cytokines that were differentially expressed genes in the fKO iWAT RNASeq dataset. (n=8-9 mice per group).

(E) Heat map of z-scores of genes from the most differentially regulated pathways between WT and fKO iWAT following high-fat feeding (n=3 mice per group). Data presented as mean +/- SEM with sample sizes listed above. The difference in means was analyzed using Student's t-test where *P<0.05 and **P<0.01.

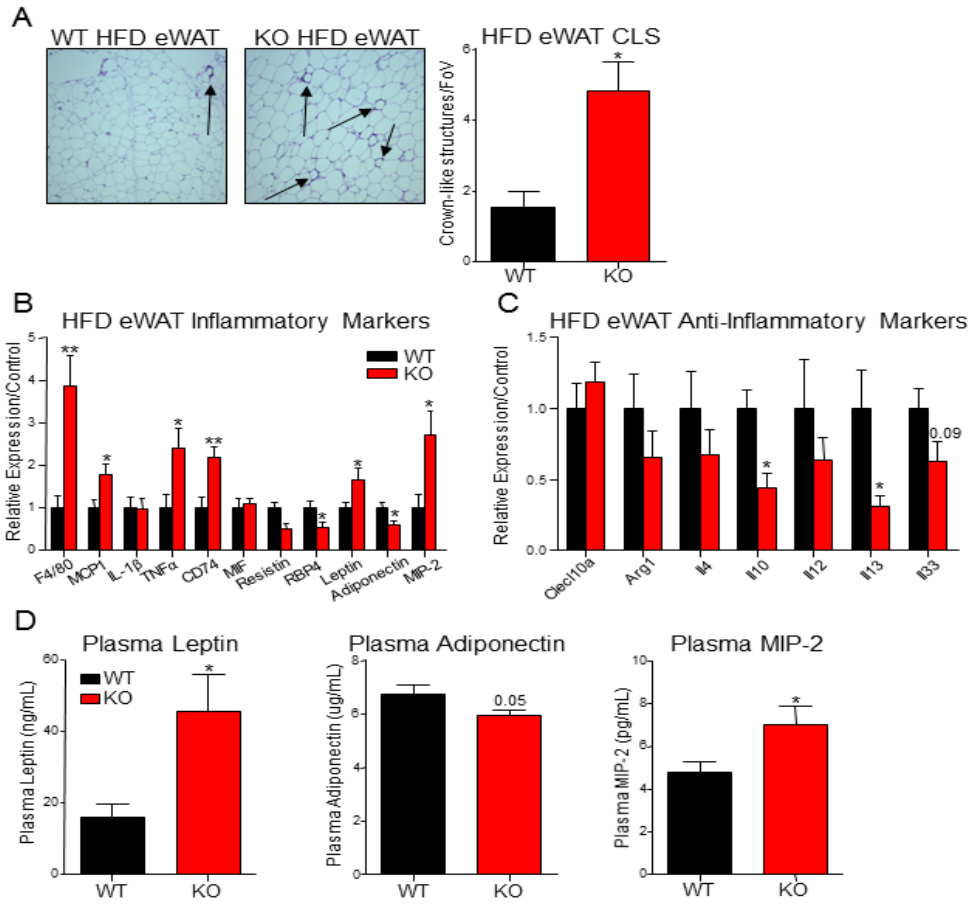

Figure 19: Ablation of CREB3L3 promotes visceral fat inflammation

(A) Representative images of H&E-stained eWAT sections following high-fat feeding and quantification of the number of crown-like structures per field of view. Arrows demarcate the presence of crown-like structures (3 images were taken per mouse. n=4-8 mice per group).

(B) Quantitative PCR for markers of inflammation in WT and fKO eWAT following high-fat feeding (n=8-9 mice per group).

(C) Quantitative PCR for anti-inflammatory markers in WT and fKO eWAT following high-fat feeding (n=5 mice per group).

(D) Quantification of plasma leptin and MIP-2 concentration following high-fat feeding using multiplex (n=4-6 mice per group). Adiponectin concentration was measured using ELISA (n=13-16 mice per group). Data presented as mean +/- SEM. The difference in means was analyzed using Student's t-test where *P<0.05 and **P<0.01.

3. Discussion

During our initial experiments, we identified that the liver-specific transcription factor CREB3L3 is expressed in the adipose tissue and selectively downregulated in the subcutaneous fat during obesity. We hypothesized that this downregulation could contribute to the healthier outcomes seen in patients and animal models that preferentially expand the subcutaneous adipose tissues during obesity. A fat-specific knockout (fKO) mouse was created to study this hypothesis. These fKO mice had enhanced fat mass (Fig 13B), but no changes in body weight (Fig 13A), glucose tolerance, or insulin sensitivity. Despite having no changes in insulin sensitivity, the fKO mice trended towards having higher circulating insulin. This could be due to changes in the secretome of the fKO adipose tissue – either altered adipokine or metabolite release – or this could be a byproduct of this measurement being performed using samples collected from mice in the fed state, and feeding time could introduce variability to these results.

Indirect calorimetry also revealed differences in the chow-fed fKO mice. These mice had higher energy expenditure during the dark cycles (Fig 14A) and a lower RER during the light cycles (Fig 14B) compared to the WT controls. These results are interesting, given the larger fat mass of the fKO mice (Fig 13B), without changes in food intake (Fig 14D) or activity (Fig 14C). This could be due to a shift towards lipid synthesis and storage within the white adipose tissues, but higher rates of energy and lipid consumption in other tissues like the muscle and the smaller livers of the fKO mice (Fig 13C). Further investigation into the metabolic profiles of these tissues is needed to answer this question.

Despite the small changes in global metabolism in the chow-fed fKO mice, our analysis focused on the pronounced phenotype of these mice during the pathological

obese state. The differences in fat mass and adipose tissue weights were exacerbated by high-fat feeding (Fig 15B-C), and the fKO mice gained significantly more weight (Fig 15A) and had reduced insulin sensitivity compared to WT controls (Figs 15D, 16A-B, 17A-B).

To evaluate what aspect of obese adipose biology in the fKO mice contributed to the development of insulin resistance, the transcriptomes of the white adipose tissues were analyzed using RNASeq. Interestingly, the ablation of CREB3L3 had divergent effects on gene expression in the fKO eWAT and iWAT, with the majority of genes being upregulated in the eWAT, while downregulated in the iWAT (Fig 18A). The vastly different transcriptomes of the fKO eWAT and iWAT during obesity are an interesting aspect of this phenotype that requires further investigation in the future. The transcriptome analysis did highlight innate immune pathways that were upregulated in the fKO eWAT during obesity (Fig 18E). The more inflammatory nature of this tissue was confirmed using morphological, gene expression, and plasma protein analysis (Fig 19), without more hypertrophy occurring within the tissue (Fig 17D). This lack of hypertrophy suggests that adipocyte dysfunction is not solely responsible for the increased pro-inflammatory cytokine expression in the fKO eWAT, but is due in part to the ablation of CREB3L3 in these obese adipocytes. These findings make future studies into the mechanism by which CREB3L3 regulates adipose inflammation a requirement. Together, the increased eWAT inflammation provides the likely link between the increased adiposity and insulin resistance of the obese fKO mice described in this chapter.

V. CREB3L3 fKO promotes weight gain by reducing energy expenditure and metabolic flexibility

1. Intro

In the previous chapter, we established that the ablation of CREB3L3 in adipose tissue leaves mice susceptible to diet-induced obesity. Expansion of adipose tissue can occur in response to changes in energy balance – by tilting the balance towards more energy consumption, or by a reduction in energy expenditure lifting up that side of the balance. Additionally, changes in adipose biology and its ability create, store, oxidize, and release lipids can also impact the size of the tissue. In this chapter, I will describe the experiments we performed to determine the changes in global energy balance and adipose functioning responsible for the enhanced adiposity we observed in the fKO mice.

2. Results

A. Fat-specific ablation of CREB3L3 reduces global energy expenditure during obesity

In order to understand why fKO promotes adiposity upon HFD feeding, indirect calorimetry experiments were performed. After acclimation to the cage system, the fKO mice had a significant reduction in their energy expenditure (Fig 20A), suggesting that a lower metabolic rate is contributing to the larger fat mass observed in the fKO mice during obesity. Additionally, the fKO mice had a significant downward shift in their (RER) (Fig 20B), suggesting a preference to use more lipids as an energy source. This could be related with the observation that despite high insulin (Fig 15F) and hepatic insulin resistance (Fig 16A-D), the fKO mice did not develop steatosis (Fig 16E-F) and had a trend towards increased plasma ketones when fasted (Fig 20C). Interestingly, the increased body weight and lipid consumption are not due to increased food intake (Fig

21A) or behavioral changes (Fig 21B) in the fKO mice. In fact, fKO mice consumed less food when normalized to body weight (Fig 21A), which may be caused by reduced expression of the orexigenic protein, neural peptide Y (NPY) in the hypothalamus of fKO mice (Fig 21C). No changes in distance traveled or x-axis and y-axis beam breaks were observed in these mice (Fig 21B).

B. Ablation of CREB3L3 promotes whitening of brown fat

Brown adipose tissue (BAT) is a significant contributor to global energy expenditure and upon stimulation accounts for an estimated 16% of the resting metabolic rate in humans [130]. Changes in the metabolic rate of this tissue would have large impacts on the basal metabolic rate of the animal as a whole. Despite the weight of BAT not being altered by fKO in diet-induced obese mice, H&E staining revealed gross morphological changes to the BAT in the fKO mice, which exhibited significant whitening of the tissue following HFD diet (Fig 22A). Analysis of functional marker expression with qPCR showed that there was a no change in UCP1 expression, but Elovl3, Fgf21, and Cox8b were upregulated in the BAT from the fKO mice (Fig 22B). There was no significant reduction in the expression of genes involved in oxidation in the fKO BAT (Fig 22C). However, there was a 4-fold increase in the expression of Acetyl-CoA Carboxylase 1 (ACC1), the enzyme that converts acetyl-CoA to malonyl-CoA, and a 2.5-fold increase in Fatty Acid Synthase (FASN) expression (Fig 22D). Malonyl-CoA serves as a substrate for *de novo* lipogenesis and is converted to palmitate by FASN. It has also been shown to inhibit beta oxidation through inhibition of carnitine palmitoyltransferase 1 (CPT1), the enzyme responsible for the influx of fatty acyl CoA molecules into the mitochondria via the carnitine shuttle [95]. In addition to upregulation of ACC1, there is a trend towards the fKO BAT having reduced

expression of CPT1B (Fig 22C), the CPT1 isoform expressed in BAT, skeletal muscle, and the heart. Together, these data suggest that the BAT of the fKO mice is whiter due to lipid flux shifting away from fatty acid oxidation and towards more *de novo* lipogenesis and lipid accumulation.

C. fKO subcutaneous adipocytes possess less browning potential

In addition to BAT, brown-like beige adipocytes are also significant contributors to basal metabolic rate. We observed that there is a significant reduction in UCP1 and PGC1α in the iWAT of lean, chow-fed fKO mice (Fig 23A). To further determine whether deficits in browning and adaptive thermogenesis could contribute to the reduced energy expenditure in the fKO mice, beige adipocyte formation in the iWAT was analyzed following treatment with the β3-adrenregic receptor agonist, CL 316,243 (CL). β3-adrenregic receptor stimulation with CL promotes the transdifferentiation of white adipocytes to beige adipocytes, as opposed to *de novo* formation of beige adipocytes that differentiate from precursor cells following cold stimulation [144]. The iWAT from chow-fed fKO mice exhibited a blunted beiging capacity following 10 days of CL treatment. The fKO mice had lower expression of the thermogenic markers UCP1, PGC1α, Cidea, Cox8b, Elovl3, and the beige adipocyte marker Prdm16 compared to WT controls (Fig 23B).

Surprisingly, the fKO iWAT did not have reduced thermogenic marker expression following 7 days of cold exposure. Instead, there was a significant increase in the expression of some thermogenic markers, including UCP1 (Fig 23C). This suggests that the ablation of CREB3L3 specifically limits the ability of subcutaneous adipocytes to undergo transdifferentiation into beige adipocytes following pharmacological stimulation,

but does not reduce the ability for precursor cells to differentiate into beige cells upon cold exposure. To this end, we found that the fKO mice had no deficits in their ability to defend their core body temperature in response to cold (Fig 23D).

To determine the contribution of impaired beige adipocyte formation to the larger body weight of the fKO mice following high-fat feeding, a cohort of mice were housed at thermoneutrality and fed a HFD for 14 weeks. There were no differences in body weight (Fig 24A) or adipose tissue size (Figure 24B) between the WT and fKO mice at thermoneutrality. This suggests that the enhanced body weight and enlarged adipose tissues in the fKO mice during obesity are temperature-dependent and are caused by a diminished ability of the fKO iWAT to undergo adaptive thermogenesis.

D. CREB3L3 differentially regulates lipid metabolism in white adipose tissue

CREB3L3 plays an important role in regulating lipid metabolism in the liver. To determine whether CREB3L3 serves a similar function in adipose tissue, the expression of genes involved in *de novo* lipogenesis and lipolysis were assayed in the white adipose tissues from fKO mice. Several genes involved in lipid synthesis were upregulated in the fKO iWAT following high-fat feeding, including Srebp1c, Fasn, Acc2, Scd2, Dhcr24, and Elovl1 (Fig 25A). Interestingly, the opposite effect was observed in the eWAT during obesity. There were trends towards reduced expression of Srebp1c, Fasn, Acc1, and significant downregulation of Chrebp, Scd1, and Glut4 (Fig 25B). A similar differential effect was observed with the regulation of lipolysis markers in obese fKO tissues. While there were no significant differences in the expression of the lipases, either perilipin (Plin1/2) isoform, or the β3-adrenregic receptor (Adrb3) in the fKO iWAT (Fig 25C), there was a significant reduction in the expression of ATGL, LPL, and Adrb3 in the fKO eWAT following high-fat

feeding (Fig 25D). Additionally, the expression of perilipin 2 was significantly higher (Fig 25D), indicating that eWAT adipocytes have more regulatory control over lipases accessing the lipid droplet. Overall, we observed that the ablation of CREB3L3 differentially altered lipogenic and lipolytic gene expression in the iWAT and eWAT during obesity.

To further examine how these changes in gene expression could contribute to the greater adiposity observed in the fKO mice, Western blotting was performed. There was an increase in the abundance of FASN and Stearol-CoA Desaturase 1 (SCD1) in the fKO iWAT (Fig 25E) and the fKO eWAT had reduced phosphorylation of HSL, reduced abundance of ATGL, and a drastic increase in perilipin abundance (Fig 25F). To ascertain if these changes in the abundance of lipases and perilipin translate to measureable changes in the rate of lipolysis occurring in the eWAT, we performed an *ex vivo* lipolysis assay using white adipose tissue explants. Contrary to the changes in protein abundance, the fKO eWAT and iWAT did not exhibit any changes in free fatty acid release under both the basal or isoproterenol-stimulated conditions (Fig 26A). In order to confirm that there were no functional lipolysis differences in the obese fKO mice, a cohort of high-fat fed mice were fasted for 6 hours and injected with CL to induce adipocyte lipolysis. Plasma samples were collected one hour after stimulation. In agreement with the lack of differences in the *ex vivo* lipolysis assay, there were no *in vivo* differences in fatty acid content of obese fKO mice following CL stimulation (Fig 26B). Together, these findings suggest that while CREB3L3 ablation alters the expression of lipid metabolism in the white adipose tissue, there does not appear to be functional differences in lipolysis, nor do they contribute to the greater adiposity of the fKO mice during obesity.

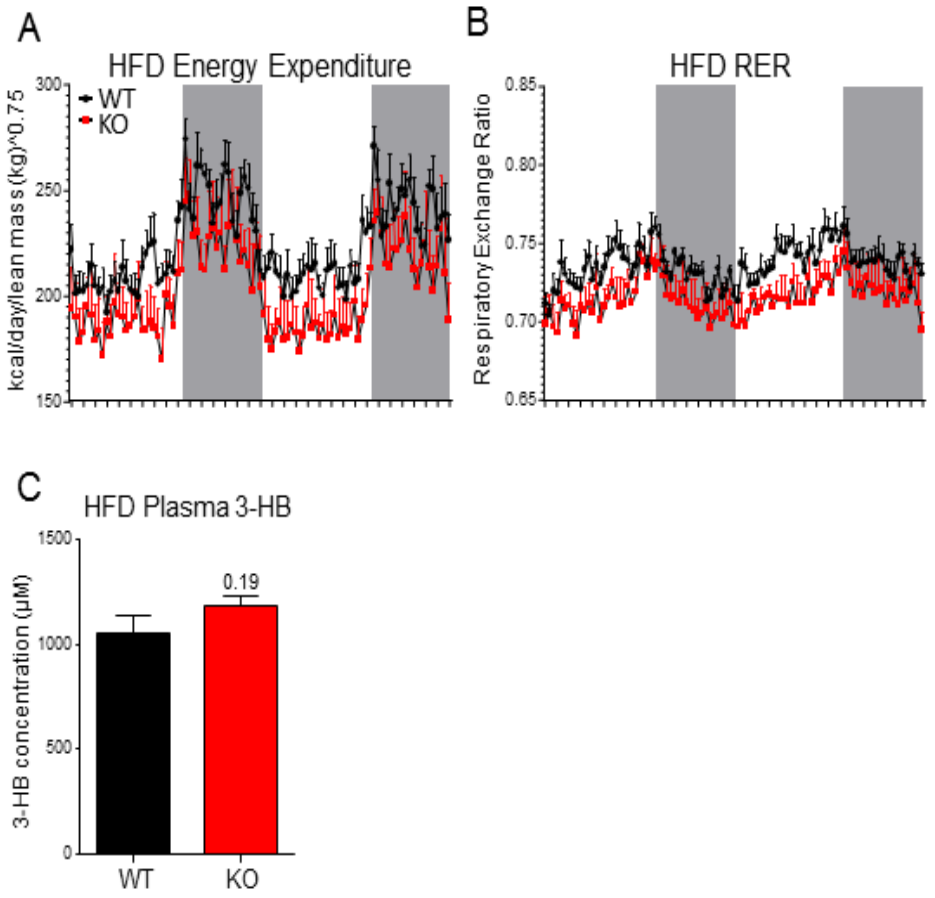

Figure 20: CREB3L3 ablation reduces energy expenditure and RER

(A-B) (A) Energy expenditure and (B) respiratory exchange ratios (RER) of WT and fKO mice fed high-fat diet (n=6-8 mice per group). Energy expenditure was normalized to the animal's lean mass. The curves for both measurements were analyzed using two-way ANOVA. P values for the column factor (genotype) for the energy expenditure and the RER were both <0.0001.

(C) Quantitative PCR of orexigenic and anorexigenic peptides in WT and fKO hypothalami following high-fat feeding (n=7 mice per group). Data presented as mean +/- SEM. The difference in means was analyzed using Student's t-test where *P<0.05 and **P<0.01.

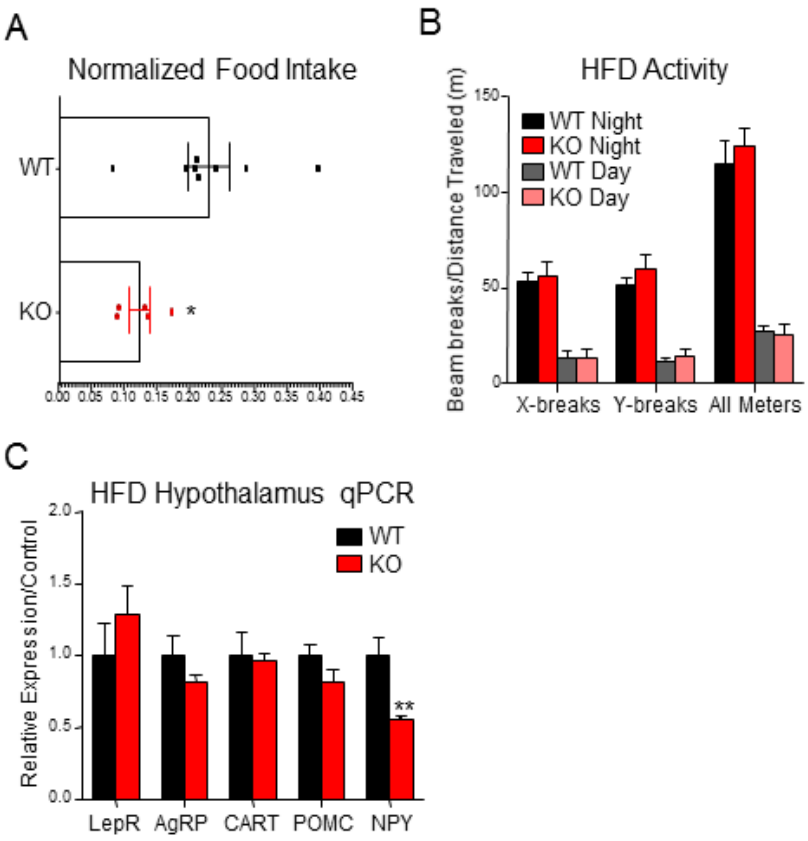

Figure 21: Adipose ablation of CREB3L3 reduces food intake

(A) Total consumption of high-fat diet while mice were in metabolic cages. Food intake was normalized to animal's body weight (n=5-8 mice per group).

(B) Activity measurements of WT and fKO mice fed high-fat diet. Data presented as x- and y-axis beam breaks and total movement per day following acclimation period (n=6-8 mice per group).

(C) Quantitative PCR of orexigenic and anorexigenic peptides in WT and fKO hypothalami following high-fat feeding (n=7 mice per group). Data presented as mean +/- SEM. The difference in means was analyzed using Student's t-test where *P<0.05 and **P<0.01.

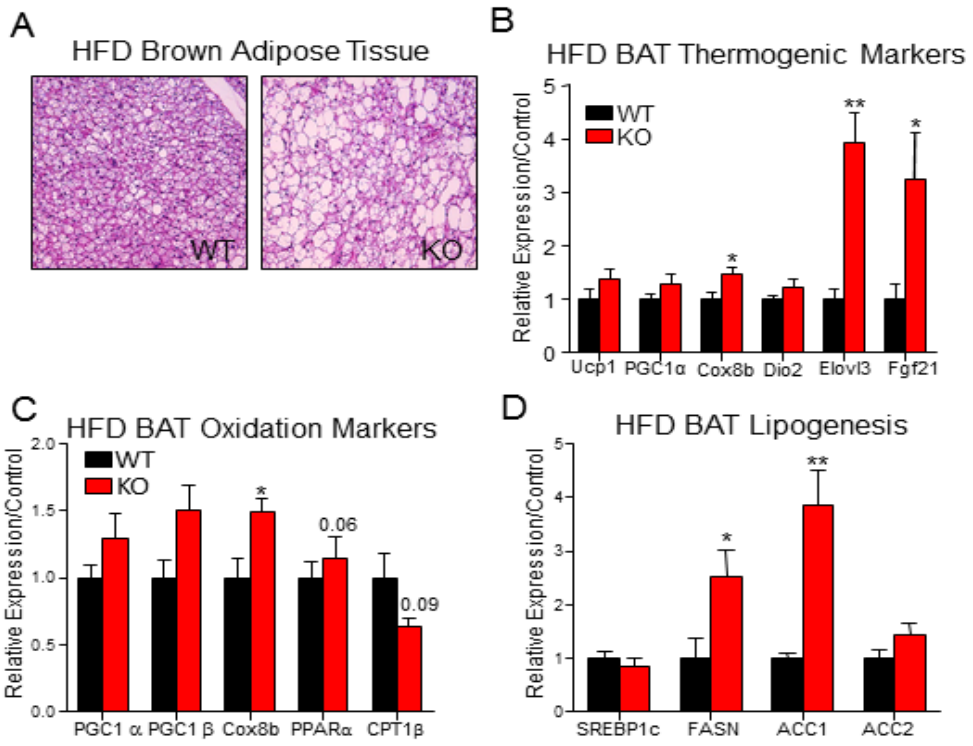

Figure 22: CREB3L3 ablation promotes lipid accumulation in obese brown fat
(A) Representative images of H&E-stained brown adipose tissue sections following high-fat feeding.

(B) Quantitative PCR for markers of thermogenesis and adipocyte browning in brown adipose tissue from WT and fKO mice following high-fat feeding (n=5 mice per group).

(C) Quantitative PCR for markers of fatty acid oxidation in WT and fKO brown adipose tissue following high-fat feeding (n=5 mice per group).

(D) Quantitative PCR for markers of *de novo* lipogenesis in WT and fKO brown adipose tissue following high-fat feeding (n=5 mice per group). Data presented as mean +/- SEM. The difference in means was analyzed using Student's t-test where *P<0.05 and **P<0.01.

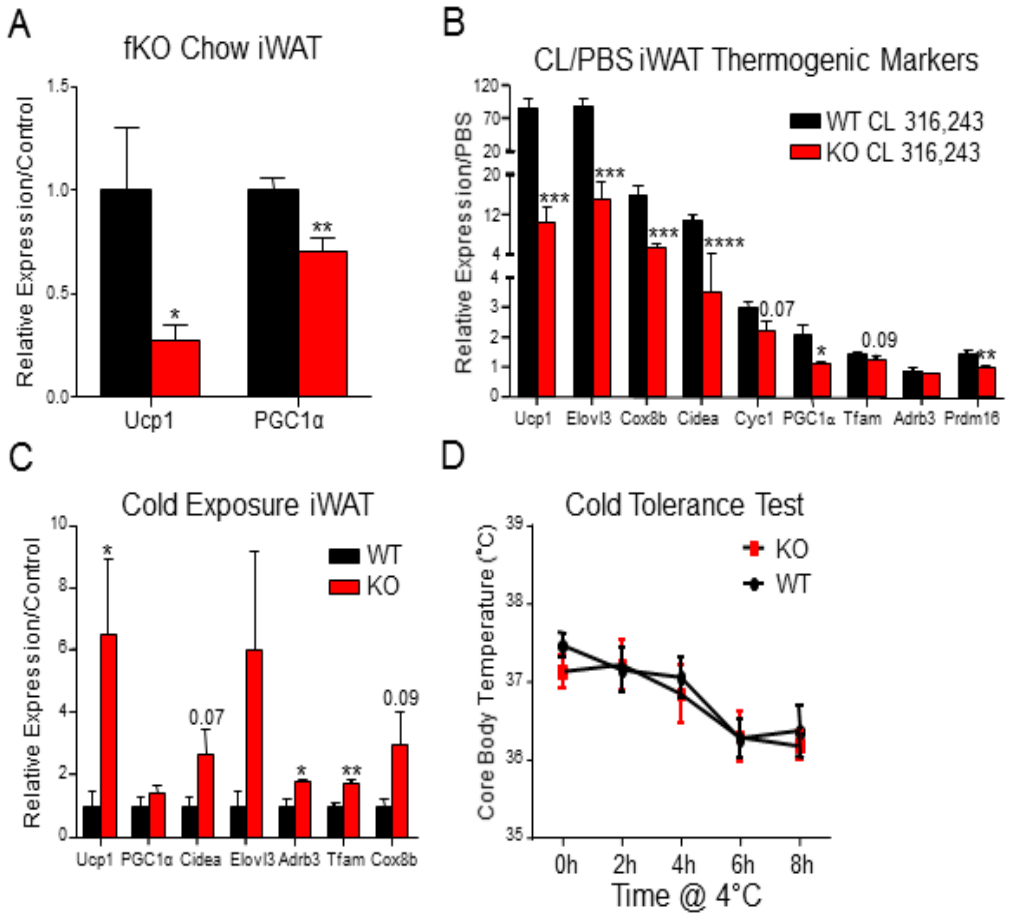

Figure 23: CREB3L3 ablation prevents β3-induced browning of iWAT adipocytes

(A) Quantitative PCR for UCP1 and PGC1a in WT and fKO inguinal adipose tissue in mice fed a chow diet (n=5-6 mice per group).

(B) Quantitative PCR for markers of thermogenesis and adipocyte browning in iWAT from lean WT and fKO mice following 10-day treatment with 316,243 (n=6 mice per group). Expression data are presented as fold change over the mean relative expression from the PBS-injected group for each genotype.

(C) qPCR for markers of thermogenesis and adipocyte browning in inguinal adipose tissue in lean WT and fKO mice housed at 6 degrees for 7d (n=3-4 mice per group).

(D) Core body temperature measured during cold tolerance tests performed at 4 degrees with chow-fed WT and fKO mice (n=8-12 mice per group). Data presented as mean +/- SEM. The difference in means was analyzed using Student's t-test where *P<0.05 and **P<0.01, ***P<0.001, and ****P<0.0001.

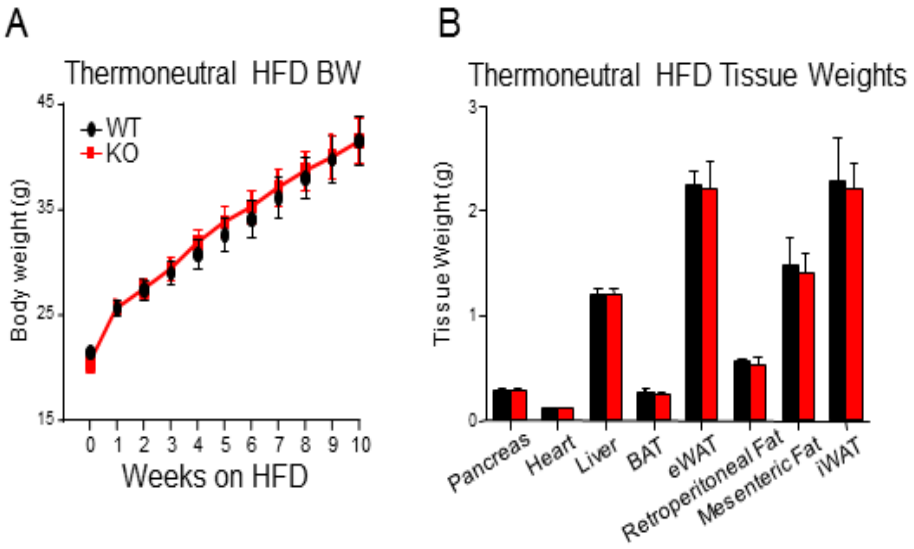

Figure 24: Body weight effects of CREB3L3 ablation lost at thermoneutrality
(A) Body weight measurements for WT and fKO mice consuming high-fat diet while housed at thermoneutrality for 10 wks (n=7-9 mice per group).

(B) Tissue weight measurements for WT and fKO mice after consuming high-fat diet while housed at thermoneutrality for 10 wks (n=7-9 mice per group). Data presented as mean +/- SEM.

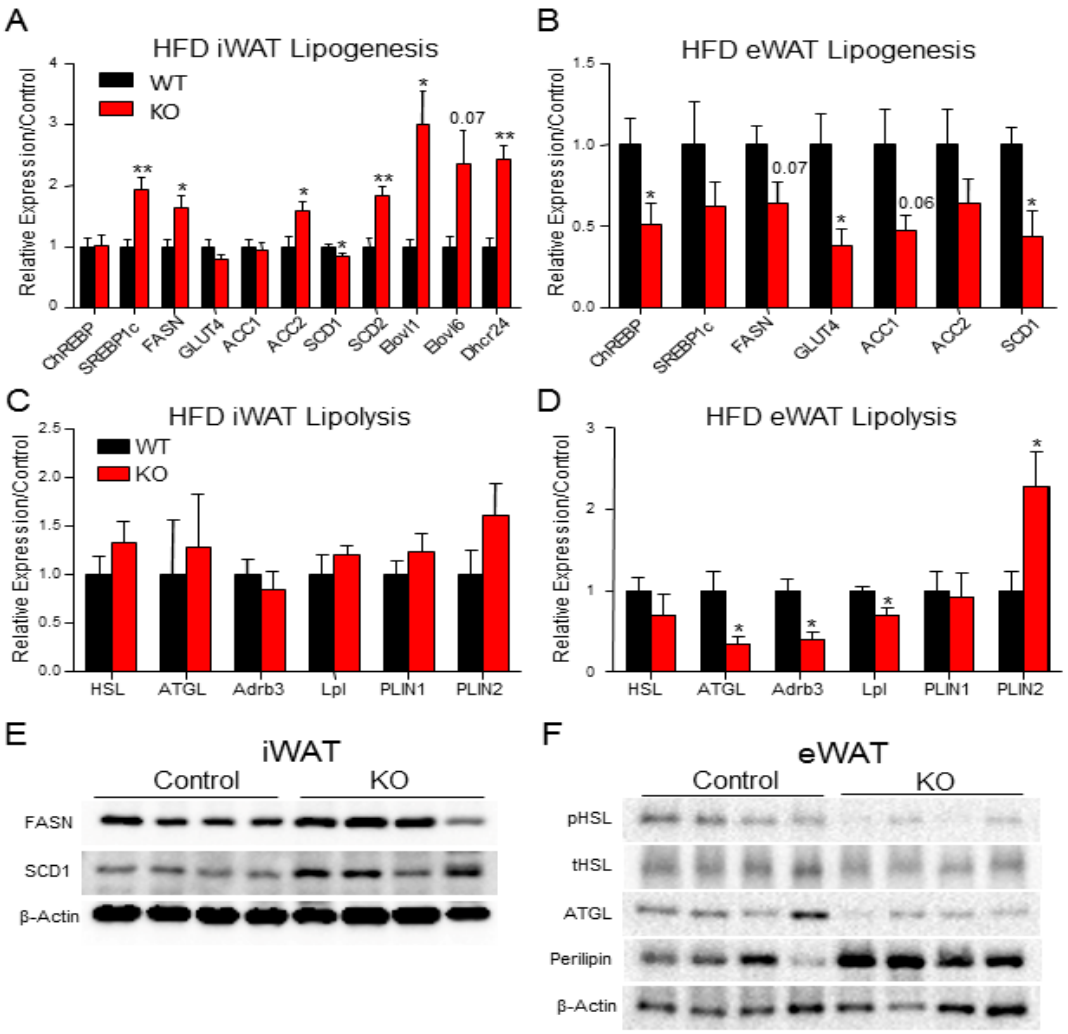

Figure 25: CREB3L3 differentially regulates lipid metabolism in obese iWAT and eWAT (A-B) Quantitative PCR for markers of lipid synthesis in WT and fKO (A) iWAT or (B) eWAT following high-fat feeding (n=5 mice per group).

(C-D) Quantitative PCR for markers of lipolysis in WT and fKO (C) iWAT or (D) eWAT following high-fat feeding (n=5 mice per group).

(E) Western blot measuring abundance of FASN and SCD in high fat-fed WAT and fKO iWAT.

(F) Western blot measuring abundance of pHSL, HSL, ATGL, and perilipin in high fat-fed WAT and fKO eWAT. Data presented as mean +/- SEM. The difference in means was analyzed using Student's t-test where *P<0.05 and **P<0.01.

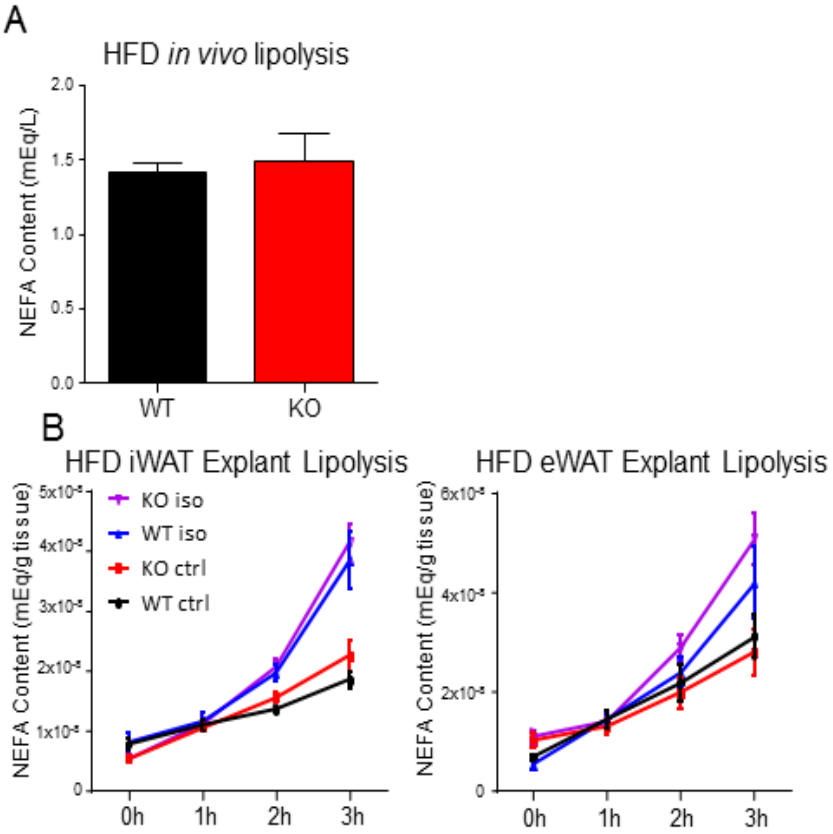

Figure 26: CREB3L3 ablation does not alter free fatty release from obese WAT

(A) Non-esterified fatty acids (NEFA) content measured in plasma collected from high-fat fed WT and fKO mice 1h after injection with CL316,243 (n=5-8 mice per group).

(B) NEFA content measured in conditioned media from iWAT explants harvested from WT and fKO mice fed high-fat diet with or without isoproterenol (iso) (n=5-10 mice per group).

(C) NEFA content measured in conditioned media from eWAT explants harvested from WT and fKO mice fed high-fat diet with or without isoproterenol (iso) (n=5-10 mice per group). Data presented as mean +/- SEM.

3. Discussion

In this chapter, we sought to explain why the fKO mice have enhanced adiposity during obesity. We found that the ablation of CREB3L3 in adipose tissue leads to a reduction in global energy expenditure (Fig 20A). This appears to be due to reduced oxidative capacity (Fig 22C-D) in the brown fat and a whitening of this tissue (Fig 22A), in addition to diminished ability of fKO subcutaneous adipocytes to undergo browning (Fig 23B). Ambient temperature is sufficient to induce browning of white adipose tissue, but browning is not needed by mice to maintain body temperature when mice are housed at thermoneutrality [242]. This would suggest that the greater adiposity observed in high-fat fed fKO mice is due to the impaired ability of subcutaneous adipocytes to undergo browning, as adiposity differences were lost when fKO mice were housed at thermoneutrality (Fig 24B).

The reduced energy expenditure following high-fat feeding was in opposition to the increased energy expenditure observed in the fKO mice on chow diet (Fig 14A). This maybe be due to increased metabolic and oxidative rates occurring in other metabolic organs in the chow-fed mice, as suggested by the lower RER in these mice (Fig 14B), despite the fKO mice having a larger fat mass (Fig 13B). This may also be the case in the fKO mice fed high-fat diet. These mice also exhibited a lower RER (Fig 20B), in addition to having a trend towards more circulating ketone bodies (Fig 20C) and livers that did not become more steatotic (Fig 16E-F), despite upregulation of PPARγ and other markers of de novo lipogenesis (Fig 16D). While the fKO mice are able to balance out changes in adipose energy expenditure with increased hepatic lipid oxidation under chow feeding, the increased energy and lipid intake with high-fat feeding provides a positive energy balance and the phenotype of the adipose tissue becomes more pronounced. While the

high-fat fed fKO mice did consume less food compared to WT controls (Fig 21A) and exhibited a reduction in hypothalamic NPY expression (Fig 21C), this may be a compensatory measure to combat their weight gain and feeding measurements at earlier time points during high-fat feeding are needed to determine its cause.

In addition to the changes in energy expenditure observed in the fKO mice, altered lipid metabolism may also contribute to the enhanced adiposity observed in these mice. We observed differential expression of genes involved in lipogenesis (Fig 25A-B) and lipolysis (Fig 25C-D) in the fKO iWAT and eWAT following HFD. This could be due to a multitude of factors and could provide insight into transcriptional differences between subcutaneous and visceral fat. Therefore mechanistic studies to further investigate this differential expression are needed. In an attempt to determine the functional significance of these changes in gene expression, we performed *in vivo* and *ex vivo* lipolysis assays and determined there were no significant differences in the rates of lipolysis in the obese fKO eWAT or iWAT (Fig 26A-B). The lack of differences may be due to the reduced insulin sensitivity of the fKO eWAT during obesity (Fig 17A-B). Additionally, the increased eWAT expression of the lipid droplet protein isoform perilipin 2 (Fig 26D) might be from other cell types [78], and provide no barrier to lipolysis in adipocytes. Taken together, we found no functional differences linking changes in gene expression and protein abundance to the enlarged adipose tissues of the fKO mice. Therefore, the reduced expenditure, particularly the limited ability of the fKO mice to perform adaptive thermogenesis, is responsible for the enhanced adiposity of the fKO mice fed a high-fat diet.

VI. Increasing expression of CREB3L3 in subcutaneous adipose tissue prevents diet-induced obesity

1. Introduction

CREB3L3 message is selectively downregulated in the iWAT of obese mice (Fig 8A). This natural knockdown following high-fat feeding could limit our ability to make inferences about the role of this transcription factor in the subcutaneous adipose biology of the fKO mice. To better study the role of this transcription factor in obese iWAT, we aimed to reintroduce CREB3L3 into this tissue by iWAT-specific overexpression. In this chapter I will describe our experiments to induce iWAT CREB3L3 overexpression and our subsequent examination of the metabolic consequences.

2. Results

A. Increased expression of CREB3L3 in subcutaneous adipose tissue prevents diet-induced obesity

In order to induce CREB3L3 overexpression in adipose tissues, we injected an empty AAV (sham) or an AAV containing the processed form of CREB3L3 (smaller band in OE iWAT, control mesenteric fat, fasting liver, Fig 9C) directly into the eWAT and iWAT of young adult mice. After recovering from surgery, the mice were placed on HFD. While injection with the CREB3L3-AAV created robust overexpression of the CREB3L3 N-terminus (Fig 27A), and improved glucose tolerance (Fig 27B) and insulin sensitivity (Fig 27C) following high-fat feeding, we discovered that the livers of the overexpression mice also had elevated CREB3L3 expression (Fig 27D). Due to the leakiness of this overexpression system, we sought to add an element that would limit overexpression solely to adipocytes.

To achieve this, we utilized flip-excision (FLEx) technology, where the desired reading frame is inverted and housed between both loxP and lox2272 sites (Fig 27E). Cre recombination results in the inversion of the reading frame and overexpression only in the tissues expressing Cre recombinase. Using this strategy, CREB3L3 was overexpressed in the iWAT of Adipo-Cre mice via direct injection of our CREB3L3-FLEx-AAV (Fig 27F).

Despite having no significant difference in their body weights before the surgery, the mice with subcutaneous overexpression (sOE) weighed less than sham littermate controls lacking the Adipo-Cre BAC, that received the same CREB3L3-FLEx-AAV (Fig 28A). This difference was exacerbated during high-fat feeding. Strikingly, increased expression of CREB3L3 reduced body weight gain in mice with diet-induced obesity. The sOE mice were 14.4 grams heavier following 12 weeks on HFD. Control mice that were also injected with the virus gained 23.4 grams over the same time period (Fig 28B). This difference in body weight was due to significant reductions in iWAT, BAT, mesenteric fat, pancreas, and liver size in the sOE mice (Fig 28C). Interestingly, there were no changes in the eWAT and retroperitoneal fat, although this could be due to compensatory fat storage (Fig 28C). Overall, the sOE mice had a dramatic reduction in their fat mass, in addition to a small reduction in lean mass (Fig 28D).

B. Subcutaneous adipose overexpression of CREB3L3 prevents obesity associated metabolic dysfunction

Consistent with their leaner phenotype, the sOE mice had improved insulin sensitivity (Fig 29A), in addition to having improved glucose tolerance compared to the sham control mice (Fig 29B). The improved body weight and insulin sensitivity of the sOE mice are not due to increased energy expenditure (Fig 30A) or reduced food intake, which is actually

increased when normalized to body weight (Fig 30B). However, the sOE mice exhibit increased activity (Fig 30C). This may explain the changes in body composition (Fig 28B-D). Additionally, an upward shift in the RER curve during the light cycle suggest that sOE creates a preference for carbohydrates (Fig 30D), which was further supported by a drop in their fasted ketone bodies (Fig 30E).

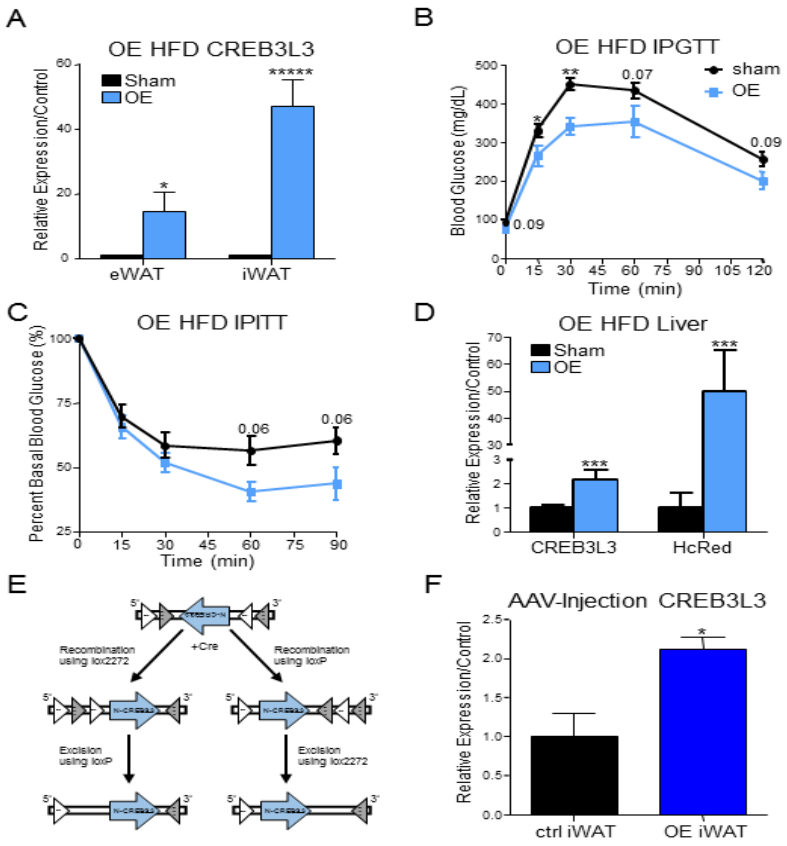

Figure 27: Adipose expression of CREB3L3 is induced using AAV

(A) qPCR for CREB3L3 message in eWAT and iWAT following high-fat feeding in mice injected with the CREB3L3-AAV (OE) or empty AAV (sham) (n=6-10 mice per group).

(B-C) Intraperitoneal (B) glucose and (C) insulin tolerance tests performed with high fat-fed sham and OE mice (n=6-10 mice per group).

(D) qPCR for CREB3L3 and HcRed message in livers following high-fat feeding in mice injected with the CREB3L3-AAV (OE) or empty AAV (sham) (n=6-9 mice per group).

(E) Schematic depicting the recombination and inversion of CREB3L3 within the flip-excision (FLEx) AAV in the presence of Cre recombinase.

(F) qPCR for the expression of CREB3L3 message in inguinal fat pads harvested two weeks following injection with the CREB3L3 FLEx AAV in Adiponectin-Cre (sOE) or littermates lacking the Cre BAC (ctrl) (n= 3-4 mice per group). Data presented as mean +/- SEM. The difference in means was analyzed using Student's t-test where *P<0.05, **P<0.01, ***P<0.001, and *****P<0.00001.

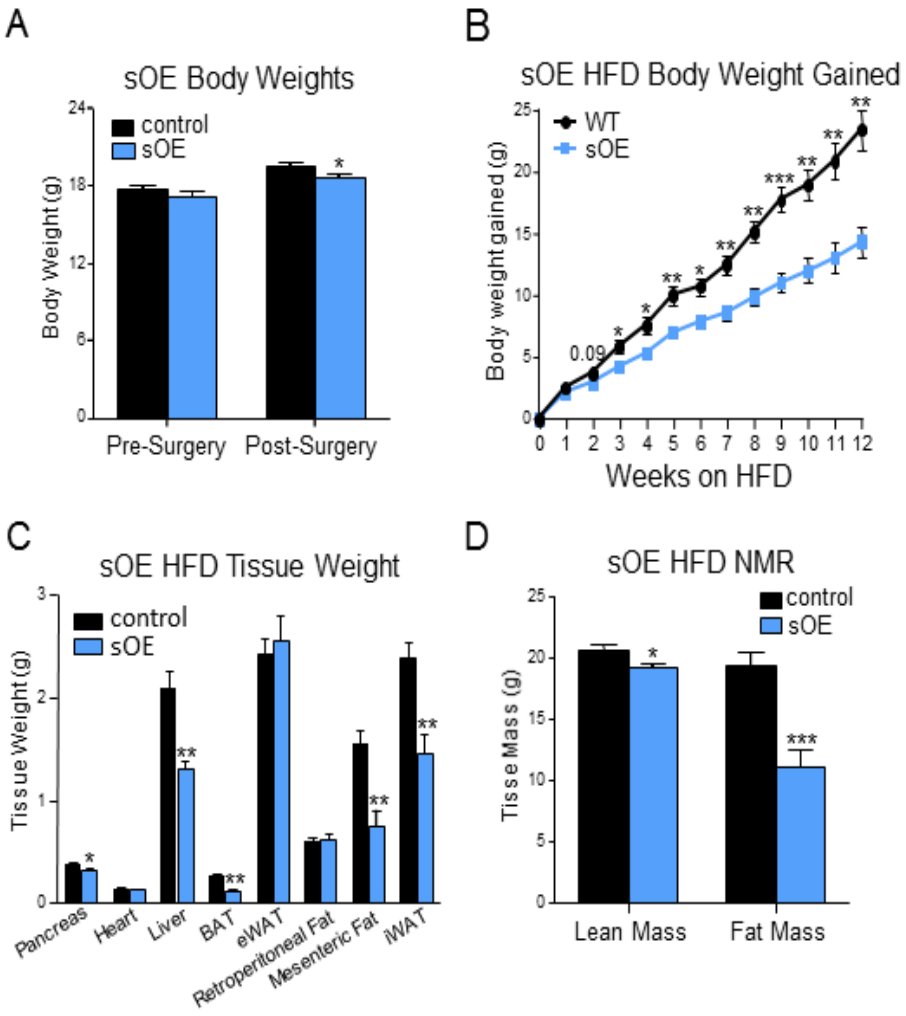

Figure 28: Increased expression of CREB3L3 in iWAT prevents diet-induced obesity

(A) Body weight measurements of sham ctrl and sOE mice 2 wks after injection with the CREB3L3 FLEx AAV (n=6-9 mice per group).

(B) Measurements of the body weight gained by sham control and subcutaneous overexpression (sOE) mice after high-fat feeding (n=6-9 mice per group).

(C) Tissue weights measurements for sham control and sOE mice after high-fat feeding (n=6-9 mice per group).

(D) Body composition of sham and sOE mice following high-fat feeding measured by NMR (n=6-9 mice per group). Data presented as mean +/- SEM. The difference in means was analyzed using Student's t-test where *P<0.05, **P<0.01, and ***P<0.001.

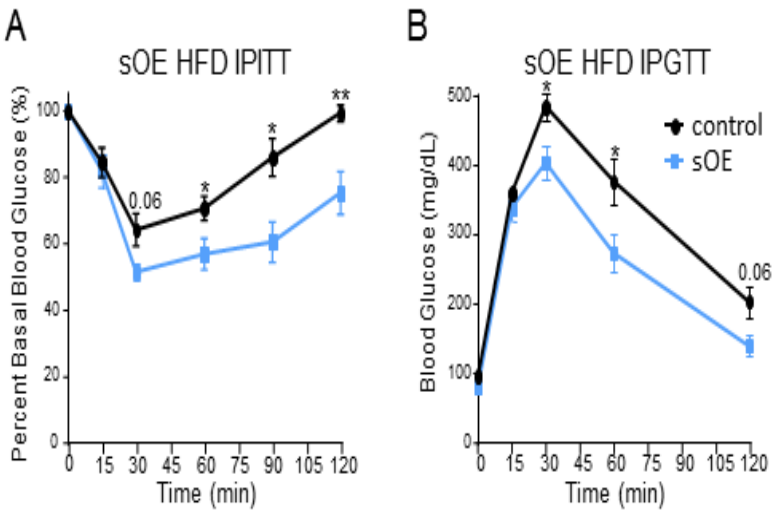

Figure 29: Increased iWAT CREB3L3 prevents glucose intolerance and insulin resistance

(A-B) Intraperitoneal (A) insulin and (B) glucose tolerance tests performed with sham control and sOE mice (n=5-7 mice per group). Data presented as mean +/- SEM. The difference in means was analyzed using Student's t-test where *P<0.05, **P<0.01.

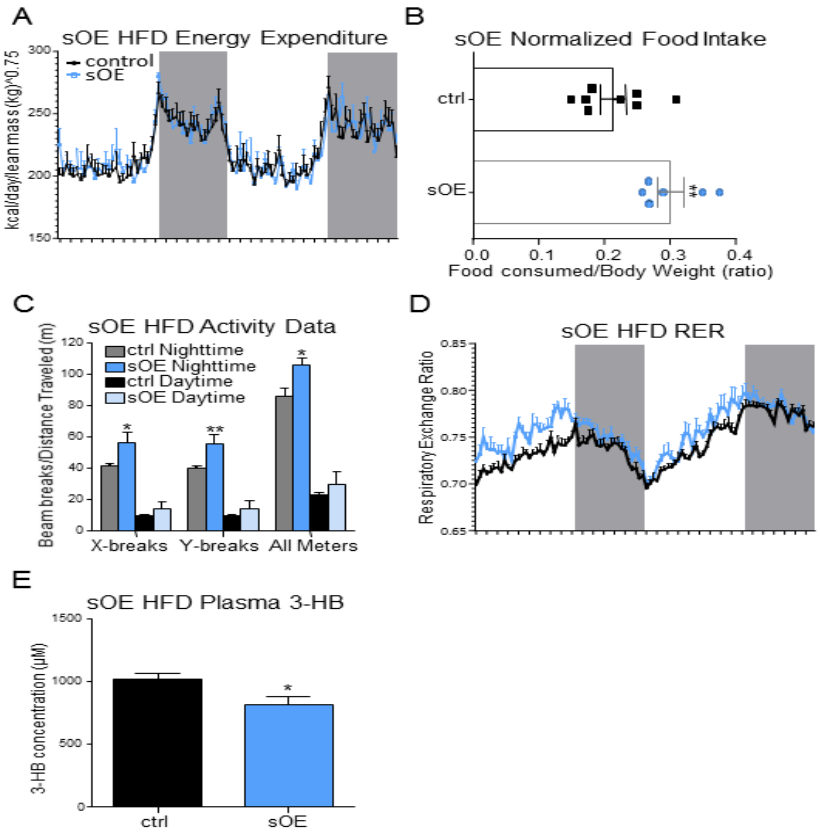

Figure 30: Increased iWAT CREB3L3 shifts global energy homeostasis

(A) Energy expenditure of sham sham ctrl and sOE mice fed high-fat diet (n=6-9 mice per group) normalized to the animal's lean mass. The curves were analyzed using two-way ANOVA. P value for the column factor (genotype) was 0.4992.

(B) Total consumption of high-fat diet while sham ctrl and sOE mice were in metabolic cages. Food intake was normalized to animal's body weight (n=6-8 mice per group).

(C) Activity measurements of sham ctrl and sOE mice fed HFD. Total movement and x- and y-axis beam breaks after acclimation period are shown (n=5-8 mice per group).

(D) Respiratory exchange ratios (RER) of sham ctrl and sOE mice fed HFD (n=6-9 mice per group). Curves were analyzed using two-way ANOVA. P value for the column factor (genotype) was <0.0001.

(E) Quantification of fasted plasma 3-hydroxybutyrate from sOE mice following high-fat feeding (n=6-8 mice per group). Data presented as mean +/- SEM. The difference in means was analyzed using Student's t-test where *P<0.05 and **P<0.01.

3. Discussion

In this chapter, we overexpressed CREB3L3 in the iWAT to study its role in the tissue during obesity. Since CREB3L3 is downregulated in the iWAT during obesity, the similar expression levels in the WT and fKO tissue might hinder the phenotype of the fKO mice during high-fat feeding. We hypothesized that overexpressing CREB3L3 in the subcutaneous fat could induce a more robust iWAT phenotype during obesity. Our initial attempt at overexpressing CREB3L3 in both iWAT and eWAT by injecting a CREB3L3-AAV directly into both tissues did dramatically overexpress CREB3L3 in these WAT (Fig 27A). However, this approach did not create the desired adipose-specific overexpression, as the vector leaked into the circulation and CREB3L3 along with its connected HcRed tag were also expressed in the livers of these mice (Fig 28D). Due to this setback, we designed a new AAV that would only allow CREB3L3 to be overexpressed in adipose tissues. We therefore injected our CREB3L3-FLEx-AAV into the iWAT of Adipo-Cre mice, to create a subcutaneous fat-specific overexpression (sOE) model.

While these mice recovered from surgery, the sOE mice gained less weight than control mice that lack the Adipo-Cre BAC (Fig 28A). This change in body weight was exacerbated when the mice were put on HFD (Fig 28B), and resulted in reduced fat mass and iWAT, BAT, mesenteric fat, pancreas, and liver weights. However, no changes in eWAT weight was observed in the sOE mice (Fig 28C). While these mice had improved glucose tolerance (Fig 29B) and insulin sensitivity (Fig 29A), they did not exhibit increased energy expenditure (Fig 30A), despite their leaner phenotype (Fig 28D) and the reduced energy expenditure in the fKO mice fed HFD (Fig 20A). These mice were significantly more active than Cre-null CREB3L3 FLEx-AAV-injected control mice (Fig 30C), which could contribute to their leaner phenotype.

We also may not have observed changes in energy expenditure due to one of the limitations of our approach to inducing overexpression via AAV injection. The AAV virus was injected into mice at 5 weeks of age when the inguinal fat depot is still developing and expanding. As the inguinal fat continues to expand in these adolescent mice, especially as they undergo high-fat feeding, many more adipocytes differentiate from adipose-derived stem cells. Adipocytes do not proliferate, but do turnover due to adipocyte death, especially when under dietary stress [207]. Therefore, the proportion of adipocytes that overexpress our gene of interest likely decreases over the course of dietary treatment. After monitoring the body weight during 12 weeks of high-fat feeding, then performing tolerance tests, the pool of adipocytes in the sOE inguinal fat that still overexpressed CREB3L3 when the sOE mice underwent indirect calorimetry measurements was likely diminished. Despite these limitations, the sOE mice maintained their resistance to diet-induced obesity, and still exhibited reduced fat mass and improved glucose tolerance and insulin sensitivity after the 12 weeks of high-fat feeding, despite consuming more food relative to body weight (Figure 30D). However, optimization of our FLEx-AAV system is needed in order to achieve better metabolic characterizations of the resultant mouse models.

Additionally, the sOE mice also had a higher RER than controls, signifying a global preference for carbohydrate utilization (Fig 30B), as well as elevated circulating ketone bodies (Fig 30E). This is the opposite of the lipid preference observed in the fKO mice following chow and high-fat feeding. Since ketone bodies are produced in the liver [93], this suggests the presence of a CREB3L3-dependent crosstalk mechanism by which adipose tissue inhibits hepatic fatty acid oxidation and ketone body production, which requires further investigation. Together, our findings in this chapter describe a new

approach to fat depot-specific genetic modification, as well as establish CREB3L3 as an anti-obesogenic factor.

VII. General Conclusions and Future Directions

Body weight regulation has become a crucial public health issue over the past few decades and as of 2015-2016, 39.6 percent of American adults are obese [50]. Due to the substantial contributions of brown and beige fat to body weight reduction as both high energy-usage tissues and as endocrine organs, they have been the targets of recent therapeutic investigation [12]. Additionally, the chronic low-level inflammation that occurs in the adipose tissue during obesity spurs the development of metabolic syndrome and a host of deadly comorbidities [51]. While increased adiposity typically leads to deleterious changes in whole-body metabolism, the expansion of different adipose tissues does not contribute equally to the development of metabolic dysfunction. It is well-known that expansion of visceral adipose tissue is associated with metabolic dysfunction, whereas subcutaneous adipose expansion might even be protective [52]. It has been shown that visceral and subcutaneous adipocytes are derived from different developmental origins [53], but studies investigating the differences between mature subcutaneous and visceral adipocytes are lacking.

In this study, we discovered that adipose expression of CREB3L3 is differentially modulated by these tissues during obesity. Previous studies reported the expression levels of CREB3L3 in a variety of tissues, but did not examine the expression of this ER-bound transcription factor in adipose tissues [17; 26; 54]. Here we report that CREB3L3 is not a liver-specific protein, and both CREB3L3 message and protein can be detected in the subcutaneous, brown, and multiple visceral adipose tissues (Fig 9A-C). In addition to being present in the adipose tissue, we also found that CREB3L3 is selectively downregulated in the human and murine subcutaneous fat during obesity, while the expression in the visceral fat is largely unchanged (Fig 8A-C). This differential expression

pattern is caused by the elevated ER stress occurring in obese adipose tissues [243], and further investigation is needed to identify the exact mechanism responsible for this differential expression. These findings led us to hypothesize that the downregulation of CREB3L3 in obese subcutaneous fat could contribute to the divergent metabolic profiles of subcutaneous and visceral fat during obesity.

Using *in vivo* fat-specific ablation of this transcription factor, we have identified the contributions of CREB3L3 to both subcutaneous and visceral adipose biology. In the subcutaneous fat, the ablation of CREB3L3 leads to a reduction in the ability of the tissue to undergo browning and perform adaptive thermogenesis, leading to a blunted basal metabolic rate in obese fKO mice. In the visceral fat, the ablation of CREB3L3 leads to enhanced macrophage infiltration, altered adipokine expression, and increased inflammatory cytokines in the obese state. These are key features of each subtype of white adipose tissue and the enhanced adiposity and hepatic insulin resistance observed in the fKO mice following high-fat feeding suggests that the modulation of CREB3L3 and its activity can have substantial effects on the global metabolic homeostasis of obese mice.

Another potential role that CREB3L3 plays in obese adipose tissue is the differential regulation of lipolysis and lipid synthesis in the inguinal and epididymal fat. CREB3L3 has previously been shown to suppress lipogenesis in the liver by suppressing SREBP1c expression [218]. While we observed a concordant disinhibition of lipogenesis and SREBP1c expression in the inguinal and brown fat of fKO mice after high-fat feeding, genes involved in lipid synthesis were actually downregulated in the fKO epididymal fat during obesity. Similarly, genes important to lipolysis were downregulated in the obese epididymal fat, but their expression was unchanged in the inguinal fat of the fKO mice.

This differential regulation of lipid metabolism in the inguinal and epididmyal fat during obesity suggests that CREB3L3 could contribute to the unique metabolic profiles of subcutaneous and visceral adipose tissue during obesity. This potential role of CREB3L3 in adipose tissue heterogeneity deserves further investigation.

One of the reasons we do not fully understand the heterogeneity between subcutaneous and visceral adipocytes is the difficulty in producing fat-depot specific genetic manipulations. This is due to the lack of depot-specific genes from which the promoter can be used to drive the expression of Cre recombinase. In this study, we describe the creation of a subcutaneous fat-specific overexpression model via injection of a CREB3L3 FLEx-AAV directly into the subcutaneous fat pads of mice expressing Adiponectin Cre (Fig 27F). Adipose-specific viral transductions have proven to be difficult due to the tendency for viral vectors to transduce non-adipocyte cell types and the size of the adiponectin promoter is prohibitive when working with the smaller packaging capacity of AAVs. Previously, groups have cloned “mini” aP2 promoters [55] or micro RNAs into the AAV vectors to prevent off-target expression in the heart and liver [56]. Our system makes use of an inverted reading frame of interest to prevent expression in non-adipocytes. Since the element needed for adipocyte specificity is programmed into the adipocytes themselves, the investigator is afforded more cloning flexibility and does not need to accommodate any adipose-specific elements into the AAV. To our knowledge, this is the first demonstration of using a viral vector in conjunction with adiponectin-Cre to manipulate gene expression in a specific fat depot.

Using this overexpression system, we created a CREB3L3 subcutaneous fat-specific overexpression model (sOE). These mice were resistant to diet-induced obesity, further demonstrating the importance of CREB3L3 in body weight regulation. One of the

unique features of our overexpression system is the degree to which our gene of interest is overexpressed. Whereas many transgenic and viral-induced overexpression systems force expression to supraphysiological levels that drastically alter cellular biology, our FLEx-AAV system induced a more modest 2-fold increase in CREB3L3 expression (Fig 27F). This may be due to the added recombination and inversion step, which further reduces the probability of reading frame induction beyond the necessary adipocyte AAV transduction. The reduced amplitude of overexpression that occurs in our system as a result highlights the physiological relevance of fluctuations in CREB3L3 expression and the robustness of the sOE phenotype that arose from this relatively small change in gene expression underpins the ability of CREB3L3 to modulate body weight.

Given the advance in the ability to create fat depot-specific genetic modifications, while using larger genetic elements in that our FLEx-AAV technology represents, I cannot help but be excited about its research potential. Improving our ability to target gene expression modulation to a specific fat depot has the potential to highlight the mechanisms that define the variety of behaviors that different fat depots exhibit. This concept affords investigators the flexibility to up or downregulate expression of a target gene in any fat depot (surgical limitations apply) under any physiological or pathological condition. While optimization is needed to ensure that changes in target gene expression are maintained over time as the tissue expands and adipocytes turn over, our sOE mice demonstrate the potential of this technique to isolate the effects of a gene within specific fat depots. Based on our findings, it would be interesting to determine if CREB3L3 sOE increases the ability of iWAT adipocytes to form beige cells in response to β3-adrengergic stimulation. Ultimately, injecting the CREB3L3-FLEx-AAV into the iWAT of obese Adipo-Cre mice would be the most clinically relevant experiment in future investigations and

would demonstrate the ability of CREB3L3 activity in subcutaneous adipocytes to induce weight loss in an already obese animal.

The resistance of sOE mice to diet-induced obesity, when coupled with enhancement of diet-induced obesity in the fKO mice demonstrated the important role that CREB3L3 plays in body weight and fat mass regulation. While the blunting of adaptive thermogenesis in the fKO subcutaneous fat appears to contribute to this phenomenon, the exact mechanism underpinning the body weight regulatory effects of CREB3L3 requires further study. Additionally, the enhanced inflammation within the epididymal fat of the fKO mice during obesity suggests that CREB3L3 could play a role in limiting the extent of inflammation within obese visceral fat. Further investigation into the role of CREB3L3 in the regulation of adipose inflammation is needed. Together, through its contributions to regulating both adiposity and inflammation, we have identified the importance of CREB3L3 in the transcriptional control of the behavior of adipose tissue during obesity.

In my concluding thoughts, I have realized that my research has furthered our understanding of adipose tissue biology and led to the creation of a novel technique that could improve the way we study the heterogeneity of adipose tissue. We discovered that this transcription factor with key roles in hepatic lipid metabolism is present in adipose tissue and a modest increase in its expression using that technique afforded mice resistance to diet-induced obesity. With a better understanding of how CREB3L3 activity is regulated in adipocytes, perhaps an agonist of this anti-obesogenic factor could be developed as a sorely-needed weight loss therapeutic to limit the burden of obesity on the individual and society.

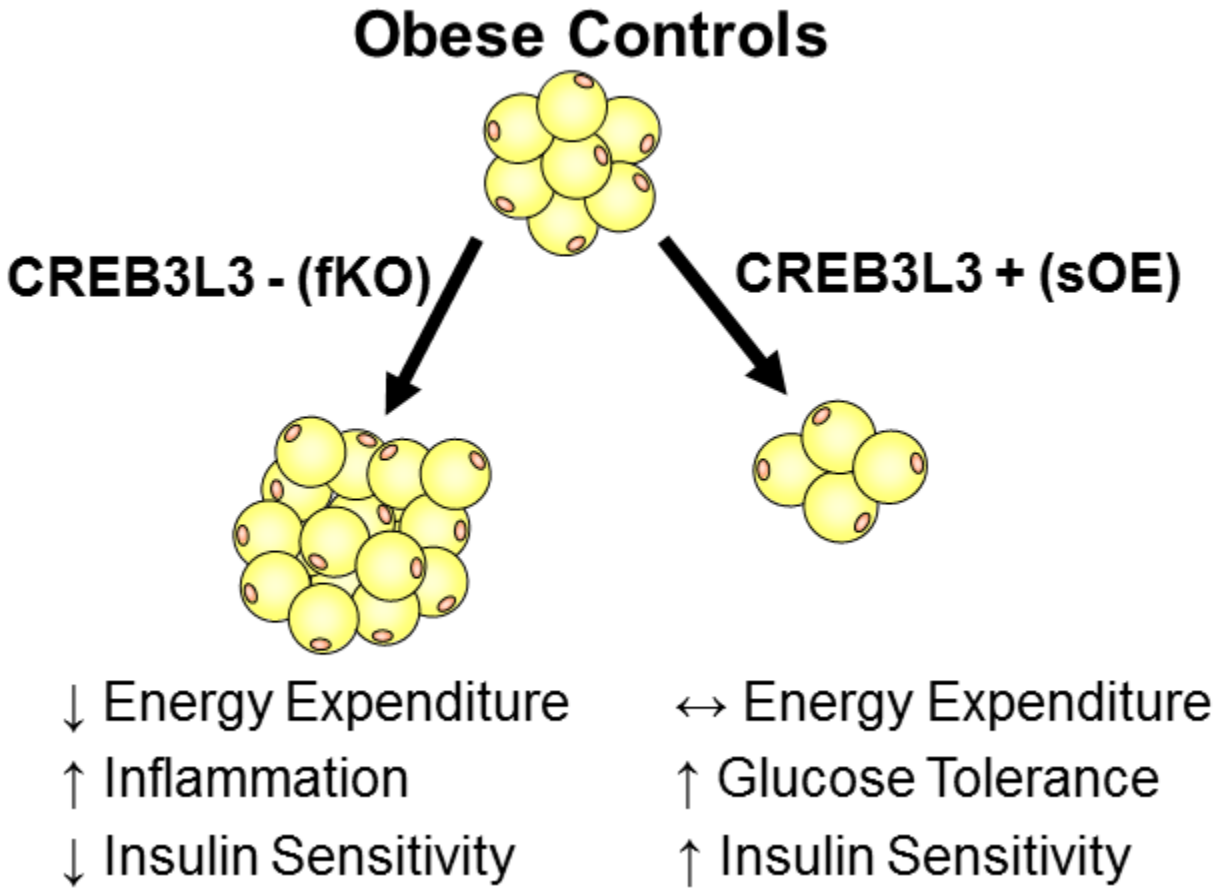

Figure 31: Summary of the effects that CREB3L3 modulation has on energy and metabolic homeostasis.

VIII. Appendices

Copyright Clearance Center Marketplace™

The Company of Biologists Ltd. - License Terms and Conditions

This is a License Agreement between Maximilian McCann ("You") and The Company of Biologists Ltd. ("Publisher") provided by Copyright Clearance Center ("CCC"). The license consists of your order details, the terms and conditions provided by The Company of Biologists Ltd., and the CCC terms and conditions.

All payments must be made in full to CCC.

Order Date	04-Mar-2021	Type of Use	Republish in a thesis/dissertation
Order license ID	1101846-1		
ISSN	1477-9129	Publisher	COMPANY OF BIOLOGISTS,
		Portion	Image/photo/illustration

LICENSED CONTENT

Publication Title	Development	Country	United Kingdom of Great Britain and Northern Ireland
Author/Editor	Company of Biologists.		
Date	12/31/1986	Rightsholder	The Company of Biologists Ltd.
Language	English		
		Publication Type	e-Journal
		URL	http://dev.biologists.org/

REQUEST DETAILS

Portion Type	Image/photo/illustration	Distribution	United States
Number of images / photos / illustrations	1	Translation	Original language of publication
Format (select all that apply)	Print, Electronic	Copies for the disabled?	No
		Minor editing privileges?	No
Who will republish the content?	Academic institution	Incidental promotional use?	No
Duration of Use	Life of current edition	Currency	USD
Lifetime Unit Quantity	Up to 499		
Rights Requested	Main product		

NEW WORK DETAILS

Title	The Role of CREB3L3 in Adipose Biology and Obesity	Institution name	University of Illinois at Chicago
		Expected presentation date	2021-03-18
Instructor name	Maximilian McCann		

ADDITIONAL DETAILS

Order reference number	N/A

ELSEVIER LICENSE TERMS AND CONDITIONS

Mar 23, 2021

This Agreement between Mr. Maximilian McCann ("You") and Elsevier ("Elsevier") consists of your license details and the terms and conditions provided by Elsevier and Copyright Clearance Center.

License Number	5006171295631
License date	Feb 11, 2021
Licensed Content Publisher	Elsevier
Licensed Content Publication	Cell Metabolism
Licensed Content Title	SnapShot: Niche Determines Adipocyte Character I
Licensed Content Author	Devika P. Bagchi,Isabel Forss,Susanne Mandrup,Ormond A. MacDougald
Licensed Content Date	Jan 9, 2018
Licensed Content Volume	27
Licensed Content Issue	1
Licensed Content Pages	2
Start Page	264
End Page	264.e1
Type of Use	reuse in a thesis/dissertation
Portion	figures/tables/illustrations
Number of figures/tables/illustrations	1
Format	both print and electronic
Are you the author of this Elsevier article?	No
Will you be translating?	No
Title	The role of CREB3L3 in adipose biology and obesity
Institution name	University of Illinois at Chicago
Expected presentation date	Mar 2021
Portions	Figure 1
Requestor Location	Mr. Maximilian McCann 531 W Deming Pl Apt 520 CHICAGO, IL 60614 United States Attn: Mr. Maximilian McCann
Publisher Tax ID	98-0397604
Total	**0.00 USD**
Terms and Conditions	

INTRODUCTION

1. The publisher for this copyrighted material is Elsevier. By clicking "accept" in connection with completing this licensing transaction, you agree that the following terms and conditions apply to this transaction (along with the Billing and Payment terms and conditions established by Copyright Clearance Center, Inc. ("CCC"), at the time that you opened your Rightslink account and that are available at any time at http://myaccount.copyright.com).

GENERAL TERMS

2. Elsevier hereby grants you permission to reproduce the aforementioned material subject to the terms and conditions indicated.

SPRINGER NATURE LICENSE TERMS AND CONDITIONS

Mar 23, 2021

This Agreement between Mr. Maximilian McCann ("You") and Springer Nature ("Springer Nature") consists of your license details and the terms and conditions provided by Springer Nature and Copyright Clearance Center.

License Number	5022091026460
License date	Mar 04, 2021
Licensed Content Publisher	Springer Nature
Licensed Content Publication	Nature Medicine
Licensed Content Title	Brown and beige fat: development, function and therapeutic potential
Licensed Content Author	Matthew Harms et al
Licensed Content Date	Sep 29, 2013
Type of Use	Thesis/Dissertation
Requestor type	academic/university or research institute
Format	print and electronic
Portion	figures/tables/illustrations
Number of figures/tables/illustrations	1
High-res required	no
Will you be translating?	no
Circulation/distribution	1 - 29
Author of this Springer Nature content	no
Title	The role of CREB3L3 in adipose biology and obesity
Institution name	University of Illinois at Chicago
Expected presentation date	Mar 2021
Portions	Figure 3
Requestor Location	Mr. Maximilian McCann 531 W Deming Pl Apt 520 CHICAGO, IL 60614 United States Attn: Mr. Maximilian McCann
Total	**0.00 USD**
Terms and Conditions	

Springer Nature Customer Service Centre GmbH
Terms and Conditions

This agreement sets out the terms and conditions of the licence (the **Licence**) between you and **Springer Nature Customer Service Centre GmbH** (the **Licensor**). By clicking 'accept' and completing the transaction for the material (**Licensed Material**), you also confirm your acceptance of these terms and conditions.

1. Grant of License

1. 1. The Licensor grants you a personal, non-exclusive, non-transferable, world-wide licence to reproduce the Licensed Material for the purpose specified in your order only. Licences are granted for the specific use requested in the order and for no other use, subject to the conditions below.

Copyright Clearance Center Marketplace™

American Society for Clinical Investigation - License Terms and Conditions

This is a License Agreement between Maximilian McCann ("You") and American Society for Clinical Investigation ("Publisher") provided by Copyright Clearance Center ("CCC"). The license consists of your order details, the terms and conditions provided by American Society for Clinical Investigation, and the CCC terms and conditions.

All payments must be made in full to CCC.

Order Date	04-Mar-2021	Type of Use	Republish in a thesis/dissertation
Order license ID	1101845-1		
ISSN	0021-9738	Publisher	AMERICAN SOCIETY FOR CLINICAL INVESTIGATION
		Portion	Image/photo/illustration

LICENSED CONTENT

Publication Title	The journal of clinical investigation	Country	United States of America
		Rightsholder	American Society for Clinical Investigation
Author/Editor	AMERICAN SOCIETY FOR CLINICAL INVESTIGATION., Robinson, George Canby	Publication Type	Journal
Date	12/31/1923		
Language	English		

REQUEST DETAILS

Portion Type	Image/photo/illustration	Distribution	United States
Number of images / photos / illustrations	1	Translation	Original language of publication
Format (select all that apply)	Print, Electronic	Copies for the disabled?	No
		Minor editing privileges?	No
Who will republish the content?	Academic institution	Incidental promotional use?	No
Duration of Use	Life of current edition	Currency	USD
Lifetime Unit Quantity	Up to 499		
Rights Requested	Main product		

NEW WORK DETAILS

Title	The Role of CREB3L3 in Adipose Biology and Obesity	Institution name	University of Illinois at Chicago
		Expected presentation date	2021-03-18
Instructor name	Maximilian McCann		

ADDITIONAL DETAILS

Order reference number	N/A

ELSEVIER LICENSE TERMS AND CONDITIONS

Mar 23, 2021

This Agreement between Mr. Maximilian McCann ("You") and Elsevier ("Elsevier") consists of your license details and the terms and conditions provided by Elsevier and Copyright Clearance Center.

License Number	5022100885230
License date	Mar 04, 2021
Licensed Content Publisher	Elsevier
Licensed Content Publication	Cell
Licensed Content Title	Endoplasmic Reticulum Stress Activates Cleavage of CREBH to Induce a Systemic Inflammatory Response
Licensed Content Author	Kezhong Zhang,Xiaohua Shen,Jun Wu,Kenjiro Sakaki,Thomas Saunders,D. Thomas Rutkowski,Sung Hoon Back,Randal J. Kaufman
Licensed Content Date	Feb 10, 2006
Licensed Content Volume	124
Licensed Content Issue	3
Licensed Content Pages	13
Start Page	587
End Page	599
Type of Use	reuse in a thesis/dissertation
Portion	figures/tables/illustrations
Number of figures/tables/illustrations	2
Format	both print and electronic
Are you the author of this Elsevier article?	No
Will you be translating?	No
Title	The role of CREB3L3 in adipose biology and obesity
Institution name	University of Illinois at Chicago
Expected presentation date	Mar 2021
Portions	Figure 1 & Figure 7
Requestor Location	Mr. Maximilian McCann 531 W Deming Pl Apt 520 CHICAGO, IL 60614 United States Attn: Mr. Maximilian McCann
Publisher Tax ID	98-0397604
Total	**0.00 USD**
Terms and Conditions	

INTRODUCTION

1. The publisher for this copyrighted material is Elsevier. By clicking "accept" in connection with completing this licensing transaction, you agree that the following terms and conditions apply to this transaction (along with the Billing and Payment terms and conditions established by Copyright Clearance Center, Inc. ("CCC"), at the time that you opened your Rightslink account and that are available at any time at http://myaccount.copyright.com).

GENERAL TERMS

JOHN WILEY AND SONS LICENSE TERMS AND CONDITIONS

Mar 23, 2021

This Agreement between Mr. Maximilian McCann ("You") and John Wiley and Sons ("John Wiley and Sons") consists of your license details and the terms and conditions provided by John Wiley and Sons and Copyright Clearance Center.

License Number	5022101067795
License date	Mar 04, 2021
Licensed Content Publisher	John Wiley and Sons
Licensed Content Publication	Hepatology
Licensed Content Title	Hepatocyte nuclear factor 4α is implicated in endoplasmic reticulum stress–induced acute phase response by regulating expression of cyclic adenosine monophosphate responsive element binding protein H
Licensed Content Author	Stephen A. Duncan, Randal J. Kaufman, Jixuan Li, et al
Licensed Content Date	Sep 26, 2008
Licensed Content Volume	48
Licensed Content Issue	4
Licensed Content Pages	9
Type of Use	Dissertation/Thesis
Requestor type	University/Academic
Format	Print and electronic
Portion	Figure/table
Number of figures/tables	1
Will you be translating?	No
Title	The role of CREB3L3 in adipose biology and obesity
Institution name	University of Illinois at Chicago
Expected presentation date	Mar 2021
Portions	Figure 2A
Requestor Location	Mr. Maximilian McCann 531 W Deming Pl Apt 520 CHICAGO, IL 60614 United States Attn: Mr. Maximilian McCann
Publisher Tax ID	EU826007151
Total	**0.00 USD**
Terms and Conditions	

TERMS AND CONDITIONS

This copyrighted material is owned by or exclusively licensed to John Wiley & Sons, Inc. or one of its group companies (each a"Wiley Company") or handled on behalf of a society with which a Wiley Company has exclusive publishing rights in relation to a particular work (collectively "WILEY"). By clicking "accept" in connection with completing this licensing transaction, you agree that the following terms and conditions apply to this transaction (along with the billing and payment terms and conditions established by the Copyright Clearance Center Inc., ("CCC's Billing and Payment terms and conditions"), at the time that you opened your RightsLink account (these are available at any time at http://myaccount.copyright.com).

Terms and Conditions

IX. Cited Literature

[1] Zhang, K., Shen, X., Wu, J., Sakaki, K., Saunders, T., Rutkowski, D.T., et al., 2006. Endoplasmic reticulum stress activates cleavage of CREBH to induce a systemic inflammatory response. Cell 124(3):587-599.
[2] Luebke-Wheeler, J., Zhang, K., Battle, M., Si-Tayeb, K., Garrison, W., Chhinder, S., et al., 2008. Hepatocyte nuclear factor 4alpha is implicated in endoplasmic reticulum stress-induced acute phase response by regulating expression of cyclic adenosine monophosphate responsive element binding protein H. Hepatology 48(4):1242-1250.
[3] Hales CM, C.M., Fryar CD, Ogden CL, 2017. Prevalence of obesity among adults and youth: United States, 2015–2016, NCHS data brief. National Center for Health Statistics, Hyattsville, MD.
[4] Bagchi, D.P., Forss, I., Mandrup, S., MacDougald, O.A., 2018. SnapShot: Niche Determines Adipocyte Character I. Cell Metab 27(1):264-264.e261.
[5] Harms, M., Seale, P., 2013. Brown and beige fat: development, function and therapeutic potential. Nat Med 19(10):1252-1263.
[6] Shoelson, S.E., Lee, J., Goldfine, A.B., 2006. Inflammation and insulin resistance. J Clin Invest 116(7):1793-1801.
[7] Rutkowski, J.M., Stern, J.H., Scherer, P.E., 2015. The cell biology of fat expansion. J Cell Biol 208(5):501-512.
[8] Tam, P.P., Loebel, D.A., 2007. Gene function in mouse embryogenesis: get set for gastrulation. Nat Rev Genet 8(5):368-381.
[9] Flemming, W., 1871. Ueber Bildung und Rückbildung der Fettzelle im Bindegewebe, und Bemerkungen über die Structur des Letzteren. Archiv für mikroskopische Anatomie 7(1):32-80.
[10] Flemming, W., 1879. Beitrage zur Kenntniss der Zelle und ihrer Lebenserscheinungen. Archiv für mikroskopische Anatomie 16(1):302-436.
[11] Billon, N., Iannarelli, P., Monteiro, M.C., Glavieux-Pardanaud, C., Richardson, W.D., Kessaris, N., et al., 2007. The generation of adipocytes by the neural crest. Development 134(12):2283-2292.
[12] Sebo, Z.L., Rodeheffer, M.S., 2019. Assembling the adipose organ: adipocyte lineage segregation and adipogenesis in vivo. Development 146(7).
[13] Tajbakhsh, S., Spörle, R., 1998. Somite development: constructing the vertebrate body. Cell 92(1):9-16.
[14] Sanchez-Gurmaches, J., Guertin, D.A., 2014. Adipocytes arise from multiple lineages that are heterogeneously and dynamically distributed. Nat Commun 5:4099.
[15] Sanchez-Gurmaches, J., Hung, C.M., Sparks, C.A., Tang, Y., Li, H., Guertin, D.A., 2012. PTEN loss in the Myf5 lineage redistributes body fat and reveals subsets of white adipocytes that arise from Myf5 precursors. Cell Metab 16(3):348-362.
[16] Teboul, L., Hadchouel, J., Daubas, P., Summerbell, D., Buckingham, M., Rigby, P.W., 2002. The early epaxial enhancer is essential for the initial expression of the skeletal muscle determination gene Myf5 but not for subsequent, multiple phases of somitic myogenesis. Development 129(19):4571-4580.
[17] Jukkola, T., Trokovic, R., Maj, P., Lamberg, A., Mankoo, B., Pachnis, V., et al., 2005. Meox1Cre: a mouse line expressing Cre recombinase in somitic mesoderm. Genesis 43(3):148-153.
[18] Sebo, Z.L., Jeffery, E., Holtrup, B., Rodeheffer, M.S., 2018. A mesodermal fate map for adipose tissue. Development 145(17).
[19] Chau, Y.Y., Bandiera, R., Serrels, A., Martínez-Estrada, O.M., Qing, W., Lee, M., et al., 2014. Visceral and subcutaneous fat have different origins and evidence supports a mesothelial source. Nat Cell Biol 16(4):367-375.
[20] Krueger, K.C., Costa, M.J., Du, H., Feldman, B.J., 2014. Characterization of Cre recombinase activity for in vivo targeting of adipocyte precursor cells. Stem Cell Reports 3(6):1147-1158.
[21] Sanchez-Gurmaches, J., Hsiao, W.Y., Guertin, D.A., 2015. Highly selective in vivo labeling of subcutaneous white adipocyte precursors with Prx1-Cre. Stem Cell Reports 4(4):541-550.

[22] Rosen, E.D., Spiegelman, B.M., 2014. What we talk about when we talk about fat. Cell 156(1-2):20-44.
[23] Gupta, R.K., Arany, Z., Seale, P., Mepani, R.J., Ye, L., Conroe, H.M., et al., 2010. Transcriptional control of preadipocyte determination by Zfp423. Nature 464(7288):619-623.
[24] Kang, S., Akerblad, P., Kiviranta, R., Gupta, R.K., Kajimura, S., Griffin, M.J., et al., 2012. Regulation of early adipose commitment by Zfp521. PLoS Biol 10(11):e1001433.
[25] Okamura, M., Kudo, H., Wakabayashi, K., Tanaka, T., Nonaka, A., Uchida, A., et al., 2009. COUP-TFII acts downstream of Wnt/beta-catenin signal to silence PPARgamma gene expression and repress adipogenesis. Proc Natl Acad Sci U S A 106(14):5819-5824.
[26] Xu, Z., Yu, S., Hsu, C.H., Eguchi, J., Rosen, E.D., 2008. The orphan nuclear receptor chicken ovalbumin upstream promoter-transcription factor II is a critical regulator of adipogenesis. Proc Natl Acad Sci U S A 105(7):2421-2426.
[27] Kanazawa, A., Tsukada, S., Kamiyama, M., Yanagimoto, T., Nakajima, M., Maeda, S., 2005. Wnt5b partially inhibits canonical Wnt/beta-catenin signaling pathway and promotes adipogenesis in 3T3-L1 preadipocytes. Biochem Biophys Res Commun 330(2):505-510.
[28] Garten, A., Schuster, S., Kiess, W., 2012. The insulin-like growth factors in adipogenesis and obesity. Endocrinol Metab Clin North Am 41(2):283-295, v-vi.
[29] Qiang, G., Whang Kong, H., Xu, S., Pham, H.A., Parlee, S.D., Burr, A.A., et al., 2016. Lipodystrophy and severe metabolic dysfunction in mice with adipose tissue-specific insulin receptor ablation. Mol Metab 5(7):480-490.
[30] Rosen, E.D., MacDougald, O.A., 2006. Adipocyte differentiation from the inside out. Nat Rev Mol Cell Biol 7(12):885-896.
[31] Hu, E., Tontonoz, P., Spiegelman, B.M., 1995. Transdifferentiation of myoblasts by the adipogenic transcription factors PPAR gamma and C/EBP alpha. Proc Natl Acad Sci U S A 92(21):9856-9860.
[32] Tontonoz, P., Hu, E., Spiegelman, B.M., 1994. Stimulation of adipogenesis in fibroblasts by PPAR gamma 2, a lipid-activated transcription factor. Cell 79(7):1147-1156.
[33] Mikkelsen, T.S., Xu, Z., Zhang, X., Wang, L., Gimble, J.M., Lander, E.S., et al., 2010. Comparative epigenomic analysis of murine and human adipogenesis. Cell 143(1):156-169.
[34] Schmidt, S.F., Jørgensen, M., Chen, Y., Nielsen, R., Sandelin, A., Mandrup, S., 2011. Cross species comparison of C/EBPα and PPARγ profiles in mouse and human adipocytes reveals interdependent retention of binding sites. BMC Genomics 12:152.
[35] Soccio, R.E., Tuteja, G., Everett, L.J., Li, Z., Lazar, M.A., Kaestner, K.H., 2011. Species-specific strategies underlying conserved functions of metabolic transcription factors. Mol Endocrinol 25(4):694-706.
[36] Siersbæk, R., Nielsen, R., John, S., Sung, M.H., Baek, S., Loft, A., et al., 2011. Extensive chromatin remodelling and establishment of transcription factor 'hotspots' during early adipogenesis. Embo j 30(8):1459-1472.
[37] Rosen, E.D., Hsu, C.H., Wang, X., Sakai, S., Freeman, M.W., Gonzalez, F.J., et al., 2002. C/EBPalpha induces adipogenesis through PPARgamma: a unified pathway. Genes Dev 16(1):22-26.
[38] Wu, Z., Rosen, E.D., Brun, R., Hauser, S., Adelmant, G., Troy, A.E., et al., 1999. Cross-regulation of C/EBP alpha and PPAR gamma controls the transcriptional pathway of adipogenesis and insulin sensitivity. Mol Cell 3(2):151-158.
[39] Park, B.O., Ahrends, R., Teruel, M.N., 2012. Consecutive positive feedback loops create a bistable switch that controls preadipocyte-to-adipocyte conversion. Cell Rep 2(4):976-990.
[40] Lefterova, M.I., Zhang, Y., Steger, D.J., Schupp, M., Schug, J., Cristancho, A., et al., 2008. PPARgamma and C/EBP factors orchestrate adipocyte biology via adjacent binding on a genome-wide scale. Genes Dev 22(21):2941-2952.

[41] Chusyd, D.E., Wang, D., Huffman, D.M., Nagy, T.R., 2016. Relationships between Rodent White Adipose Fat Pads and Human White Adipose Fat Depots. Front Nutr 3:10.
[42] Manolopoulos, K.N., Karpe, F., Frayn, K.N., 2010. Gluteofemoral body fat as a determinant of metabolic health. Int J Obes (Lond) 34(6):949-959.
[43] Walker, G.E., Verti, B., Marzullo, P., Savia, G., Mencarelli, M., Zurleni, F., et al., 2007. Deep subcutaneous adipose tissue: a distinct abdominal adipose depot. Obesity (Silver Spring) 15(8):1933-1943.
[44] Lundbom, J., Hakkarainen, A., Lundbom, N., Taskinen, M.R., 2013. Deep subcutaneous adipose tissue is more saturated than superficial subcutaneous adipose tissue. Int J Obes (Lond) 37(4):620-622.
[45] Cancello, R., Zulian, A., Gentilini, D., Maestrini, S., Della Barba, A., Invitti, C., et al., 2013. Molecular and morphologic characterization of superficial- and deep-subcutaneous adipose tissue subdivisions in human obesity. Obesity (Silver Spring) 21(12):2562-2570.
[46] Kelley, D.E., Thaete, F.L., Troost, F., Huwe, T., Goodpaster, B.H., 2000. Subdivisions of subcutaneous abdominal adipose tissue and insulin resistance. Am J Physiol Endocrinol Metab 278(5):E941-948.
[47] Bagchi, D.P., Forss, I., Mandrup, S., MacDougald, O.A., 2018. SnapShot: Niche Determines Adipocyte Character II. Cell Metab 27(1):266-266.e261.
[48] Wilkosz, S., Ireland, G., Khwaja, N., Walker, M., Butt, R., de Giorgio-Miller, A., et al., 2005. A comparative study of the structure of human and murine greater omentum. Anat Embryol (Berl) 209(3):251-261.
[49] Bjørndal, B., Burri, L., Staalesen, V., Skorve, J., Berge, R.K., 2011. Different adipose depots: their role in the development of metabolic syndrome and mitochondrial response to hypolipidemic agents. J Obes 2011:490650.
[50] Zhang, Z., Shao, M., Hepler, C., Zi, Z., Zhao, S., An, Y.A., et al., 2019. Dermal adipose tissue has high plasticity and undergoes reversible dedifferentiation in mice. The Journal of Clinical Investigation 129(12):5327-5342.
[51] Alexander, C.M., Kasza, I., Yen, C.L., Reeder, S.B., Hernando, D., Gallo, R.L., et al., 2015. Dermal white adipose tissue: a new component of the thermogenic response. J Lipid Res 56(11):2061-2069.
[52] Pujol, E., Proenza, A.M., Roca, P., Lladó, I., 2006. Changes in mammary fat pad composition and lipolytic capacity throughout pregnancy. Cell Tissue Res 323(3):505-511.
[53] Prokesch, A., Smorlesi, A., Perugini, J., Manieri, M., Ciarmela, P., Mondini, E., et al., 2014. Molecular aspects of adipoepithelial transdifferentiation in mouse mammary gland. Stem Cells 32(10):2756-2766.
[54] Morison, R., 1906. Remarks ON SOME FUNCTIONS OF THE OMENTUM. Br Med J 1(2350):76-78.
[55] Meza-Perez, S., Randall, T.D., 2017. Immunological Functions of the Omentum. Trends Immunol 38(7):526-536.
[56] Bénézech, C., Luu, N.T., Walker, J.A., Kruglov, A.A., Loo, Y., Nakamura, K., et al., 2015. Inflammation-induced formation of fat-associated lymphoid clusters. Nat Immunol 16(8):819-828.
[57] Rabkin, S.W., 2007. Epicardial fat: properties, function and relationship to obesity. Obes Rev 8(3):253-261.
[58] Sacks, H.S., Fain, J.N., Holman, B., Cheema, P., Chary, A., Parks, F., et al., 2009. Uncoupling protein-1 and related messenger ribonucleic acids in human epicardial and other adipose tissues: epicardial fat functioning as brown fat. J Clin Endocrinol Metab 94(9):3611-3615.
[59] Iacobellis, G., 2015. Local and systemic effects of the multifaceted epicardial adipose tissue depot. Nat Rev Endocrinol 11(6):363-371.
[60] Begaye, L., Simcox, J.A., 2019. Intramuscular adipocytes: a buried adipose tissue depot deserving more exploration. J Lipid Res 60(4):753-754.

[61] Greenberg, A.S., Coleman, R.A., Kraemer, F.B., McManaman, J.L., Obin, M.S., Puri, V., et al., 2011. The role of lipid droplets in metabolic disease in rodents and humans. J Clin Invest 121(6):2102-2110.
[62] Bays, H.E., González-Campoy, J.M., Bray, G.A., Kitabchi, A.E., Bergman, D.A., Schorr, A.B., et al., 2008. Pathogenic potential of adipose tissue and metabolic consequences of adipocyte hypertrophy and increased visceral adiposity. Expert Rev Cardiovasc Ther 6(3):343-368.
[63] Jacquier, N., Choudhary, V., Mari, M., Toulmay, A., Reggiori, F., Schneiter, R., 2011. Lipid droplets are functionally connected to the endoplasmic reticulum in Saccharomyces cerevisiae. J Cell Sci 124(Pt 14):2424-2437.
[64] Kassan, A., Herms, A., Fernández-Vidal, A., Bosch, M., Schieber, N.L., Reddy, B.J., et al., 2013. Acyl-CoA synthetase 3 promotes lipid droplet biogenesis in ER microdomains. J Cell Biol 203(6):985-1001.
[65] Walther, T.C., Chung, J., Farese, R.V., Jr., 2017. Lipid Droplet Biogenesis. Annu Rev Cell Dev Biol 33:491-510.
[66] Kuerschner, L., Moessinger, C., Thiele, C., 2008. Imaging of lipid biosynthesis: how a neutral lipid enters lipid droplets. Traffic 9(3):338-352.
[67] Stone, S.J., Levin, M.C., Zhou, P., Han, J., Walther, T.C., Farese, R.V., Jr., 2009. The endoplasmic reticulum enzyme DGAT2 is found in mitochondria-associated membranes and has a mitochondrial targeting signal that promotes its association with mitochondria. J Biol Chem 284(8):5352-5361.
[68] Wilfling, F., Wang, H., Haas, J.T., Krahmer, N., Gould, T.J., Uchida, A., et al., 2013. Triacylglycerol synthesis enzymes mediate lipid droplet growth by relocalizing from the ER to lipid droplets. Dev Cell 24(4):384-399.
[69] Wilfling, F., Haas, J.T., Walther, T.C., Farese, R.V., Jr., 2014. Lipid droplet biogenesis. Curr Opin Cell Biol 29:39-45.
[70] Beller, M., Sztalryd, C., Southall, N., Bell, M., Jäckle, H., Auld, D.S., et al., 2008. COPI complex is a regulator of lipid homeostasis. PLoS Biol 6(11):e292.
[71] Guo, Y., Walther, T.C., Rao, M., Stuurman, N., Goshima, G., Terayama, K., et al., 2008. Functional genomic screen reveals genes involved in lipid-droplet formation and utilization. Nature 453(7195):657-661.
[72] Gong, J., Sun, Z., Wu, L., Xu, W., Schieber, N., Xu, D., et al., 2011. Fsp27 promotes lipid droplet growth by lipid exchange and transfer at lipid droplet contact sites. J Cell Biol 195(6):953-963.
[73] Chakravarty, B., Gu, Z., Chirala, S.S., Wakil, S.J., Quiocho, F.A., 2004. Human fatty acid synthase: Structure and substrate selectivity of the thioesterase domain. Proceedings of the National Academy of Sciences of the United States of America 101(44):15567.
[74] Green, C.D., Ozguden-Akkoc, C.G., Wang, Y., Jump, D.B., Olson, L.K., 2010. Role of fatty acid elongases in determination of de novo synthesized monounsaturated fatty acid species. J Lipid Res 51(7):1871-1877.
[75] Shimano, H., Shimomura, I., Hammer, R.E., Herz, J., Goldstein, J.L., Brown, M.S., et al., 1997. Elevated levels of SREBP-2 and cholesterol synthesis in livers of mice homozygous for a targeted disruption of the SREBP-1 gene. J Clin Invest 100(8):2115-2124.
[76] Herman, M.A., Peroni, O.D., Villoria, J., Schön, M.R., Abumrad, N.A., Blüher, M., et al., 2012. A novel ChREBP isoform in adipose tissue regulates systemic glucose metabolism. Nature 484(7394):333-338.
[77] Frühbeck, G., Méndez-Giménez, L., Fernández-Formoso, J.A., Fernández, S., Rodríguez, A., 2014. Regulation of adipocyte lipolysis. Nutr Res Rev 27(1):63-93.
[78] Sztalryd, C., Brasaemle, D.L., 2017. The perilipin family of lipid droplet proteins: Gatekeepers of intracellular lipolysis. Biochim Biophys Acta Mol Cell Biol Lipids 1862(10 Pt B):1221-1232.
[79] Lafontan, M., Langin, D., 2009. Lipolysis and lipid mobilization in human adipose tissue. Progress in Lipid Research 48(5):275-297.

[80] Bartness, T.J., Song, C.K., 2007. Thematic review series: Adipocyte Biology. Sympathetic and sensory innervation of white adipose tissue. Journal of Lipid Research 48(8):1655-1672.
[81] De Matteis, R., Arch, J.R.S., Petroni, M.L., Ferrari, D., Cinti, S., Stock, M.J., 2002. Immunohistochemical identification of the β3-adrenoceptor in intact human adipocytes and ventricular myocardium: effect of obesity and treatment with ephedrine and caffeine. International Journal of Obesity 26(11):1442-1450.
[82] Buemann, B., Toubro, S., Astrup, A., 2000. Effects of the two beta3-agonists, ZD7114 and ZD2079 on 24 hour energy expenditure and respiratory quotient in obese subjects. Int J Obes Relat Metab Disord 24(12):1553-1560.
[83] Redman, L.M., de Jonge, L., Fang, X., Gamlin, B., Recker, D., Greenway, F.L., et al., 2007. Lack of an effect of a novel beta3-adrenoceptor agonist, TAK-677, on energy metabolism in obese individuals: a double-blind, placebo-controlled randomized study. J Clin Endocrinol Metab 92(2):527-531.
[84] Lafontan, M., Berlan, M., 1995. Fat cell alpha 2-adrenoceptors: the regulation of fat cell function and lipolysis. Endocr Rev 16(6):716-738.
[85] Langin, D., 2006. Adipose tissue lipolysis as a metabolic pathway to define pharmacological strategies against obesity and the metabolic syndrome. Pharmacol Res 53(6):482-491.
[86] Jaworski, K., Sarkadi-Nagy, E., Duncan, R.E., Ahmadian, M., Sul, H.S., 2007. Regulation of triglyceride metabolism. IV. Hormonal regulation of lipolysis in adipose tissue. Am J Physiol Gastrointest Liver Physiol 293(1):G1-4.
[87] Yip, R.G.-C., Goodman, H.M., 1999. Growth Hormone and Dexamethasone Stimulate Lipolysis and Activate Adenylyl Cyclase in Rat Adipocytes by Selectively Shifting Giα2 to Lower Density Membrane Fractions*. Endocrinology 140(3):1219-1227.
[88] Lafontan, M., 2005. Fat cells: afferent and efferent messages define new approaches to treat obesity. Annu Rev Pharmacol Toxicol 45:119-146.
[89] Djurhuus, C.B., Gravholt, C.H., Nielsen, S., Mengel, A., Christiansen, J.S., Schmitz, O.E., et al., 2002. Effects of cortisol on lipolysis and regional interstitial glycerol levels in humans. Am J Physiol Endocrinol Metab 283(1):E172-177.
[90] Bousquet-Mélou, A., Galitzky, J., Lafontan, M., Berlan, M., 1995. Control of lipolysis in intra-abdominal fat cells of nonhuman primates: comparison with humans. J Lipid Res 36(3):451-461.
[91] Taniguchi, A., Kataoka, K., Kono, T., Oseko, F., Okuda, H., Nagata, I., et al., 1987. Parathyroid hormone-induced lipolysis in human adipose tissue. J Lipid Res 28(5):490-494.
[92] McCarty, M.F., Thomas, C.A., 2003. PTH excess may promote weight gain by impeding catecholamine-induced lipolysis-implications for the impact of calcium, vitamin D, and alcohol on body weight. Med Hypotheses 61(5-6):535-542.
[93] Puchalska, P., Crawford, P.A., 2017. Multi-dimensional Roles of Ketone Bodies in Fuel Metabolism, Signaling, and Therapeutics. Cell Metab 25(2):262-284.
[94] Jang, H.S., Noh, M.R., Kim, J., Padanilam, B.J., 2020. Defective Mitochondrial Fatty Acid Oxidation and Lipotoxicity in Kidney Diseases. Front Med (Lausanne) 7:65.
[95] McGarry, J.D., Brown, N.F., 1997. The mitochondrial carnitine palmitoyltransferase system. From concept to molecular analysis. Eur J Biochem 244(1):1-14.
[96] Malandrino, M.I., Fucho, R., Weber, M., Calderon-Dominguez, M., Mir, J.F., Valcarcel, L., et al., 2015. Enhanced fatty acid oxidation in adipocytes and macrophages reduces lipid-induced triglyceride accumulation and inflammation. Am J Physiol Endocrinol Metab 308(9):E756-769.
[97] Krishnan, J., Danzer, C., Simka, T., Ukropec, J., Walter, K.M., Kumpf, S., et al., 2012. Dietary obesity-associated Hif1α activation in adipocytes restricts fatty acid oxidation and energy expenditure via suppression of the Sirt2-NAD+ system. Genes Dev 26(3):259-270.
[98] Choo, H.J., Kim, J.H., Kwon, O.B., Lee, C.S., Mun, J.Y., Han, S.S., et al., 2006. Mitochondria are impaired in the adipocytes of type 2 diabetic mice. Diabetologia 49(4):784-791.

[99] Keller, M.P., Attie, A.D., 2010. Physiological insights gained from gene expression analysis in obesity and diabetes. Annu Rev Nutr 30:341-364.
[100] Ingalls, A.M., Dickie, M.M., Snell, G.D., 1950. Obese, a new mutation in the house mouse. J Hered 41(12):317-318.
[101] Coleman, D.L., 1973. Effects of parabiosis of obese with diabetes and normal mice. Diabetologia 9(4):294-298.
[102] Leinninger, G.M., Jo, Y.H., Leshan, R.L., Louis, G.W., Yang, H., Barrera, J.G., et al., 2009. Leptin acts via leptin receptor-expressing lateral hypothalamic neurons to modulate the mesolimbic dopamine system and suppress feeding. Cell Metab 10(2):89-98.
[103] Myers, M.G., Jr., Münzberg, H., Leinninger, G.M., Leshan, R.L., 2009. The geometry of leptin action in the brain: more complicated than a simple ARC. Cell Metab 9(2):117-123.
[104] La Cava, A., Matarese, G., 2004. The weight of leptin in immunity. Nat Rev Immunol 4(5):371-379.
[105] Carbone, F., La Rocca, C., Matarese, G., 2012. Immunological functions of leptin and adiponectin. Biochimie 94(10):2082-2088.
[106] Eguchi, J., Wang, X., Yu, S., Kershaw, E.E., Chiu, P.C., Dushay, J., et al., 2011. Transcriptional control of adipose lipid handling by IRF4. Cell Metab 13(3):249-259.
[107] Combs, T.P., Berg, A.H., Obici, S., Scherer, P.E., Rossetti, L., 2001. Endogenous glucose production is inhibited by the adipose-derived protein Acrp30. J Clin Invest 108(12):1875-1881.
[108] Goldstein, B.J., Scalia, R.G., Ma, X.L., 2009. Protective vascular and myocardial effects of adiponectin. Nat Clin Pract Cardiovasc Med 6(1):27-35.
[109] Yoon, M.J., Lee, G.Y., Chung, J.J., Ahn, Y.H., Hong, S.H., Kim, J.B., 2006. Adiponectin increases fatty acid oxidation in skeletal muscle cells by sequential activation of AMP-activated protein kinase, p38 mitogen-activated protein kinase, and peroxisome proliferator-activated receptor alpha. Diabetes 55(9):2562-2570.
[110] Ceddia, R.B., Somwar, R., Maida, A., Fang, X., Bikopoulos, G., Sweeney, G., 2005. Globular adiponectin increases GLUT4 translocation and glucose uptake but reduces glycogen synthesis in rat skeletal muscle cells. Diabetologia 48(1):132-139.
[111] Kim, J.Y., van de Wall, E., Laplante, M., Azzara, A., Trujillo, M.E., Hofmann, S.M., et al., 2007. Obesity-associated improvements in metabolic profile through expansion of adipose tissue. J Clin Invest 117(9):2621-2637.
[112] Wolf, A.M., Wolf, D., Rumpold, H., Enrich, B., Tilg, H., 2004. Adiponectin induces the anti-inflammatory cytokines IL-10 and IL-1RA in human leukocytes. Biochemical and Biophysical Research Communications 323(2):630-635.
[113] Steppan, C.M., Lazar, M.A., 2004. The current biology of resistin. J Intern Med 255(4):439-447.
[114] Savage, D.B., Sewter, C.P., Klenk, E.S., Segal, D.G., Vidal-Puig, A., Considine, R.V., et al., 2001. Resistin / Fizz3 expression in relation to obesity and peroxisome proliferator-activated receptor-gamma action in humans. Diabetes 50(10):2199-2202.
[115] Graham, T.E., Kahn, B.B., 2007. Tissue-specific alterations of glucose transport and molecular mechanisms of intertissue communication in obesity and type 2 diabetes. Horm Metab Res 39(10):717-721.
[116] Cao, H., Sekiya, M., Ertunc, M.E., Burak, M.F., Mayers, J.R., White, A., et al., 2013. Adipocyte lipid chaperone AP2 is a secreted adipokine regulating hepatic glucose production. Cell Metab 17(5):768-778.
[117] Timmons, J.A., Wennmalm, K., Larsson, O., Walden, T.B., Lassmann, T., Petrovic, N., et al., 2007. Myogenic gene expression signature establishes that brown and white adipocytes originate from distinct cell lineages. Proc Natl Acad Sci U S A 104(11):4401-4406.
[118] Heaton, J.M., 1972. The distribution of brown adipose tissue in the human. J Anat 112(Pt 1):35-39.

[119] Lidell, M.E., Betz, M.J., Dahlqvist Leinhard, O., Heglind, M., Elander, L., Slawik, M., et al., 2013. Evidence for two types of brown adipose tissue in humans. Nat Med 19(5):631-634.
[120] Symonds, M.E., 2013. Brown adipose tissue growth and development. Scientifica (Cairo) 2013:305763.
[121] Cannon, B., Nedergaard, J., 2004. Brown adipose tissue: function and physiological significance. Physiol Rev 84(1):277-359.
[122] Virtanen, K.A., Lidell, M.E., Orava, J., Heglind, M., Westergren, R., Niemi, T., et al., 2009. Functional brown adipose tissue in healthy adults. N Engl J Med 360(15):1518-1525.
[123] van Marken Lichtenbelt, W.D., Vanhommerig, J.W., Smulders, N.M., Drossaerts, J.M., Kemerink, G.J., Bouvy, N.D., et al., 2009. Cold-activated brown adipose tissue in healthy men. N Engl J Med 360(15):1500-1508.
[124] Saito, M., Okamatsu-Ogura, Y., Matsushita, M., Watanabe, K., Yoneshiro, T., Nio-Kobayashi, J., et al., 2009. High incidence of metabolically active brown adipose tissue in healthy adult humans: effects of cold exposure and adiposity. Diabetes 58(7):1526-1531.
[125] Cohade, C., Mourtzikos, K.A., Wahl, R.L., 2003. "USA-Fat": prevalence is related to ambient outdoor temperature-evaluation with 18F-FDG PET/CT. J Nucl Med 44(8):1267-1270.
[126] Cao, W., Daniel, K.W., Robidoux, J., Puigserver, P., Medvedev, A.V., Bai, X., et al., 2004. p38 mitogen-activated protein kinase is the central regulator of cyclic AMP-dependent transcription of the brown fat uncoupling protein 1 gene. Mol Cell Biol 24(7):3057-3067.
[127] Puigserver, P., Wu, Z., Park, C.W., Graves, R., Wright, M., Spiegelman, B.M., 1998. A cold-inducible coactivator of nuclear receptors linked to adaptive thermogenesis. Cell 92(6):829-839.
[128] Tiraby, C., Tavernier, G., Lefort, C., Larrouy, D., Bouillaud, F., Ricquier, D., et al., 2003. Acquirement of brown fat cell features by human white adipocytes. J Biol Chem 278(35):33370-33376.
[129] Ricquier, D., 2011. Uncoupling protein 1 of brown adipocytes, the only uncoupler: a historical perspective. Front Endocrinol (Lausanne) 2:85.
[130] Moonen, M.P.B., Nascimento, E.B.M., van Marken Lichtenbelt, W.D., 2019. Human brown adipose tissue: Underestimated target in metabolic disease? Biochim Biophys Acta Mol Cell Biol Lipids 1864(1):104-112.
[131] Chondronikola, M., Volpi, E., Børsheim, E., Porter, C., Annamalai, P., Enerbäck, S., et al., 2014. Brown adipose tissue improves whole-body glucose homeostasis and insulin sensitivity in humans. Diabetes 63(12):4089-4099.
[132] Lee, P., Smith, S., Linderman, J., Courville, A.B., Brychta, R.J., Dieckmann, W., et al., 2014. Temperature-acclimated brown adipose tissue modulates insulin sensitivity in humans. Diabetes 63(11):3686-3698.
[133] Seale, P., Conroe, H.M., Estall, J., Kajimura, S., Frontini, A., Ishibashi, J., et al., 2011. Prdm16 determines the thermogenic program of subcutaneous white adipose tissue in mice. J Clin Invest 121(1):96-105.
[134] Cohen, P., Levy, J.D., Zhang, Y., Frontini, A., Kolodin, D.P., Svensson, K.J., et al., 2014. Ablation of PRDM16 and beige adipose causes metabolic dysfunction and a subcutaneous to visceral fat switch. Cell 156(1-2):304-316.
[135] Ohno, H., Shinoda, K., Ohyama, K., Sharp, L.Z., Kajimura, S., 2013. EHMT1 controls brown adipose cell fate and thermogenesis through the PRDM16 complex. Nature 504(7478):163-167.
[136] Bartelt, A., Bruns, O.T., Reimer, R., Hohenberg, H., Ittrich, H., Peldschus, K., et al., 2011. Brown adipose tissue activity controls triglyceride clearance. Nat Med 17(2):200-205.
[137] Stanford, K.I., Middelbeek, R.J., Townsend, K.L., Lee, M.Y., Takahashi, H., So, K., et al., 2015. A novel role for subcutaneous adipose tissue in exercise-induced improvements in glucose homeostasis. Diabetes 64(6):2002-2014.

[138] Wang, G.X., Zhao, X.Y., Meng, Z.X., Kern, M., Dietrich, A., Chen, Z., et al., 2014. The brown fat-enriched secreted factor Nrg4 preserves metabolic homeostasis through attenuation of hepatic lipogenesis. Nat Med 20(12):1436-1443.
[139] Himms-Hagen, J., Melnyk, A., Zingaretti, M.C., Ceresi, E., Barbatelli, G., Cinti, S., 2000. Multilocular fat cells in WAT of CL-316243-treated rats derive directly from white adipocytes. Am J Physiol Cell Physiol 279(3):C670-681.
[140] Vitali, A., Murano, I., Zingaretti, M.C., Frontini, A., Ricquier, D., Cinti, S., 2012. The adipose organ of obesity-prone C57BL/6J mice is composed of mixed white and brown adipocytes. J Lipid Res 53(4):619-629.
[141] Wang, Q.A., Tao, C., Gupta, R.K., Scherer, P.E., 2013. Tracking adipogenesis during white adipose tissue development, expansion and regeneration. Nat Med 19(10):1338-1344.
[142] Berry, D.C., Jiang, Y., Graff, J.M., 2016. Mouse strains to study cold-inducible beige progenitors and beige adipocyte formation and function. Nat Commun 7:10184.
[143] Long, J.Z., Svensson, K.J., Tsai, L., Zeng, X., Roh, H.C., Kong, X., et al., 2014. A smooth muscle-like origin for beige adipocytes. Cell Metab 19(5):810-820.
[144] Jiang, Y., Berry, D.C., Graff, J.M., 2017. Distinct cellular and molecular mechanisms for β3 adrenergic receptor-induced beige adipocyte formation. Elife 6.
[145] Collins, S., Daniel, K.W., Rohlfs, E.M., Ramkumar, V., Taylor, I.L., Gettys, T.W., 1994. Impaired expression and functional activity of the beta 3- and beta 1-adrenergic receptors in adipose tissue of congenitally obese (C57BL/6J ob/ob) mice. Mol Endocrinol 8(4):518-527.
[146] Bronnikov, G., Houstěk, J., Nedergaard, J., 1992. Beta-adrenergic, cAMP-mediated stimulation of proliferation of brown fat cells in primary culture. Mediation via beta 1 but not via beta 3 adrenoceptors. J Biol Chem 267(3):2006-2013.
[147] de Jong, J.M.A., Wouters, R.T.F., Boulet, N., Cannon, B., Nedergaard, J., Petrovic, N., 2017. The β(3)-adrenergic receptor is dispensable for browning of adipose tissues. Am J Physiol Endocrinol Metab 312(6):E508-e518.
[148] Ueta, C.B., Fernandes, G.W., Capelo, L.P., Fonseca, T.L., Maculan, F.D., Gouveia, C.H., et al., 2012. β(1) Adrenergic receptor is key to cold- and diet-induced thermogenesis in mice. J Endocrinol 214(3):359-365.
[149] Soloveva, V., Graves, R.A., Rasenick, M.M., Spiegelman, B.M., Ross, S.R., 1997. Transgenic mice overexpressing the beta 1-adrenergic receptor in adipose tissue are resistant to obesity. Mol Endocrinol 11(1):27-38.
[150] Shinoda, K., Luijten, I.H., Hasegawa, Y., Hong, H., Sonne, S.B., Kim, M., et al., 2015. Genetic and functional characterization of clonally derived adult human brown adipocytes. Nat Med 21(4):389-394.
[151] Wu, J., Boström, P., Sparks, L.M., Ye, L., Choi, J.H., Giang, A.H., et al., 2012. Beige adipocytes are a distinct type of thermogenic fat cell in mouse and human. Cell 150(2):366-376.
[152] Zuriaga, M.A., Fuster, J.J., Gokce, N., Walsh, K., 2017. Humans and Mice Display Opposing Patterns of "Browning" Gene Expression in Visceral and Subcutaneous White Adipose Tissue Depots. Front Cardiovasc Med 4:27.
[153] Nakhuda, A., Josse, A.R., Gburcik, V., Crossland, H., Raymond, F., Metairon, S., et al., 2016. Biomarkers of browning of white adipose tissue and their regulation during exercise- and diet-induced weight loss. Am J Clin Nutr 104(3):557-565.
[154] Flegal, K.M., Carroll, M.D., Kuczmarski, R.J., Johnson, C.L., 1998. Overweight and obesity in the United States: prevalence and trends, 1960-1994. Int J Obes Relat Metab Disord 22(1):39-47.
[155] Hruby, A., Hu, F.B., 2015. The Epidemiology of Obesity: A Big Picture. Pharmacoeconomics 33(7):673-689.
[156] Cawley, J., Meyerhoefer, C., 2012. The medical care costs of obesity: an instrumental variables approach. J Health Econ 31(1):219-230.

[157] Coleman-Jensen, A.R., M.P.; Gregory, C.A.; Singh, A. , 2020. Household Food Insecurity in the United States in 2019, Economic Research Report. United States Department of Agriculture.
[158] Krotkiewski, M., Björntorp, P., Sjöström, L., Smith, U., 1983. Impact of obesity on metabolism in men and women. Importance of regional adipose tissue distribution. J Clin Invest 72(3):1150-1162.
[159] Salans, L.B., Horton, E.S., Sims, E.A., 1971. Experimental obesity in man: cellular character of the adipose tissue. J Clin Invest 50(5):1005-1011.
[160] Spalding, K.L., Arner, E., Westermark, P.O., Bernard, S., Buchholz, B.A., Bergmann, O., et al., 2008. Dynamics of fat cell turnover in humans. Nature 453(7196):783-787.
[161] Björntorp, P., Carlgren, G., Isaksson, B., Krotkiewski, M., Larsson, B., Sjöström, L., 1975. Effect of an energy-reduced dietary regimen in relation to adipose tissue cellularity in obese women. Am J Clin Nutr 28(5):445-452.
[162] Kral, J.G., Björntorp, P., Scherstén, T., Sjöström, L., 1977. Body composition and adipose tissue cellularity before and after jejuno-ileostomy in severely obese subjects. Eur J Clin Invest 7(5):413-419.
[163] Sun, K., Tordjman, J., Clément, K., Scherer, P.E., 2013. Fibrosis and adipose tissue dysfunction. Cell Metab 18(4):470-477.
[164] Hotamisligil, G.S., 2010. Endoplasmic reticulum stress and the inflammatory basis of metabolic disease. Cell 140(6):900-917.
[165] Trayhurn, P., 2013. Hypoxia and adipose tissue function and dysfunction in obesity. Physiol Rev 93(1):1-21.
[166] Jiang, C., Kim, J.H., Li, F., Qu, A., Gavrilova, O., Shah, Y.M., et al., 2013. Hypoxia-inducible factor 1α regulates a SOCS3-STAT3-adiponectin signal transduction pathway in adipocytes. J Biol Chem 288(6):3844-3857.
[167] Halberg, N., Khan, T., Trujillo, M.E., Wernstedt-Asterholm, I., Attie, A.D., Sherwani, S., et al., 2009. Hypoxia-inducible factor 1alpha induces fibrosis and insulin resistance in white adipose tissue. Mol Cell Biol 29(16):4467-4483.
[168] Borén, J., Taskinen, M.R., Olofsson, S.O., Levin, M., 2013. Ectopic lipid storage and insulin resistance: a harmful relationship. J Intern Med 274(1):25-40.
[169] Weir, G.C., Bonner-Weir, S., 2004. Five Stages of Evolving Beta-Cell Dysfunction During Progression to Diabetes. Diabetes 53(suppl 3):S16.
[170] Heymsfield, S.B., Greenberg, A.S., Fujioka, K., Dixon, R.M., Kushner, R., Hunt, T., et al., 1999. Recombinant leptin for weight loss in obese and lean adults: a randomized, controlled, dose-escalation trial. Jama 282(16):1568-1575.
[171] Roth, J.D., Roland, B.L., Cole, R.L., Trevaskis, J.L., Weyer, C., Koda, J.E., et al., 2008. Leptin responsiveness restored by amylin agonism in diet-induced obesity: evidence from nonclinical and clinical studies. Proc Natl Acad Sci U S A 105(20):7257-7262.
[172] Considine, R.V., Sinha, M.K., Heiman, M.L., Kriauciunas, A., Stephens, T.W., Nyce, M.R., et al., 1996. Serum immunoreactive-leptin concentrations in normal-weight and obese humans. N Engl J Med 334(5):292-295.
[173] Zhao, S., Zhu, Y., Schultz, R.D., Li, N., He, Z., Zhang, Z., et al., 2019. Partial Leptin Reduction as an Insulin Sensitization and Weight Loss Strategy. Cell Metab 30(4):706-719.e706.
[174] Cnop, M., Havel, P.J., Utzschneider, K.M., Carr, D.B., Sinha, M.K., Boyko, E.J., et al., 2003. Relationship of adiponectin to body fat distribution, insulin sensitivity and plasma lipoproteins: evidence for independent roles of age and sex. Diabetologia 46(4):459-469.
[175] Li, S., Shin, H.J., Ding, E.L., van Dam, R.M., 2009. Adiponectin levels and risk of type 2 diabetes: a systematic review and meta-analysis. Jama 302(2):179-188.
[176] Aron-Wisnewsky, J., Tordjman, J., Poitou, C., Darakhshan, F., Hugol, D., Basdevant, A., et al., 2009. Human adipose tissue macrophages: m1 and m2 cell surface markers in subcutaneous and omental depots and after weight loss. J Clin Endocrinol Metab 94(11):4619-4623.

[177] Lumeng, C.N., Bodzin, J.L., Saltiel, A.R., 2007. Obesity induces a phenotypic switch in adipose tissue macrophage polarization. J Clin Invest 117(1):175-184.
[178] Feuerer, M., Herrero, L., Cipolletta, D., Naaz, A., Wong, J., Nayer, A., et al., 2009. Lean, but not obese, fat is enriched for a unique population of regulatory T cells that affect metabolic parameters. Nat Med 15(8):930-939.
[179] Winer, S., Chan, Y., Paltser, G., Truong, D., Tsui, H., Bahrami, J., et al., 2009. Normalization of obesity-associated insulin resistance through immunotherapy. Nat Med 15(8):921-929.
[180] Tiemessen, M.M., Jagger, A.L., Evans, H.G., van Herwijnen, M.J., John, S., Taams, L.S., 2007. CD4+CD25+Foxp3+ regulatory T cells induce alternative activation of human monocytes/macrophages. Proc Natl Acad Sci U S A 104(49):19446-19451.
[181] Odegaard, J.I., Ricardo-Gonzalez, R.R., Goforth, M.H., Morel, C.R., Subramanian, V., Mukundan, L., et al., 2007. Macrophage-specific PPARgamma controls alternative activation and improves insulin resistance. Nature 447(7148):1116-1120.
[182] Hotamisligil, G.S., Shargill, N.S., Spiegelman, B.M., 1993. Adipose expression of tumor necrosis factor-alpha: direct role in obesity-linked insulin resistance. Science 259(5091):87-91.
[183] Weisberg, S.P., Hunter, D., Huber, R., Lemieux, J., Slaymaker, S., Vaddi, K., et al., 2006. CCR2 modulates inflammatory and metabolic effects of high-fat feeding. J Clin Invest 116(1):115-124.
[184] Taniguchi, C.M., Emanuelli, B., Kahn, C.R., 2006. Critical nodes in signalling pathways: insights into insulin action. Nature Reviews Molecular Cell Biology 7(2):85-96.
[185] Gual, P., Le Marchand-Brustel, Y., Tanti, J.F., 2005. Positive and negative regulation of insulin signaling through IRS-1 phosphorylation. Biochimie 87(1):99-109.
[186] Wu, H., Ballantyne, C.M., 2020. Metabolic Inflammation and Insulin Resistance in Obesity. Circ Res 126(11):1549-1564.
[187] Brown, M.S., Goldstein, J.L., 2008. Selective versus total insulin resistance: a pathogenic paradox. Cell Metab 7(2):95-96.
[188] ter Horst, K.W., Vatner, D.F., Zhang, D., Cline, G.W., Ackermans, M.T., Nederveen, A.J., et al., 2021. Hepatic Insulin Resistance Is Not Pathway Selective in Humans With Nonalcoholic Fatty Liver Disease. Diabetes Care 44(2):489.
[189] Hamdy, O., Porramatikul, S., Al-Ozairi, E., 2006. Metabolic obesity: the paradox between visceral and subcutaneous fat. Curr Diabetes Rev 2(4):367-373.
[190] Snijder, M.B., Dekker, J.M., Visser, M., Bouter, L.M., Stehouwer, C.D., Kostense, P.J., et al., 2003. Associations of hip and thigh circumferences independent of waist circumference with the incidence of type 2 diabetes: the Hoorn Study. Am J Clin Nutr 77(5):1192-1197.
[191] Tankó, L.B., Bagger, Y.Z., Alexandersen, P., Larsen, P.J., Christiansen, C., 2003. Central and peripheral fat mass have contrasting effect on the progression of aortic calcification in postmenopausal women. Eur Heart J 24(16):1531-1537.
[192] Tran, T.T., Yamamoto, Y., Gesta, S., Kahn, C.R., 2008. Beneficial effects of subcutaneous fat transplantation on metabolism. Cell Metab 7(5):410-420.
[193] Hocking, S.L., Chisholm, D.J., James, D.E., 2008. Studies of regional adipose transplantation reveal a unique and beneficial interaction between subcutaneous adipose tissue and the intra-abdominal compartment. Diabetologia 51(5):900-902.
[194] Mathis, D., 2013. Immunological goings-on in visceral adipose tissue. Cell Metab 17(6):851-859.
[195] Ferrara, D., Montecucco, F., Dallegri, F., Carbone, F., 2019. Impact of different ectopic fat depots on cardiovascular and metabolic diseases. Journal of Cellular Physiology 234(12):21630-21641.
[196] Turer, A.T., Khera, A., Ayers, C.R., Turer, C.B., Grundy, S.M., Vega, G.L., et al., 2011. Adipose tissue mass and location affect circulating adiponectin levels. Diabetologia 54(10):2515-2524.
[197] Lee, M.J., Wu, Y., Fried, S.K., 2013. Adipose tissue heterogeneity: implication of depot differences in adipose tissue for obesity complications. Mol Aspects Med 34(1):1-11.

[198] Cancello, R., Tordjman, J., Poitou, C., Guilhem, G., Bouillot, J.L., Hugol, D., et al., 2006. Increased infiltration of macrophages in omental adipose tissue is associated with marked hepatic lesions in morbid human obesity. Diabetes 55(6):1554-1561.
[199] Xiao, Y., Liu, D., Cline, M.A., Gilbert, E.R., 2020. Chronic stress, epigenetics, and adipose tissue metabolism in the obese state. Nutrition & Metabolism 17(1):88.
[200] Tchkonia, T., Thomou, T., Zhu, Y., Karagiannides, I., Pothoulakis, C., Jensen, M.D., et al., 2013. Mechanisms and metabolic implications of regional differences among fat depots. Cell Metab 17(5):644-656.
[201] Kiefer, F.W., Vernochet, C., O'Brien, P., Spoerl, S., Brown, J.D., Nallamshetty, S., et al., 2012. Retinaldehyde dehydrogenase 1 regulates a thermogenic program in white adipose tissue. Nat Med 18(6):918-925.
[202] Lee, Y.H., Petkova, A.P., Mottillo, E.P., Granneman, J.G., 2012. In vivo identification of bipotential adipocyte progenitors recruited by β3-adrenoceptor activation and high-fat feeding. Cell Metab 15(4):480-491.
[203] Qiang, G., Kong, H.W., Fang, D., McCann, M., Yang, X., Du, G., et al., 2016. The obesity-induced transcriptional regulator TRIP-Br2 mediates visceral fat endoplasmic reticulum stress-induced inflammation. Nat Commun 7:11378.
[204] Shao, M., Ishibashi, J., Kusminski, C.M., Wang, Q.A., Hepler, C., Vishvanath, L., et al., 2016. Zfp423 Maintains White Adipocyte Identity through Suppression of the Beige Cell Thermogenic Gene Program. Cell Metab 23(6):1167-1184.
[205] Jeffery, E., Wing, A., Holtrup, B., Sebo, Z., Kaplan, J.L., Saavedra-Peña, R., et al., 2016. The Adipose Tissue Microenvironment Regulates Depot-Specific Adipogenesis in Obesity. Cell Metab 24(1):142-150.
[206] Tchoukalova, Y.D., Votruba, S.B., Tchkonia, T., Giorgadze, N., Kirkland, J.L., Jensen, M.D., 2010. Regional differences in cellular mechanisms of adipose tissue gain with overfeeding. Proc Natl Acad Sci U S A 107(42):18226-18231.
[207] Strissel, K.J., Stancheva, Z., Miyoshi, H., Perfield, J.W., 2nd, DeFuria, J., Jick, Z., et al., 2007. Adipocyte death, adipose tissue remodeling, and obesity complications. Diabetes 56(12):2910-2918.
[208] Tchkonia, T., Giorgadze, N., Pirtskhalava, T., Tchoukalova, Y., Karagiannides, I., Forse, R.A., et al., 2002. Fat depot origin affects adipogenesis in primary cultured and cloned human preadipocytes. Am J Physiol Regul Integr Comp Physiol 282(5):R1286-1296.
[209] Gesta, S., Blüher, M., Yamamoto, Y., Norris, A.W., Berndt, J., Kralisch, S., et al., 2006. Evidence for a role of developmental genes in the origin of obesity and body fat distribution. Proc Natl Acad Sci U S A 103(17):6676-6681.
[210] Omori, Y., Imai, J., Watanabe, M., Komatsu, T., Suzuki, Y., Kataoka, K., et al., 2001. CREB-H: a novel mammalian transcription factor belonging to the CREB/ATF family and functioning via the box-B element with a liver-specific expression. Nucleic Acids Res 29(10):2154-2162.
[211] Pelham, H.R., 1991. Recycling of proteins between the endoplasmic reticulum and Golgi complex. Curr Opin Cell Biol 3(4):585-591.
[212] Xu, X., Park, J.G., So, J.S., Hur, K.Y., Lee, A.H., 2014. Transcriptional regulation of apolipoprotein A-IV by the transcription factor CREBH. J Lipid Res 55(5):850-859.
[213] Zhang, C., Wang, G., Zheng, Z., Maddipati, K.R., Zhang, X., Dyson, G., et al., 2012. Endoplasmic reticulum-tethered transcription factor cAMP responsive element-binding protein, hepatocyte specific, regulates hepatic lipogenesis, fatty acid oxidation, and lipolysis upon metabolic stress in mice. Hepatology 55(4):1070-1082.
[214] Lee, M.W., Chanda, D., Yang, J., Oh, H., Kim, S.S., Yoon, Y.S., et al., 2010. Regulation of hepatic gluconeogenesis by an ER-bound transcription factor, CREBH. Cell Metab 11(4):331-339.

[215] Danno, H., Ishii, K.A., Nakagawa, Y., Mikami, M., Yamamoto, T., Yabe, S., et al., 2010. The liver-enriched transcription factor CREBH is nutritionally regulated and activated by fatty acids and PPARalpha. Biochem Biophys Res Commun 391(2):1222-1227.
[216] Nakagawa, Y., Satoh, A., Yabe, S., Furusawa, M., Tokushige, N., Tezuka, H., et al., 2014. Hepatic CREB3L3 controls whole-body energy homeostasis and improves obesity and diabetes. Endocrinology 155(12):4706-4719.
[217] Takei, K., Han, S.I., Murayama, Y., Satoh, A., Oikawa, F., Ohno, H., et al., 2017. Selective peroxisome proliferator-activated receptor-α modulator K-877 efficiently activates the peroxisome proliferator-activated receptor-α pathway and improves lipid metabolism in mice. J Diabetes Investig 8(4):446-452.
[218] Min, A.K., Jeong, J.Y., Go, Y., Choi, Y.K., Kim, Y.D., Lee, I.K., et al., 2013. cAMP response element binding protein H mediates fenofibrate-induced suppression of hepatic lipogenesis. Diabetologia 56(2):412-422.
[219] Zheng, Z., Kim, H., Qiu, Y., Chen, X., Mendez, R., Dandekar, A., et al., 2016. CREBH Couples Circadian Clock With Hepatic Lipid Metabolism. Diabetes 65(11):3369-3383.
[220] Bhattacharya, A., Sun, S., Wang, H., Liu, M., Long, Q., Yin, L., et al., 2018. Hepatic Sel1L-Hrd1 ER-associated degradation (ERAD) manages FGF21 levels and systemic metabolism via CREBH. Embo j 37(22).
[221] Kim, H., Mendez, R., Zheng, Z., Chang, L., Cai, J., Zhang, R., et al., 2014. Liver-enriched transcription factor CREBH interacts with peroxisome proliferator-activated receptor α to regulate metabolic hormone FGF21. Endocrinology 155(3):769-782.
[222] Vecchi, C., Montosi, G., Zhang, K., Lamberti, I., Duncan, S.A., Kaufman, R.J., et al., 2009. ER stress controls iron metabolism through induction of hepcidin. Science 325(5942):877-880.
[223] Kim, J.H., Kim, K., Kim, I., Seong, S., Nam, K.I., Kim, K.K., et al., 2018. Endoplasmic Reticulum-Bound Transcription Factor CREBH Stimulates RANKL-Induced Osteoclastogenesis. J Immunol 200(5):1661-1670.
[224] Lee, J.H., Giannikopoulos, P., Duncan, S.A., Wang, J., Johansen, C.T., Brown, J.D., et al., 2011. The transcription factor cyclic AMP-responsive element-binding protein H regulates triglyceride metabolism. Nat Med 17(7):812-815.
[225] Johansen, C.T., Wang, J., McIntyre, A.D., Martins, R.A., Ban, M.R., Lanktree, M.B., et al., 2012. Excess of rare variants in non-genome-wide association study candidate genes in patients with hypertriglyceridemia. Circ Cardiovasc Genet 5(1):66-72.
[226] Cefalù, A.B., Spina, R., Noto, D., Valenti, V., Ingrassia, V., Giammanco, A., et al., 2015. Novel CREB3L3 Nonsense Mutation in a Family With Dominant Hypertriglyceridemia. Arterioscler Thromb Vasc Biol 35(12):2694-2699.
[227] Kikuchi, T., Orihara, K., Oikawa, F., Han, S.I., Kuba, M., Okuda, K., et al., 2016. Intestinal CREBH overexpression prevents high-cholesterol diet-induced hypercholesterolemia by reducing Npc1l1 expression. Mol Metab 5(11):1092-1102.
[228] Kim, H., Zheng, Z., Walker, P.D., Kapatos, G., Zhang, K., 2017. CREBH Maintains Circadian Glucose Homeostasis by Regulating Hepatic Glycogenolysis and Gluconeogenesis. Molecular and Cellular Biology 37(14):e00048-00017.
[229] Tang, Q.-Q., Otto, T.C., Lane, M.D., 2003. Mitotic clonal expansion: A synchronous process required for adipogenesis. Proceedings of the National Academy of Sciences 100(1):44.
[230] Nakagawa, Y., Shimano, H., 2018. CREBH Regulates Systemic Glucose and Lipid Metabolism. Int J Mol Sci 19(5).
[231] Liew, C.W., Boucher, J., Cheong, J.K., Vernochet, C., Koh, H.J., Mallol, C., et al., 2013. Ablation of TRIP-Br2, a regulator of fat lipolysis, thermogenesis and oxidative metabolism, prevents diet-induced obesity and insulin resistance. Nat Med 19(2):217-226.

[232] LI, Y., WANG, X., QIANG, G., MCCANN, M.A., GIL, V., BLÜHER, M., et al., 2020. 208-OR: Emc10emc10, a Novel Circulating Factor for Systemic Energy and Metabolic Homeostasis. Diabetes 69(Supplement 1):208-OR.
[233] Hotamisligil, G.S., 2010. Endoplasmic Reticulum Stress and the Inflammatory Basis of Metabolic Disease. Cell 140(6):900-917.
[234] Chin, K.T., Zhou, H.J., Wong, C.M., Lee, J.M., Chan, C.P., Qiang, B.Q., et al., 2005. The liver-enriched transcription factor CREB-H is a growth suppressor protein underexpressed in hepatocellular carcinoma. Nucleic Acids Res 33(6):1859-1873.
[235] Haywood, N.J., Slater, T.A., Matthews, C.J., Wheatcroft, S.B., 2019. The insulin like growth factor and binding protein family: Novel therapeutic targets in obesity & diabetes. Mol Metab 19:86-96.
[236] Yu, S., Matsusue, K., Kashireddy, P., Cao, W.Q., Yeldandi, V., Yeldandi, A.V., et al., 2003. Adipocyte-specific gene expression and adipogenic steatosis in the mouse liver due to peroxisome proliferator-activated receptor gamma1 (PPARgamma1) overexpression. J Biol Chem 278(1):498-505.
[237] Wolf Greenstein, A., Majumdar, N., Yang, P., Subbaiah, P.V., Kineman, R.D., Cordoba-Chacon, J., 2017. Hepatocyte-specific, PPARγ-regulated mechanisms to promote steatosis in adult mice. J Endocrinol 232(1):107-121.
[238] Michael, M.D., Kulkarni, R.N., Postic, C., Previs, S.F., Shulman, G.I., Magnuson, M.A., et al., 2000. Loss of insulin signaling in hepatocytes leads to severe insulin resistance and progressive hepatic dysfunction. Mol Cell 6(1):87-97.
[239] Tandon, P., Wafer, R., Minchin, J.E.N., 2018. Adipose morphology and metabolic disease. J Exp Biol 221(Pt Suppl 1).
[240] La Cava, A., 2017. Leptin in inflammation and autoimmunity. Cytokine 98:51-58.
[241] Ouchi, N., Walsh, K., 2007. Adiponectin as an anti-inflammatory factor. Clin Chim Acta 380(1-2):24-30.
[242] Cannon, B., Nedergaard, J., 2011. Nonshivering thermogenesis and its adequate measurement in metabolic studies. J Exp Biol 214(Pt 2):242-253.
[243] Ozcan, U., Cao, Q., Yilmaz, E., Lee, A.H., Iwakoshi, N.N., Ozdelen, E., et al., 2004. Endoplasmic reticulum stress links obesity, insulin action, and type 2 diabetes. Science 306(5695):457-461.

X. Vita

Maximilian A. McCann
Ph.D. Candidate
Email: mccann7@uic.edu

Department of Physiology & Biophysics
University of Illinois at Chicago, College of Medicine

Education

2014-Present **Ph.D. Candidate: Department of Physiology and Biophysics**
University of Illinois at Chicago (Chicago, IL)

2010-2014 **Bachelor of Science (B.S.) in Neuroscience**
University of Pittsburgh (Pittsburgh, PA)

Research Experience

2014-Present Graduate Student
Department of Physiology & Biophysics, University of Illinois at Chicago
Advisor: Dr. Chong Wee Liew
Thesis Title: Transcription factor CREB3L3 prevents whole-body metabolic dysfunction by regulating adipose function

2011-2014 Undergraduate Research Assistant
College of Nursing, University of Pittsburgh
Advisor: Dr. Yvette Conley
Project Title: Mitochondrial Genetics of Traumatic Brain Injury Recovery

Awards

2014 Phi Beta Kappa Honors Society
2014 Neuroscience Research Excellence Award awarded by the University of Pittsburgh
2016 Travel Award for Combined Annual Meeting of the CSCTR/AMFR
2016 Provost Deiss Award for Graduate Research
2018 Travel Award for Combined Annual Meeting of the CSCTR/AMFR
2018 Poster Award at Chicago Diabetes Day
2018 Poster Award at UIC Diabetes & Obesity Research Day
2018 Mark R. Lambrecht Award for Scholarship and Commitment

Funding

American Heart Association Predoctoral Fellowship (2016-2018)
UIC University Fellowship (2014-2015, 2018-2019)

Special Coursework

10th Annual Course Isotope Tracers in Metabolic Research
Sponsored by the Mouse Metabolic Phenotyping Center at Vanderbilt University
October 30 - November 3, 2017, Nashville, TN

Publications

1. McCann M, Li Y, Muñoz M, Gil V, Qiang G, Cordoba-Chacon J, Blüher M, Duncan S, Liew CW (2021) *Adipose expression of CREB3L3 modulates body weight during obesity*. Sci. Rep [Under Review]

2. Lee SM, Muratalla J, Diaz-Ruiz A, Remon-Ruiz P, **McCann M**, Liew CW, Kineman RD, Cordoba-Chacon J (2021) *Hepatocyte-specific PPARγ mediates the steatogenic actions of rosiglitazone in the liver of diet-induced obese male mice*. [In Preparation]

3. Wang X, Qiang G, Li Y, Wang K, **McCann M**, Gil V, Yu Y, Li S, Yang Z, Xu S, Cordoba-Chacon J, Kineman R, DeJesus D, Sun B, Chen K, Wang X, Zhou L, Hu R, Ding Q, Gao D, Kulkarni R, Blüher M, Liew CW (2021) *Emc10, a novel circulating actor, promotes diet-induced obesity via suppression of adipocyte thermogenesis.* Nat Metab [Under Review]

4. Batra A, Warren C, Ke Y, **McCann M**, Halas M, Capote A, Liew CW, Solaro RJ, Rosas P (2021) *Deletion of P21 Activated Kinase-1 Induces Age-dependent Increased Visceral Adiposity and Cardiac Dysfunction in Female Mice*. Mol Cell Biochem: Mar;476(3):1337-1349. PMID: 33389497

5. Ryba D, Warren C, Karam C, Davis R, Chowdhury S, Alvarez M, **McCann M**, Liew CW, Wieczorek D, Solaro RJ, Wolska B (2019) *The Sphingosine-1-Phosphate Receptor Modulator, FTY720, Improves Diastolic Dysfunction and Reverses Remodeling in Hypertrophic Cardiomyopathy*. Circ Heart Fail. 2019: 12(11): e005835. PMID: 31684756

6. Liew CW, Xu S, Wang X, **McCann M**, Whang Kong H, Carley AC, Pang J, Fantuzzi G, O'Donnell JM, Lewandowski ED (2017) *Multiphasic Regulation of Systemic and Peripheral Organ Metabolic Responses to Cardiac Hypertrophy*. Circ Heart Fail. 2017: 10(4): pii: e003864. PMID: 28404627

7. Qiang G, Whang Kong H, Fang D, **McCann M**, Yang X, Du G, Blüher M, Zhu J, Liew CW (2016) *An obesity-induced transcriptional regulator, TRIP-Br2, mediates visceral fat endoplasmic reticulum stress-induced inflammation*. Nat. Commun. 2016: 25(7): 11378. PMID: 27109496

Oral Presentations

1. McCann M, Qiang G, Gil V, Whang Kong H, Duncan S, Liew CW. Transcription factor CREB3L3 is a novel regulator of adipocyte biology and metabolism. 2016 American Diabetes Association 76th Scientific Sessions, New Orleans, LA.

2. McCann M, Qiang G, Gil V, Whang Kong H, Zhang K, Duncan S, Liew CW. Adipose CREB3L3 mediates obesity-induced metabolic dysfunction. 2016 UIC Diabetes & Obesity Research Day, Chicago, IL.

3. McCann M, Qiang G, Gil V, Whang Kong H, Zhang K, Duncan S, Liew CW. Adipose CREB3L3 mediates obesity-induced metabolic dysfunction. 2017 Combined Annual

Meeting of Central Society for Clinical and Translational Research and Midwestern Section of the American Federation for Medical Research, Chicago, IL.

4. McCann M, Qiang G, Gil V, Whang Kong H, Zhang K, Duncan S, Liew CW. Adipose CREB3L3 mediates obesity-induced metabolic dysfunction. 2017 American Diabetes Association 77th Scientific Sessions, San Diego, CA.

5. McCann M, Qiang G, Gil V, Whang Kong H, Zhang K, Duncan S, Liew CW. Adipose CREB3L3 mediates obesity-induced metabolic dysfunction. 2017 Graduate Education in Medical Sciences Research Symposium, Chicago, IL.

6. McCann M, Qiang G, Gil V, Whang Kong H, Zhang K, Liew CW. Ablation of Adipose CREB3L3 Protects Mice from Obesity-Induced Metabolic Dysfunction. 2018 American Diabetes Association 78th Scientific Sessions, Orlando, FL.

7. McCann M, Qiang G, Gil V, Whang Kong H, Zhang K, Liew CW. Ablation of Adipose CREB3L3 Protects Mice from Obesity-Induced Metabolic Dysfunction. 2019 Midthesis Departmental Seminar. Department of Physiology and Biophysics, University of Illinois at Chicago. Chicago, IL.

8. McCann M, Qiang G, Li S, Li Y, Gil V, Zhang K, Liew CW. Ablating Adipose CREB3L3 Preserves Metabolic Health During Obesity. 2019 Combined Annual Meeting of Central Society for Clinical and Translational Research and Midwestern Section of the American Federation for Medical Research, Chicago, IL.

9. McCann M, Qiang G, Li S, Li Y, Gil V, Zhang K, Liew CW. Ablating Adipose CREB3L3 Preserves Metabolic Health During Obesity. 2019 American Diabetes Association 79th Scientific Sessions, San Fransisco, CA.

Poster Presentations

1. McCann M, Qiang G, Gil V, Whang Kong H, Duncan S, Liew CW. Transcription factor CREB3L3 is a novel regulator of adipocyte biology and metabolism. 2016 Combined Annual Meeting of Central Society for Clinical and Translational Research and Midwestern Section of the American Federation for Medical Research, Chicago, IL.

2. McCann M, Qiang G, Gil V, Whang Kong H, Duncan S, Liew CW. Transcription factor CREB3L3 is a novel regulator of adipocyte biology and metabolism. 2016 UIC Graduate Education in Medical Sciences Research Symposium.

3. McCann M, Qiang G, Gil V, Whang Kong H, Zhang K, Duncan S, Liew CW. Transcription factor CREB3L3 is a novel regulator of adipocyte biology and metabolism. 2016 UIC College of Medicine Research Forum.

4. McCann M, Qiang G, Gil V, Whang Kong H, Zhang K, Duncan S, Liew CW. Adipose CREB3L3 mediates obesity-induced metabolic dysfunction. 2017 Combined Annual Meeting of Central Society for Clinical and Translational Research and Midwestern Section of the American Federation for Medical Research, Chicago, IL.

5. McCann M, Mkrtschjan M, Gil V, Russell B, Liew CW. Firm that flab: Matrix stiffness promotes adipocyte thermogenesis. 2017 UIC College of Medicine Research Forum.

6. McCann M, Mkrtschjan M, Gil V, Russell B, Liew CW. Matrix stiffness promotes adipocyte thermogenesis. 2018 Combined Annual Meeting of Central Society for Clinical and Translational Research and Midwestern Section of the American Federation for Medical Research, Chicago, IL.

7. McCann M, Mkrtschjan M, Gil V, Russell B, Liew CW. Matrix stiffness promotes adipocyte thermogenesis. 2018 Chicago Diabetes Day, Chicago, IL.

8. McCann M, Qiang G, Gil V, Whang Kong H, Zhang K, Duncan S, Liew CW. Adipose CREB3L3 mediates obesity-induced metabolic dysfunction. 2018 UIC Graduate Education in Medical Sciences Research Symposium.

9. McCann M, Mkrtschjan M, Gil V, Russell B, Liew CW. Matrix stiffness promotes adipocyte thermogenesis. 2018 UIC Diabetes & Obesity Research Day, Chicago, IL.

10. McCann M, Li S, Li Y, Gil V, Liew CW. Calpain inhibition improves glucose homeostasis in obese mice. 2018 UIC College of Medicine Research Forum.

11. McCann M, Qiang G, Li S, Li Y, Gil V, Zhang K, Liew CW. Ablating Adipose CREB3L3 Preserves Metabolic Health During Obesity. 2019 Chicago Diabetes Day, Chicago, IL.

12. McCann M, Li S, Li Y, Gil V, Liew CW. Calpain inhibition improves glucose homeostasis in obese mice. 2019 Graduate Education in Medical Sciences Research Symposium.

13. McCann M, Qiang G, Whang Kong H, Zhang K, Duncan S, Liew CW. Ablating adipose CREB3L3 preserves metabolic health during obesity. 2019 UIC Diabetes & Obesity Research Day, Chicago, IL.

14. McCann M, Gil V, Muñoz M, Zhang K, Duncan S, Liew CW. Ablation of adipose CREB3L3 prevents browning and promotes inflammation. 2020 American Diabetes Association 80th Scientific Sessions, Chicago, IL. (Virtual Poster)

15. McCann M, Gil V, Muñoz M, Zhang K, Duncan S, Liew CW. Ablation of adipose CREB3L3 prevents browning and promotes inflammation. 2020 UIC Diabetes & Obesity Research Day, Chicago, IL.